

Yale University

EliScholar – A Digital Platform for Scholarly Publishing at Yale

Yale Medicine Thesis Digital Library

School of Medicine

1979

Electron microscopy of the fetal glomerulus fine structure and functional development

Westley Hubbard Reeves

Yale University

Follow this and additional works at: <http://elischolar.library.yale.edu/ymtdl>

Recommended Citation

Reeves, Westley Hubbard, "Electron microscopy of the fetal glomerulus fine structure and functional development" (1979). *Yale Medicine Thesis Digital Library*. 3056.

<http://elischolar.library.yale.edu/ymtdl/3056>

This Open Access Thesis is brought to you for free and open access by the School of Medicine at EliScholar – A Digital Platform for Scholarly Publishing at Yale. It has been accepted for inclusion in Yale Medicine Thesis Digital Library by an authorized administrator of EliScholar – A Digital Platform for Scholarly Publishing at Yale. For more information, please contact elischolar@yale.edu.

YALE MEDICAL LIBRARY



3 9002 08676 0411

ELECTRON MICROSCOPY OF THE FETAL GLOMERULUS
FINE STRUCTURE AND FUNCTIONAL DEVELOPMENT




WESTLEY HUBBARD REEVES

1979

YALE



MEDICAL LIBRARY



Digitized by the Internet Archive
in 2017 with funding from
The National Endowment for the Humanities and the Arcadia Fund

ELECTRON MICROSCOPY OF THE FETAL GLOMERULUS
FINE STRUCTURE AND FUNCTIONAL DEVELOPMENT

by

Westley Hubbard Reeves

A Thesis Submitted to the Yale University School of Medicine
in Partial Fulfillment of the Requirement for
the Degree of Doctor of Medicine

February 27, 1979

Dedicated to the Memory of My Grandmother
Grace S. Hubbard

ACKNOWLEDGEMENT

I am greatly indebted to my thesis advisor, Dr. Marilyn G. Farquhar, who gave me both the opportunity and guidance to make this work possible. It is my sincere desire that at least some of her outstanding qualities as an investigator and as a person will remain with me as a permanent part of my scientific education. I am also grateful to Dr. George Palade and Dr. Thomas Lentz for serving as members of my thesis committee and to Dr. Nicolai Simionescu, Dr. Maia Simionescu and Dr. James Jamieson for their valuable advice.

This work could not have been completed without the excellent technical advice and assistance of Philippe Male, Bonnie Peng, Barbara Dannacher, Nancy Bull and Laurie Daniell. The superb photographic advice of Pam Ossorio and the excellent secretarial assistance of Lynne Wooton in preparing this thesis are gratefully acknowledged.

Finally, I wish to express my appreciation to my many friends in the cell biology department and especially to Dr. John Caulfield and to Dr. Yashpal Kanwar who functioned virtually as second research advisors and who were a valuable source of stimulation and companionship throughout the course of this work.

TABLE OF CONTENTS

ACKNOWLEDGEMENTS.....	iii
SUMMARY.....	vii
I. INTRODUCTION.....	1
II. REVIEW OF LITERATURE.....	3
<u>General Description of Glomerular Development.....</u>	3
Light Microscope Studies.....	3
Early Electron Microscope Studies.....	3
<u>Development of the Vascular Glomerulus.....</u>	6
Brief Overview of the Vascularization Process.....	6
Development of the Endothelium.....	6
<u>Development of the Basement Membrane.....</u>	7
Definition of Basement Membrane.....	7
Studies of the Fetal GBM.....	8
Basement Membrane Biochemistry.....	9
Origin of Basement Membranes.....	11
Function of Basement Membranes.....	11
Charge Barrier of the GBM.....	13
Presence of Proteoglycans in Basement Membranes...	14
Possible Role of Glycosaminoglycans in Basement Membranes.....	16
<u>Development of the Epithelium.....</u>	18
Junctions.....	18
Epithelial Surface Polyanion.....	19
<u>Epithelial Changes in Glomerular Disease.....</u>	20
Epithelial Morphology.....	20

Epithelial Cell Surface Polyanion.....	21
Other Models of Glomerular Disease.....	21
Functional Alterations in Glomerular Disease.....	21
<u>Function of the Developing Glomerulus.....</u>	23
<u>Purpose of this Investigation.....</u>	23
III. MATERIALS AND METHODS.....	25
Animals Used.....	25
Collection and Fixation of Tissues.....	25
Sectioning and Staining.....	27
Special Materials.....	28
General Morphology.....	28
Colloidal Iron.....	28
Native Ferritin.....	29
Cationized Ferritin.....	30
Ruthenium Red.....	30
Alcian Blue.....	31
Enzyme Digestion Studies.....	32
IV. RESULTS.....	33
<u>Stages of Glomerular Development.....</u>	33
<u>Development of the Visceral Epithelium, Basement</u> <u>Membrane and Endothelium in Newborn Rat.....</u>	36
Vesicle Stage.....	36
S-shaped Stage.....	36
Developing Capillary Loop Stage.....	44
Maturing Glomerulus Stage.....	52
<u>Colloidal Iron Staining of Developing Glomeruli.....</u>	52
Light Microscopy.....	52
Electron Microscopy.....	55
Enzyme Digestion.....	63
<u>Tracer Studies.....</u>	63
Native Ferritin.....	63
<u>Staining with Cationic Probes.....</u>	75
Cationized Ferritin.....	75

Ruthenium Red.....	78
Alcian Blue.....	83
V. DISCUSSION.....	93
<u>Development of the Glomerular Endothelium</u>	93
<u>Formation of the Basement Membrane</u>	95
Development of Anionic Sites in the Laminae Rarae.	96
Colloidal Iron and Alcian Blue Staining.....	98
<u>Epithelial Differentiation</u>	99
Junctions in Developing Glomeruli.....	101
Epithelial Cell Surface Polyanion.....	102
Function of Sialoprotein.....	105
<u>Analogy With Aminonucleoside Nephrosis</u>	106
Epithelium.....	106
Basement Membrane and Endothelium.....	107
<u>Tracer Studies</u>	108
Native Ferritin.....	108
Cationized Ferritin as a Tracer.....	109
VI. CONCLUSIONS.....	111
VII. BIBLIOGRAPHY.....	114

SUMMARY

The development of glomerular structure and function was studied at the ultrastructural level in the newborn rat kidney in order to better understand the factors involved in the formation and maintenance of the normal filtration surface and in the prevention of proteinuria. Special attention was given to the differentiation of the fine structure organization of the glomerulus, the formation of glomerular charged sites on the epithelial cell surface and in the basement membrane, and the factors regulating the passage of large molecules across the developing glomerular capillary wall. A variety of special stains, cationic probes and tracers were used in pursuing these studies.

Four stages of glomerular development were defined: vesicle, S-shaped body, developing capillary loop, and maturing stages, and specific events in the differentiation of the glomerulus were related to these stages.

The earliest stage is the renal vesicle. It consists of a cluster of epithelial cells, the metanephrogenic blastem, which eventually develops a lumen in its center. These cells are the precursors of the glomerular and tubular epithelia.

A cleft forms in the renal vesicle, marking the beginning of the S-shaped body stage. Cells on one side of this cleft differentiate into glomerular epithelium while those on the other side of the cleft differentiate into tubular epithelium. Large (~ 30 nm in diameter) proteoglycan granules, stainable with ruthenium red, appear in the cleft; these may (by analogy with other systems) induce mesenchymal invasion into the cleft.

The invading mesenchymal cells differentiate into endothelial and mesangial cells. The endothelium forms a continuous layer, lacking fenestrae at this stage. The epithelium consists of a simple columnar layer of cells, lacking foot processes, with occluding junctions at their apices where they face the early Bowman's space. Small amounts of epithelial surface polyanion, stainable with colloidal iron, appear above the level of the junctions at the epithelial cell apices. The glomerular basement membrane is first detected at this stage and is probably secreted jointly by the epithelium and endothelium.

Just before the appearance of capillary loops, a number of important events occur. First, endothelial fenestrae appear; these early fenestrae are closed by negatively charged diaphragms which are impermeable to cationized ferritin and to which cationized ferritin binds. Secondly, the large (~ 30 nm diameter) proteoglycan granules disappear and are replaced by smaller (10-15 nm diameter) ruthenium red stainable proteoglycan granules randomly distributed within the basement membrane. Thirdly, the epithelial occluding zonulae and surface polyanion migrate in phase toward the base of the epithelium. As the junctions approach the basement membrane, they fragment into less extensive fasciae and maculae. Increasing amounts of epithelial cell surface polyanion appear progressively closer to the basement membrane, but always above the level of the occluding junctions. When the junctions and surface polyanion reach the base, the epithelial cells send out broad processes which interdigitate with the epithelial processes of adjacent cells to form the early foot processes, marking the beginning of the capillary loop stage.

During the capillary loop stage, the endothelium thins, increasing numbers of fenestrae are formed, and the fenestral diaphragms are gradually lost. The ruthenium red stainable granules in the basement membrane become

arranged in two layers on either side of the lamina densa. The early broad epithelial processes develop into more extensively interdigitated foot processes. Many slits are still closed by focal (i.e., macular) occluding junctions. As the slits begin to open, junctions gradually disappear and epithelial cell surface polyanion appears on the surfaces of the foot processes.

In the maturing glomerulus stage, the endothelium and basement membranes gradually assume their mature configuration, and the epithelial junctions are lost altogether and normal foot process and slit architecture prevails.

All three layers of the glomerular capillary wall appear to play a role in regulating the movement of large molecules across the developing capillary wall, a process that begins late in the S-shaped body stage or early in the developing capillary loop stage. Proteinuria is minimized at all stages by a number of mechanisms. The broad epithelium contains few fenestrae (which are closed by fenestral diaphragms) at early stages, and limits access to the thin basement membrane seen at these stages. As the basement membrane matures and becomes more capable of restricting the movement of large molecules, the endothelium thins and forms larger numbers of patent (i.e., without diaphragms) fenestrae, allowing greater access to the basement membrane. The epithelium serves as a monitor of glomerular filtration at all stages by taking up large molecules which pass through the basement membrane by pinocytosis. The broad epithelial processes and slits which are closed by occluding junctions may further prevent the loss of particles that pass through the basement membrane. As the basement membrane approaches its mature state, the junctions disappear and the slits open.

Thus, the establishment of glomerular function is a gradual process

which results from the closely synchronized maturation of the endothelium, basement membrane and epithelium, such that proteinuria is minimized at all stages of development.

Prior to the development of extensive interdigitation, the differentiating glomerular epithelium bears a number of striking similarities to the nephrotic epithelium: foot processes are broad, reduced in number and often joined by focal occluding junctions; slit diaphragms are reduced in number and displaced away from the basement membrane; and ladder-like structures occur in the filtration slits. The epithelial changes seen in aminonucleoside nephrosis (an experimental model of minimal change disease in children) therefore appear to represent a "dedifferentiation" to a more primitive organization, and the events that occur early in the disease process represent a rerun in reverse of events that occur during normal glomerular development.

The new findings of this study are: 1) the identification of stages of glomerular development demonstrable by light microscopy which correlate with important ultrastructural events in the differentiation of the glomerulus, 2) the demonstration of transient endothelial fenestral diaphragms in developing glomeruli, 3) the identification of two classes of ruthenium red stainable proteoglycan granules in developing glomeruli, 4) the delineation of the sequence of events which occurs during the development of the visceral epithelium from an undifferentiated columnar epithelium to the flattened, mature epithelium containing interdigitating foot processes, 5) the finding of ladder-like structures between developing glomerular epithelial cells, 6) the demonstration of the similarity between the nephrotic glomerular epithelium and a certain stage in fetal development, 7) the identification of sialoglycoprotein on the surface of developing glomerular epithelial cells and the association of this epithelial cell

surface polyanion with the presence of foot processes and open slits, and
8) a better understanding of the steps involved in the sequential development of the glomerular filtration apparatus.

INTRODUCTION

During development, the glomerulus develops from an undifferentiated cluster of cells to a three-layered structure consisting of endothelium (and mesangium), basement membrane and epithelium. Although the general aspects of glomerular development are understood, the development of the mature fenestrated endothelium, the formation of the basement membrane, the differentiation of the interdigitating foot processes from the early columnar epithelium and the appearance of epithelial polyanion are aspects of glomerular development about which there is little information. The experiments reported in this thesis were carried out to define the sequential changes that occur during glomerular development in an attempt to achieve a better understanding of the factors involved in the formation and maintenance of the normal filtration surface.

An attempt was also made to determine the previously poorly defined functional changes that occur at the same time as glomerular structure develops. An understanding of the development of glomerular function is of importance in understanding the function of the normal mature glomerulus and the loss of this function in glomerular disease. For example, in experimental and human glomerular diseases, the complex epithelial organization is frequently lost, the foot processes and slits are reduced in number and the epithelium assumes a more primitive arrangement resembling that found in immature glomeruli. Along with the loss of foot process organization, there is a loss of epithelial polyanion and alteration of the anionic charge of the basement membrane

in certain glomerular diseases. It will be shown that in many respects, the glomerular changes seen in aminonucleoside nephrosis (a model of minimal change disease in children) represent a dedifferentiation to a more primitive organization, and that the events that occur early in this disease process represent a rerun in reverse of events that occur during normal glomerular development.

REVIEW OF LITERATURE

GENERAL DESCRIPTION OF GLOMERULAR DEVELOPMENT.

Light Microscope Studies. The development of the glomerulus has been extensively studied at the light microscope (LM) level since late in the nineteenth century (Toldt (1874); Golgi (1889); and Herring (1900)) see reviews (23,73). From light microscopy studies (4,23,42,73) the following picture of glomerular development emerged (see illustrations A-G): The ampulla of the collecting duct induces the formation of the early renal vesicle from cells of mesenchymal origin (A). The renal vesicle and ampulla are originally separated (as shown by serial sectioning) (B) and later fuse as do the thin basement membranes surrounding each of these structures. After fusion, the progenitor cells of the glomerular epithelium migrate toward the lumen of the vesicle (C) while cells in the outer part of the vesicle wall form the future Bowman's capsule. A cleft is formed as a result of this cell migration (D) into which mesenchyme migrates (E). The glomerular visceral epithelium becomes arranged into a single layer with nuclei near the apices of the cells; and endothelial cells are seen in the cleft (F). These cells rearrange to form several capillary loops (G), after which the glomerulus slowly matures to the adult form. Further characterization of glomerular development was not possible until electron microscopy became available.

Early Electron Microscope Studies. Although several earlier investigators had studied glomerular development by electron microscopy (EM) (57), the earliest EM study which added to what was already known at

ILLUSTRATIONS A-G. Summary of glomerular development as revealed by light microscopy.

A. The ampulla (Am) of the collecting duct induces the formation of the metanephrogenic blastem from mesenchymal cells.

B. The metanephrogenic blastem organizes to form the renal vesicle (V), the earliest recognizable precursor of the glomerulus. Note that both the ampulla of the collecting duct (Am) and the renal vesicle are covered by thin basement membranes. Cells are separated by wide intercellular spaces in this and the following diagrams for clarity. This is not meant to imply the existence of wide intercellular spaces at this stage (in fact, as will be shown later, the cells are closely apposed at this stage and are joined by occluding junctions).

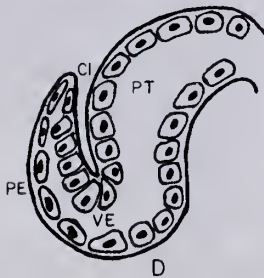
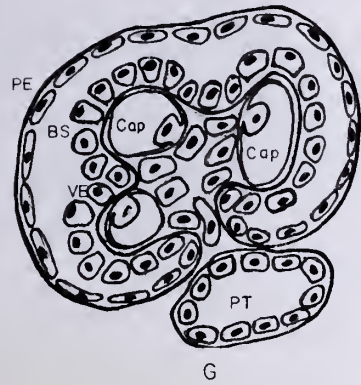
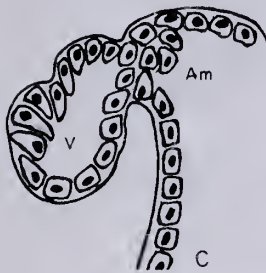
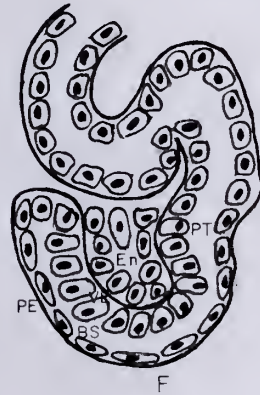
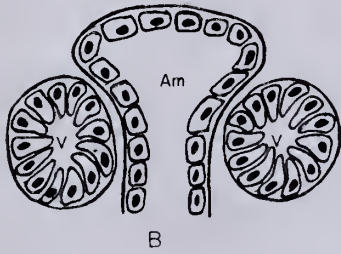
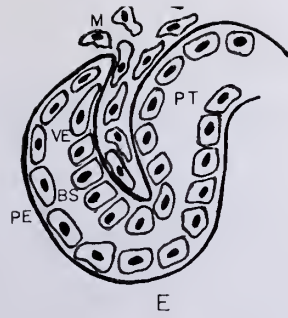
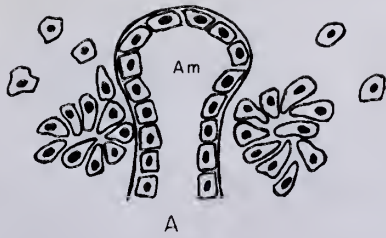
C. The renal vesicle (V) and its basement membrane fuse with the ampulla (Am) and its basement membrane. Note the notching of the vesicle epithelium near the top of the diagram. The cells above this notch migrate downward to form the glomerular visceral epithelium while those below the notch migrate upward to form Bowman's capsule (ie. the parietal epithelium).

D. A cleft forms as a result of the cell migrations, which is devoid of cells (Cl). The parietal epithelium (PE) and visceral epithelium (VE) begin to differentiate and the early Bowman's space is continuous with the lumen of the proximal tubule (PT).

E. Mesenchymal cells (M) migrate into the glomerular cleft. These cells will differentiate into endothelium and mesangium. Bowman's space (BS) widens and the visceral and parietal epithelium (VE and PE, respectively) continue their development. Note continuity of the early glomerular basement membrane and the basement membranes of the parietal epithelium and proximal tubule (PT).

F. Mesenchymal cells differentiate into endothelium (En) which rearranges to form a capillary loop. The visceral epithelium (VE) begins to flatten somewhat from a pseudostratified columnar to a simple columnar arrangement.

G. The endothelial cells rearrange to form multiple capillary loops (Cap). The visceral epithelium (VE) is cuboidal and nearly mature in configuration, Bowman's space is wider and the parietal epithelium (PE) begins to flatten and approach its adult configuration. The proximal tubule (PT) is represented in cross section.



ILLUSTRATIONS A-G

the LM level was that of Vernier and Birch-Anderson (103) who described the development of the definitive epithelial foot processes from earlier broad epithelial processes. Large numbers of small filaments located within the cytoplasm adjacent to the basement membrane were seen within these broad epithelial processes. The gradual widening of the basement membrane during glomerular differentiation was reported and the appearance of endothelial fenestrae after the broad epithelial processes had begun to form was described. The more specific aspects of the development of mature foot processes from the broad epithelial processes, the development of basement membrane fine structure and the specific details of endothelial differentiation were not studied.

DEVELOPMENT OF THE VASCULAR GLOMERULUS.

Brief Overview of the Vascularization Process. It is beyond the scope of this thesis to study the process of vascularization of the glomerulus, and this is reviewed elsewhere (23). Briefly stated, the origin of the vascular glomerulus is controversial. One group of investigators (57,103) believe that glomerular capillaries form in situ and later become connected to afferent and efferent arterioles. A second school of thought (4,70,73) supports the belief that the glomerular capillaries are connected to the afferent and efferent arterioles from the start. The latter interpretation is believed to be the most probable (70) because injection of India ink into the renal artery followed by microdissection studies shows a single afferent and efferent arteriole running through the S-shaped body which at later stages reorganizes to form the vascular glomerulus.

Development of the Endothelium. Of more pertinence to this study is the development of the endothelium. Early in development the endothelium is broad and unfenestrated, whereas later it becomes thinner and

fenestrae appear (103). Vernier and Birch-Anderson (103) believe that fenestrae do not appear until early, broad epithelial processes have formed (ie. the developing capillary loop stage), but this point remains in doubt.

Others (106) have studied the development of the endothelium using ferritin as a tracer and have concluded that the endothelium represents the major barrier to large molecules in the immature glomerulus and that access to the basement membrane is gained by the development of fenestrae. They also concluded that small molecules (e.g. horseradish peroxidase) are able to pass through junctions between endothelial cells. These authors do not distinguish between the various stages of glomerular development and further fail to recognize that tracer molecules (the size of horseradish peroxidase), can diffuse laterally in the plane of the basement membrane and thus may appear to have passed through a thickened endothelium when in fact they have gained access to the basement membrane through fenestrae outside of the plane of section.

DEVELOPMENT OF THE BASEMENT MEMBRANE.

Definition of Basement Membrane. The term "basement membrane" refers to the PAS positive material seen by light microscopy under epithelia, around muscle fibers and in other sites. Electron microscopy has shown that basement membranes are moderately electron dense and form continuous sheets located at the bases of epithelial cells, endothelial cells, and in general, wherever a cell population (other than connective tissue cells) adjoins connective tissue matrix (26). Thus, a thin, continuous sheet (20-50nm in thickness) of basement membrane material is found, for example, at the dermal-epidermal junction in skin, at the bases of all epithelia which line hollow structures

(e.g. the gastrointestinal tract, reproductive tract and urinary tract), and in many other locations (26). The glomerular basement membrane (GBM) is unusual in that it faces cell layers on both sides rather than facing connective tissue matrix on one side and cells on the other, a property that it shares with the basement membranes of smooth muscle and the lens capsule. The mature GBM is also unusual in its width (120-150nm) and in its function as a filter (see below). It is a trilaminar structure, consisting of a subendothelial layer of moderate electron density, a middle electron dense layer and a superepithelial layer of moderate electron density, the lamina rara interna, lamina densa, and lamina rara externa, respectively. The fine structure of the mature GBM will be discussed later (p.95) in connection with the fine structure development of the embryonic GBM.

Studies of the Fetal GBM. The glomerular basement membrane has been shown to originate from the fusion of the loose extracellular material coating the endothelial and epithelial cells during the S-shaped body stage with elimination of intervening mesenchyme so as to form a single basement membrane with endothelium on one side and epithelium on the other (99). The subsequent development of the glomerular basement membrane has not been well studied. LM studies of developing glomeruli stained with alcian blue show increased staining along the basement membrane at more mature developmental stages (53). This staining was removed by 24 hour neuraminidase digestion. Studies at the EM level are needed, however, to determine whether it is the basement membrane that stains with increased intensity at later stages (as suggested by the authors)(53) or whether the foot processes adherent to the basement membrane (and not distinguishable from it at the LM level) are responsible for the increased staining instead.

Because it is more permeable to ferritin than the adult glomerular basement membrane (104), Vernier and Birch-Anderson consider the GBM to be the main filter of the developing glomerulus. In contrast, Weber and Blackbourn (106) found no difference in permeability to ferritin between the fetal and the adult basement membrane and regard the endothelium and its fenestrae as the most important glomerular filter in developing glomeruli. Neither of these studies has considered all stages of glomerular development, a fact which, as will be shown below, may account for their different conclusions.

Basement Membrane Biochemistry. An understanding of the formation and function of the developing basement membrane is of importance in understanding the structure and function of the mature basement membrane. The extensive studies of the mature basement membrane by Kefalides (48-50) and Spiro and associates (86,97) have been hampered by the great degree of cross-linking of basement membrane components which is found in mature basement membranes, but a number of important new concepts regarding basement membranes have resulted from these studies.

Basement membranes are composed of collagenous and non-collagenous glycoproteins (48-50). Basement membrane collagen differs from other types of collagen in that it contains fewer glycine residues, more hydroxylysine and a large number of half-cystine residues. In addition, basement membrane collagen lacks the characteristic banding of interstitial collagens (ie. it lacks the typical ~64nm periodicity) due to the fact that it is probably secreted as procollagen, with a non-helical extension still present in the basement membrane, making it impossible for the individual molecules to line up in the usual manner. Three identical α_1 chains arranged in a triple helix are believed to form

basement membrane collagen; this has been termed Type IV collagen by Kefalides.

Non-collagenous glycoproteins have been described, one of low molecular weight and the other of high molecular weight, to which are linked heteropolysaccharide units, consisting of galactose, mannose, hexosamines, fucose and sialic acid, but not glucose (48). Three antigenic components of basement membrane have been isolated which are thought to correspond to collagen and to the two non-collagenous glycoproteins (49,50). Although glycosaminoglycans were previously thought to be absent, heparan sulfate has recently been identified as yet another component of the glomerular basement membrane (45).

The molecules which form basement membrane are thought to be cross-linked by hydrogen bonds, disulfide bonds and aldehyde-derived covalent bonds (49). These cross-links make basement membrane highly insoluble, and Kefalides was forced to digest his basement membrane preparations with pronase or pepsin in order to solubilize it. Spiro points out that there are other methods of solubilizing basement membrane (e.g., 0.5M SDS, 8M urea or 0.1N NaOH) and that the "subunits" of basement membrane described by Kefalides may be artifacts of the enzyme digestion used to isolate them (86,97). The polar end of a procollagen-like molecule to which the heteropolysaccharide might be expected to be linked, would be digested by pronase or pepsin treatment, leaving only resistant fragments ("type IV collagen"). Thus, "Type IV collagen" and the two glycoproteins might be artificial subunits, resulting from enzymatic digestion rather than the true subunits secreted originally into the basement membrane, and the question of whether the heteropolysaccharide is part of the procollagen molecule or a separate glycoprotein is still unanswered. Studies of the formation of the GBM (before extensive

cross-linking occurs) might answer this question.

Origin of Basement Membranes. The origin of basement membranes was controversial until recently, although there was evidence for the epithelial origin of basement membranes as far back as the 1960s when it was shown that 1) glomerular epithelium contains well-developed rough endoplasmic reticulum, often with dilated cisternae containing material morphologically similar to basement membrane (24, 31) and 2) when silver nitrate is given to weanling rats in their drinking water and then withheld, new basement membrane which is formed after the silver nitrate has been withheld is found in apposition to the epithelium, suggesting that the epithelium is at least partly responsible for basement membrane secretion (56).

Recent studies show that both epithelium (36) and endothelium (41) can synthesize basement membrane. Hay and Dodson (36) have shown both morphologically and by autoradiography using ^3H -proline that corneal epithelium in culture secretes both interstitial type striated collagen and basement membrane. Jaffe et al (41) have shown by autoradiography using ^3H -proline followed by collagenase digestion as well as by immunofluorescence microscopy using anti-GBM antisera that cultured endothelial cells secrete material that is morphologically, immunologically and biochemically like basement membrane collagen as well as microfibrils and elastic fibers.

Function of Basement Membranes. Basement membranes are thought to serve three main functions (26); they may: 1) maintain the separation of cell populations; 2) attach cell layers to their associated connective tissue elements, and 3) serve as filters. A fourth function, that of support of cells in a more or less rigid framework might be added.

The importance of the mature basement membrane as a filter has been known since the studies of Farquhar, Wissig and Palade in 1961 (31).

Since that time, the filtration function of the glomerular basement membrane (GBM) has been studied extensively; this work has been recently reviewed (25-27) and will only be briefly summarized here.

Using ferritin as a tracer, it has been shown (31) that ferritin concentration in the glomerulus drops sharply along the subendothelial surface of the lamina densa in the basement membrane, and later, ferritin accumulates in the mesangium. The following conclusions were drawn concerning the role of each of the three glomerular layers in filtration:

- 1) The basement membrane is the principal filtration barrier for particles the size of ferritin (11 nm diameter).

- 2) The endothelium acts as a valve, which controls access to the filter by varying the number and size of its fenestrae.

- 3) The epithelium monitors filtration by partially recovering (by pinocytosis) the proteins that pass through the filter (i.e., the filter is not perfect).

- 4) The mesangium reconditions and unclogs the filter by phagocytizing particles which accumulate against it.

Results of tracer studies using horseradish peroxidase and myeloperoxidase (35) at first seemed to contradict this scheme and rather indicated to some that the basement membrane is a coarse filter and that the slit diaphragm functions as the critical glomerular filter. However, the peroxidatic tracers, are basic (e.g., the isoelectric point of myeloperoxidase is 10) and would be expected to bind to the negatively charged sialoproteins on the cell surface (see p. 16). Recent studies using dextrans of various molecular weights as tracers (15) and involving immunocytochemical localization of endogenous albumin (43) have provided further

evidence that the basement membrane is the critical glomerular filter.

Charge Barrier of the GBM: The glomerular filtration barrier for charged particles is still debated. Brenner and associates were the first to study in detail the differences in handling of charged and uncharged particles by the glomerulus although qualitative differences had been recognized previously. Using neutral dextran and dextran sulfate (a polyanion), it has been shown that for a given molecular radius, dextran sulfate clearance is less than neutral dextran clearance, up to a radius of 4.2 nm at which point fractional clearances of both forms of dextran approach zero (12,20). This is of importance in understanding the renal handling of albumin which is a polyanion in physiologic solution. Albumin (with a molecular radius of 3.6 nm was found to be filtered more like dextran sulfate of radius 3.6 nm than like neutral dextran of the same molecular radius. These results suggest that polyanions are repelled electrostatically by a fixed component of the glomerular capillary wall (13,20). Since the presence of anionic charge on the surface of the glomerular epithelial cell (43,59,66) and endothelial cell (79) is well known, and the glomerular basement membrane has recently been shown to contain anionic charge as well (44,58,79), any or all of these layers may contribute to the electrostatic repulsion of polyanions. Although the epithelium has been postulated to play a role in this process (20,66), recent studies (78,79) have provided further evidence that, as originally stated by Farquhar and Palade (29), large negatively charged molecules such as anionic ferritin are restricted mainly at the level of the GBM. A role for epithelial polyanion is restricting polyanionic particles of smaller size cannot be ruled out at this time, and endothelial cell polyanion may prove to play a role in transport across the glomerular capillary

wall, but the bulk of evidence now available points to the GBM as the major barrier to the transport of anionic molecules across the glomerular capillary wall.

Although cationized ferritins and native ferritin have similar clearances (as expected by virtue of their large radius- see p.10 and refs 35,36), their distributions within the basement membrane after injection into the circulation differ. Cationized ferritins of varying pI have been found to penetrate the GBM in increasing amounts as the pI is increased. While native anionic ferritin fails to penetrate beyond the lamina rara interna, strongly cationized ferritin moves across all layers of the GBM, although it appears to be restricted from the urinary spaces between foot processes (78,79). Thus, transport of cationized ferritins differs from transport of anionic ferritin across the glomerular capillary wall. The difference in the transport of cationized ferritin and anionic ferritin was attributed to negative charge in the basement membrane, the location of which was previously unknown.

Presence of Proteoglycans in Basement Membranes. The characterization of negative charge in the GBM was aided by previous knowledge concerning connective tissue matrices and basement membranes in other tissues. Type I collagen, epiphyseal collagen (Type II collagen) and reticular connective tissue matrices (Type III collagen) all contain large ruthenium red positive (ie. negatively charged) proteoglycan granules (37), 20-70nm in diameter. Proteoglycans are protein molecules to which are linked glycosaminoglycans (formerly known as mucopolysaccharides). Glycosaminoglycans (GAGs) are complex polysaccharides with a high concentration of negative charge; The biochemistry of these compounds is reviewed below (p.16). The presence of proteoglycans in other connective tissue matrices has led to the search for these substances in basement membranes

(ie. matrices composed in part of type IV collagen)(see above). Proteoglycans are not preserved by the usual fixation methods, but can be retained by the addition of cationic dyes (e.g. ruthenium red, alcian blue and cationized ferritin)(62,63). Ruthenium red has proved to be the most useful of the cationic dyes.

Studies of basement membranes secreted by embryonic corneal epithelium (101), arterial smooth muscle (107) and embryonic lens, notochord and neural tube (38) have shown the presence of ruthenium red stainable (i.e. negatively charged) proteoglycan granules. In corneal epithelial basement membrane, spherical, 10nm diameter, granules were found at periodic intervals 55-60nm apart, in two rows, one in the outer and one in the inner face of the basement membrane. The fact that ruthenium red staining was prevented by treatment with chondroitinase ABC but not by leech hyaluronidase and that the epithelium synthesizes chondroitin sulfate but not dermatan sulfate or chondroitin suggests that these granules contain chondroitin sulfate. The granules in basement membranes secreted by other embryonic tissues (38) were also found to be composed at least in part of chondroitin sulfate. The ruthenium red positive granules in basement membranes secreted by arterial smooth muscle are similar morphologically but have not been identified chemically. In general, the proteoglycan granules of basement membranes have been less well studied than those of connective tissue matrices. Their distribution in basement membranes appears to be more restricted than in connective tissue matrices.

The existence of similar anionic sites in the GBM has recently been shown. These sites are stainable by lysozyme (17), by ruthenium red and by cationized ferritin (44). After ruthenium red staining, they are seen to consist of parallel layers of 20nm diameter granules located in the laminae rarae interna and externa with the particles periodically

arranged in a 60 nm intervals. Binding of cationized ferritin and probably of ruthenium red to these granules is electrostatic in nature since it is displaced by treatment with solutions of high ionic strength or pH. It has further been shown by Kanwar and Farquhar (45) that these granules are not removed by neuraminidase, collagenase, chondroitinase ABC or testicular and leech hyaluronidase but are removed by pronase, heparinase or heparitinase, suggesting that they consist at least in part of heparan sulfate.

Negatively charged fibrils, the nature of which is unclear at present, have been demonstrated in the GBM using alcian blue (14). It is possible that alcian blue stains another class of anionic particles in the GBM and/or the heparan sulfate containing sites.

Possible Role of Glycosaminoglycans in Basement Membranes: The recent demonstration of the presence of heparan sulfate, one of number of compounds known collectively as glycosaminoglycans (and previously thought to be absent in the GBM) raises the question as to its function in the GBM. The biochemistry of this class compounds will be briefly considered before addressing this question.

Glycosaminoglycans (GAG's) are complex polysaccharides with backbones consisting (except for keratan sulfate) of alternating uronic acid (L-iduronic acid and/or D-glucuronic acid) and hexosamine (D-glucosamine or D-galactosamine) residues. Seven GAG's have been studied -- hyaluronate, chondroitin, chondroitin sulfate, dermatan sulfate, heparan sulfate and heparin. Except for hyaluronate, all are sulfated and occur primarily linked to proteins in the form of proteoglycans (21, 60, 100). The large size, high charge density and linkage to proteins are thought to impart unique properties to GAG's and to proteoglycans in particular, including

the ability to restrict water flow and to interfere with diffusion of other molecules, especially macromolecules, and the ability to form proteoglycan-collagen matrices and to sterically exclude macromolecules from these matrices.

GAG- protein networks are thought to affect the transport of globular proteins such as albumin by retarding translational motion while only slightly affecting rotational motion (60). In such a network, protein molecules behave as if they were enclosed in pores in which the frictional interaction with the polymer network is minimized and lateral movement is impossible due to steric hindrance. Further, physiologic studies have shown that GBM filtration data are compatible with circular pores of radius 3.6 nm, slits of half-width 2.6 nm or fiber networks with fiber half-interspaces of 2.6 nm (77). The basement membrane may utilize features of each of these models in restricting proteins of different types. By forming "pores", GAG's may function in establishing the size barrier of the GBM; because they are highly charged, GAG's may also function in establishing the charge barrier of the GBM.

GAG's are also thought to play an important role in morphogenesis (8, 9, 100). Hyaluronate is produced in large amounts during stages of development involving mesenchymal cell migration while hyaluronidase activity increases and sulfated GAG's are preferentially secreted during later stages of development involving cell differentiation. These morphologically active substances (i.e., hyaluronate and sulfated GAG's) are thought to associate with the embryonic cell surface (100) and with early basement membranes (8, 9).

DEVELOPMENT OF THE EPITHELIUM

The general aspects of development of the glomerular epithelium from a columnar to a somewhat flattened epithelium were known from LM studies; and early EM studies showed that broad epithelial processes precede mature foot process development (see above). Few studies of the more specific aspects of epithelial fine structure development exist, however.

Junctions: The developing glomerular epithelium has been studied by transmission EM (3), scanning EM (96) and freeze fracture (40). Aoki (3) was the first to describe the existence of intercellular junctions between developing epithelial cells which he characterized as zonulae adherentes. This study was carried out before en bloc staining with uranyl acetate was available and relatively low magnifications were used, thus the junction morphology is inadequate. Humbert et al., have studied these junctions by freeze fracture (40) and have shown the existence of atypical occluding junctions between epithelial cells, consisting of linear arrays of particles rather than the more usual continuous ridges. Further, the junctions between columnar epithelial cells were shown to be zonulae while the junctions between podocytes were shown to be less extensive (fasciae or maculae). The freeze fracture technique is limited, however, in that it can distinguish only between columnar epithelium and podocytes; in the words of the authors, "undifferentiated and unidentified are synonymous" (40). In addition, adhering junctions are not recognized in replicas of freeze-fracture specimens and thus, their presence or absence cannot be determined. Clearly, further studies by transmission EM are needed to adequately describe the differentiation of the epithelium and to determine the role played by intercellular junctions in this process.

Epithelial Surface Polyanion. The mature glomerular epithelium is coated with a thick (40-70 nm) layer of colloidal iron stainable material which is removed by treatment with neuraminidase and thus consists at least in part of sialic acid, presumably in the form of sialoprotein (43, 66-69). The development of this epithelial surface sialoprotein has not been studied.

Studies of mature glomeruli have shown that epithelial cell surface polyanion may be important in maintaining normal slit and foot process architecture. Perfusion of the kidney with protamine sulfate (a polycation) (90, 91) was found to result in loss of the normal foot process and slit architecture with resulting morphologic changes similar to those seen in aminonucleoside nephrosis (see below). Associated with the changes in foot process morphology was a decrease in colloidal iron stainable material on the epithelial cell surface. Both surface charge and normal foot process architecture reappeared after reperfusion with heparin. Thus, although the cell coat was originally thought to trap protein which leaks through the GBM (43), it now seems likely that the presence of anionic charge on the epithelial cell surface serves to maintain the normal foot process and slit architecture. The presence or absence of epithelial cell surface sialoprotein in developing glomeruli prior to and during foot process differentiation is of great interest in determining the general applicability of the hypothesis that epithelial surface polyanion is needed to maintain normal foot process and slit architecture, and the studies reported in this thesis will address this question.

EPITHELIAL CHANGES IN GLOMERULAR DISEASE

In experimental and human glomerular diseases, the complex organization of the mature epithelium is often lost and the glomerular epithelium assumes a more primitive arrangement. These changes in the glomerular epithelium will be considered below and the concomitant changes in glomerular function in renal disease will be briefly reviewed.

Epithelial Morphology: Aminonucleoside nephrosis, a model of minimal change disease in children, has been the model of glomerular disease most extensively studied. It is induced in rats by daily injections of puromycin aminonucleoside and regularly produces epithelial changes indistinguishable from those seen in the human disease (105). Foot process organization is altered and several morphologic changes occur. The frequency of the slits as well as the number of foot processes are reduced (19, 29, 32, 105); many slits are replaced with occluding junctions (19, 74, 84, 85), displaced slit diaphragms (19) or ladder-like structures (19, 85).

The reduction in number of foot processes and slits has been shown to be due to foot process retraction rather than to foot process "fusion" as was once thought (5, 84).

Farquhar and Palade (29) were the first to show that the junctions between nephrotic glomerular epithelial cells resemble the occluding junctions seen in other epithelia. These junctions have been further characterized by freeze-fracture as consisting of linear arrays of membrane-associated particles, similar to those described in the developing glomerular epithelium. These junctions are thought to be atypical maculae or fasciae occludentes (19, 74, 84).

Ladder-like structures are seen in aminonucleoside nephrosis in or above the slits. They are best seen in grazing section and consist of

~ 9 nm dense ridges more or less regularly spaced ~ 9 nm apart and containing a central dense line, suggesting to some (85) that these structures represent a piling up of excess slit diaphragm which occurs as the foot processes retract. Whether or not this is the case remains to be convincingly shown.

Epithelial Cell Surface Polyanion: A decrease in colloidal iron strainable material presumably sialoprotein on the epithelial cell surface has been noted in aminonucleoside nephrosis along with a reduction in glomerular sialic acid (as determined by biochemical methods) (65). It is thought, in view of the protamine perfusion studies outlined above, that this decrease in epithelial cell surface charge may be responsible for the foot process retraction that is seen (65, 90).

Other Models of Glomerular Disease: Similar epithelial changes (i.e., reduction in foot process and slit numbers with formation of occluding junctions and ladder-like structures between the widened epithelial processes) (87) have been seen in autologous immune complex nephritis, a model of human immune complex disease characterized by massive, non-selective proteinuria, and in New Zealand Black/White mice, a model of human lupus nephritis characterized by features of membranous nephropathy with non-selective proteinuria.

Functional Alterations in Glomerular Disease: Tracer studies have shown that the glomerular basement membrane is more permeable to ferritin (29) and to dextrans (16) in aminonucleoside nephrotic than in normal rats. The decreased neutral dextran clearance described in physiologic studies (7) might be explained by a reduction in exit (due to closed slits) -- i.e., neutral dextran may penetrate further into the GBM (as shown morphologically (16)), but not reach the urinary spaces because of a reduction in slit area.

Other physiologic studies (7) have demonstrated that for any given molecular size, dextran sulfate (a polyanion) clearance is greater in aminonucleoside nephrotic animals than in normal animals. In contrast, neutral dextran and DEAE dextran (a polycation) clearance were decreased in nephrotics as compared to normals. In view of this evidence, a reduction in the glomerular charge barrier seems likely in aminonucleoside nephrosis.

Recent studies have shown that lysozyme binding to anionic sites in the GBM (cf. above and ref. 17) is reduced in aminonucleoside nephrosis, which is in keeping with physiologic studies indicating that the glomerular charge barrier is reduced in nephrosis and suggesting that this reduction in charge barrier occurs at least in part at the level of GBM. Further study is required, however, to determine the relationship of the proteoglycan granules in the GBM to the decreased charge barrier seen in aminonucleoside nephrosis. The granules are still present in the GBM of nephrotic rats, although they may have reduced charge density (Kanwar, unpublished observation).

Increased GBM ferritin permeability has also been seen in autologous immune complex nephritis (88) and in NZB/W membranous nephropathy, but the defect is probably more focal than in aminonucleoside nephrosis, with ferritin appearing to penetrate the full thickness of the GBM only in the vicinity of the electron dense deposits (i.e., immediately beneath the slits). It has been suggested (13, 22, 102) that loss of glomerular anionic charge might increase immune complex and non-immune complex deposition in the GBM resulting in increased accumulation of these complexes in the mesangium, providing a stimulus for increased mesangial matrix secretion. The final outcome of this process might be focal or diffuse glomerular sclerosis (22, 102).

Function of the Developing Glomerulus: Little is known about the function of the developing kidney at the macroscopic level (23), and virtually nothing is known about function of the developing glomerulus at the microscopic level. Renal function is not necessary in utero, as is shown by the fact that anephric fetuses which are normal in other regards may be born alive, at term. Glomerular filtration begins early in development. Both the mesonephros and the metanephros produce urine. It has been shown (23) that dye is not excreted by the metanephric glomerulus until visceral epithelium has developed well-differentiated foot processes and a proximal tubule with a recognizable brush border. At earlier stages, the dye circulates within the vascular glomerulus but is not excreted. The studies of Weber and Blackburn (106), and Vernier and Birch Anderson (104) (reviewed above) represent the only ultrastructural studies of fetal glomerular function.

PURPOSE OF THIS INVESTIGATION

A number of questions concerning developing glomeruli are raised by the recent advances in our knowledge of the structure and function of the mature glomerulus and by the previous studies in developing glomeruli.

1. Can general stages of development, recognizable at the LM level, be correlated with specific events in the differentiation of glomerular fine structure?
2. How do the endothelial fenestrae form and what is their functional significance in developing glomeruli? Does their function in the immature glomerular endothelium differ in any respect from their function in the mature endothelium?

3. How is the basement membrane formed, and specifically, how, and at what stage of development are the anionic sites recently identified in the mature GBM formed?

4. What is the sequence of development of the glomerular epithelium from an undifferentiated columnar epithelium to a flattened, mature epithelium containing interdigitating foot processes?

5. How and when does epithelial surface polyanion develop? Is its presence or absence related to the structure of the glomerular epithelium at various stages in development?

6. Can the poorly differentiated fetal epithelium be related to glomerular disease states in which the complex epithelial organization is lost?

7. At what stage is functional circulation to the glomerulus established and is the developing glomerulus capable of preventing protein loss from vascular space?

These questions have been left unanswered by previous studies of developing glomeruli. The studies undertaken in this thesis are addressed to answering these and related questions in hopes of better understanding the factors involved in the formation and maintenance of the normal filtration surface and the prevention of proteinuria.

MATERIALS AND METHODS

ANIMALS USED.

The neonatal rat kidney was selected as an experimental model because, unlike the human kidney, the newborn rat kidney is not fully developed until approximately 12 days after birth (6). A gradient in the degree of development exists so that more mature glomeruli are located toward the corticomedullary junction, and immature glomeruli are located toward the capsule. Thus, all stages of development may be studied in a single kidney from a 2- to 5-day old rat. Other than the temporal differences in the development of glomeruli, the process of differentiation of the rat and human glomerulus is thought to be identical (cf. 4,42,103).

COLLECTION AND FIXATION OF TISSUES

One hundred nineteen 2- to 5-day old Sprague-Dawley rats weighing 8-14 grams from over fifteen litters were used for these studies (see Table 1) and nearly 400 glomeruli in all stages of development were studied and photographed. Each rat was anesthetized with ether and the kidneys were exposed and fixed with Karnovsky's fixative (46) either by injection of the fixative directly into the renal cortex using a hypodermic syringe and a 28 gauge needle, or by left ventricular perfusion, depending upon the experimental procedure that was to follow. Left ventricular perfusion was accomplished as follows: After exposing the kidneys and inferior vena cava, the thorax was opened by right and left paramedian incisions, avoiding the internal mammary arteries. The thorax was retracted superiorly with a small clamp and the pericardium was stripped from the heart before inserting a 28 gauge needle (attached by polyethylene tubing to the syringe containing the perfusing solution) into the left ventricle. The inferior vena cava was nicked below the level of the renal vein and perfusion was

TABLE I.

<u>PROCEDURE</u>	<u>NUMBER OF RATS</u>	<u>NUMBER OF GLOMERULI PHOTOGRAPHED</u>
Uranyl Acetate <u>en bloc</u>	8	97
Tannic Acid <u>en bloc</u>	22	53
Colloidal Iron		
Light Microscopy	1	18
Electron Microscopy	17	35
Native Ferritin	18	47
Cationized Ferritin	12	12
Ruthenium Red	3	13
Alcian Blue	22	64
Neuraminidase/Colloidal Iron	5	13
Hyaluronidase/Colloidal Iron	4	12
Collagenase	4	-
Thiosulfation/Alcian Blue	3	-

begun, first with normal saline to wash out the blood remaining in the circulation, then with fixative or other solutions to be perfused.

In situ fixation, either by hilar injection or by perfusion was continued 5-10 minutes until the kidneys were hard, at which point they were removed, cut into thin slices (0.25 to 0.50 mm thick) and fixed for an additional hour by immersion in the same fixative at 22° C. After undergoing various other treatments, these slices were post-fixed in acetate-Veronal buffered OsO_4 (AVOsO_4) for 1½ hours at 22° C or 5° C (71). After en bloc staining, if used, (see below), the tissue was dehydrated in ethanol and propylene oxide and embedded in Epon (61) for electron microscopy.

SECTIONING AND STAINING.

Thick sections (0.5 μm) were prepared from plastic-embedded blocks using a Porter-Blum MT-2B ultramicrotome and stained with basic fuchsin (15) or azure II and methylene blue for use in surveying and trimming the material prior to thin sectioning. Glomeruli were selected by trimming the block in such a way as to leave only the subcapsular region (containing immature glomeruli) and trimming away the corticomedullary region (containing more mature glomeruli). Paraffin sections (6 to 8 μm) of whole kidneys were cut on a standard microtome and stained with colloidal iron (82). Some sections were treated with testicular hyaluronidase (0.5% in phosphate buffer for 1 hour at 37° C) prior to staining in order to distinguish hyaluronic acid rich sites from sialoproteins.

Thick sections were viewed and photographed with a Zeiss photomicroscope II at an original magnification of X250 using a 40X apochromat objective.

Thin sections (50 nm) were prepared, placed on carbon-coated grids, and stained on grid for 5 minutes in uranyl acetate and for 4 minutes in lead citrate (80) before examining in a Siemens-Elmiskop 101 electron microscope.

SPECIAL MATERIALS.

The following special materials were used: Tannic acid, AR code no. 1764, from Mallinckrodt, Inc., St. Louis, MO (chiefly composed of digallic acid); Horse spleen ferritin, twice recrystallized (cadmium-free) from Calbiochem; Ruthenium Red from Ventron Corp., Danvers, MA; Alcian blue 8GX from Matheson, Coleman and Bell Manufacturing Chemists, Norwood OH; Neuraminidase (*Cl. perfringens* NEUP) from Worthington Biochemicals; Bovine testicular hyaluronidase from Sigma Chemical Company.

GENERAL MORPHOLOGY.

Kidney slices to be used for studying the stages of glomerular development and junction structure were stained en bloc with either uranyl acetate (28) (2 hours at 22° C) or with freshly prepared 1% tannic acid in 0.1M cacodylate buffer, pH 7.4 (2 hours at 5° C) (92). The blocks treated with tannic acid were washed (three rinses of 15 minutes each) in 0.1M cacodylate buffer (pH 7.4) at 22° C prior to tannic acid staining.

COLLOIDAL IRON.

Histochemical demonstration of cell surface polyanion was achieved using colloidal iron (82). Staining by colloidal iron is dependent upon affinity of free acidic groups on the cell surface for colloidal Fe^{+++} and this is detected for light microscopy by means of the Prussian Blue reaction. Demonstration of colloidal iron at the EM level is dependent upon the high electron density of the Fe^{+++} bound to the cell surface (33).

Colloidal iron was prepared by the method of Rinehart and Abul-Haj (82) from ferric chloride, glycerin and ammonium hydroxide. The mixture was extensively dialyzed against distilled water for 72 hours. The following method, modified from the procedures of others (10, 33, 43, 65) was used to stain the glomeruli for electron microscopy: Tissue was well fixed by perfusion with Karnovsky's fixative and cut into 40 μ slices using a Smith-Farquhar tissue chopper. These slices were floated for 90 minutes in a solution consisting of 4 parts colloidal iron stock and 1 part concentrated glacial acetic acid, pH 1.6. The optimal staining time has been found to be 90 minutes (65) since longer times give increasing amounts of non-specific staining. The colloidal iron-acetic acid solution was filtered through a 0.22 μ millipore filter before use to remove aggregates of the colloid. After staining in this solution, the tissue slices were rinsed briefly with 12% acetic acid and rinsed for 30 minutes in distilled water before post-fixing in $AVOsO_4$.

NATIVE FERRITIN.

Native ferritin was used as a tracer to study glomerular capillary permeability to large, anionically charged molecules.

Horse spleen ferritin (100 mg/ml in normal saline) was given to anesthetized animals by injection either into the inferior vena cava or into the left ventricle; the dose corresponded to roughly 0.05 cc of ferritin solution per 10 grams of body weight. The ferritin was allowed to circulate 10 minutes before fixing the kidney by injection of Karnovsky's fixative into the renal parenchyma. Tissue slices were further treated for 2 hours in the same fixative followed by ferrocyanide-reduced OsO_4 (47) or by $AVOsO_4$. Tissue was dehydrated and embedded without en block staining

so as to enhance the contrast of the ferritin. The sections were stained for 1 1/2 hours on grid with alkaline bismuth (1).

CATIONIZED FERRITIN

Cationized ferritin was used as a cationic probe to stain anionic groups in the glomerulus for electron microscopy. Cationized ferritin, pI 7.3 to 7.5, has been shown (44) to be optimal for staining anionic groups in the glomerular basement membrane (GBM) of the mature rat since it binds specifically to the anionic sites without staining the cell surface. At pI greater than 7.6, agglutination of red blood cells leading to thrombus formation becomes a problem. At lower pI's, there was little or no detectable agglutination of erythrocytes.

Cationized ferritin (pI 7.3) was generously provided by Dr. Yashpal Kanwar (44). A solution containing 50 mg/ml of cationized ferritin in normal saline was injected into the inferior vena cava (roughly 0.05 cc of ferritin solution per 10 grams body weight). The ferritin was allowed to circulate 5-10 minutes before the left ventricle was perfused (see above) with 10 cc of normal saline, followed by 1 cc of low salt buffer (50 mM Tris, 50 mM KCl, 5 mM MgCl₂) (54, 55) to remove non-specific binding. Kidneys were cut into slices and fixed an additional 1 1/2 hours in the same fixative before postfixation in $AVOsO_4$. A number of animals were perfused with cationized ferritin but injection of small volumes of concentrated tracer was found to give better results.

RUTHENIUM RED

Ruthenium red is an inorganic dye which binds to acid mucopolysaccharides and other anionically charged groups (62, 63). The dye has the ability to catalytically reduce OsO_4 and the intensity of staining at the EM level can be enhanced by the use of this property. Polysaccharide is

oxidized by the dye with an equivalent reduction of OsO_4 to insoluble oxidation products which accumulate in the region of bound ruthenium red (62). To produce this useful reaction, ruthenium red is mixed with OsO_4 in the perfusate. The method of Luft (62) was used with modification for these studies.

The kidneys were perfused through the left ventricle as described above, with 10 cc of normal saline followed by 1% formaldehyde in cacodylate buffer (5 cc over 2-3 minutes); 0.2% ruthenium red in Karnovsky's fixative, pH 7.3 (62, 63), was then perfused (10 cc over 5 minutes). Slices were cut and fixed for an additional 3 hours in the same mixture after which they were placed in 0.1% ruthenium red in 0.1 M cacodylate buffer at 25° C overnight. They were postfixed in 1% AVOsO_4 containing 0.05% ruthenium red at pH 7.3 for 3 hours at 25° C and were dehydrated and embedded.

ALCIAN BLUE.

Alcian blue is a cationic copper phthalocyanin which has been used to stain mucoproteins but is not truly specific.

The concept of "critical electrolyte concentration" (75, 83, 89) was utilized in hopes of increasing the specificity of alcian blue staining. Alcian blue has been found to stain sulfate groups rather than carboxyl groups with increasing specificity as MgCl_2 concentration is raised (89). Binding to carboxyl groups ceases at relatively low magnesium ion concentrations (less than 0.3 M) while binding to sulfate esters remains, even at magnesium concentrations above 1.2 M. A pH of 5.8 was chosen because at this pH the maximum number of anionic sites are available for reaction with alcian blue. Staining was carried out after perfusion fixation with Karnovsky's fixative, by perfusion of 0.1% alcian blue in

0.025 M acetate buffer, pH 5.8, containing: a) no $MgCl_2$, b) 0.4 M $MgCl_2$, c) 0.8 M $MgCl_2$, or d) 1.2 M $MgCl_2$. Parallel controls with the same $MgCl_2$ concentrations but without alcian blue were run.

Alcian blue perfusion was continued for about 5 minutes until the kidneys had turned blue, after which 1-2 cc of acetate-Veronal buffer was perfused to wash out the excess dye. Tissue slices were cut and postfixed in $AVOsO_4$ for 1 1/2 hours, followed by uranyl acetate en block for another 2 hours before dehydration and embedding.

ENZYME DIGESTION STUDIES.

Tissue was perfused with Karnovsky's fixative followed by immersion for an additional 15 minutes in the same fixative, and cut into 40μ sections using a Smith-Farquhar tissue chopper. These sections were treated for 8 hours in either: a) neuraminidase (0.05 U/ml in 0.1 M acetate buffer, pH 5.4 at $37^\circ C$), b) bovine testicular hyaluronidase (6000 U/ml in 0.1 M acetate buffer, pH 5.4 at $37^\circ C$), or c) 0.1 M acetate buffer, pH 5.4 at $37^\circ C$. Following this treatment, slices were stained with colloidal iron as described above, dehydrated and embedded.

RESULTS

STAGES OF GLOMERULAR DEVELOPMENT.

The mammalian kidney is generally accepted to be derived from two sources: the glomerulus and the uriniferous tubule from the metanephric blastem and the collecting system from the ureteric bud (reviewed ref. 23). The terminal ampulla of the ureteric bud or presumptive collecting duct is believed to induce formation of a renal vesicle (Fig. 1) from metanephrogenic tissue. The renal vesicle consists of a cluster of cells which eventually develops a lumen at its center. A cleft forms in the vesicle which is invaded by mesenchymal tissue to form an S-shaped body (Fig. 2). The cells to one side of the mesenchymal cleft become glomerular epithelium while those to the other side of the cleft become proximal tubule. Capillary endothelium and mesangium develop from mesenchymal tissue in the cleft. Further development leads to the formation of several capillary loops (Fig. 3), after which the epithelium, basement membrane and endothelium gradually assume their adult form (Fig. 4). Thus, glomerular development is a continuous process which for convenience has been divided into stages; the number and naming of the stages varies from one investigator to another. For the purpose of this thesis, it has proved to be convenient to recognize the following four stages: (1) vesicle, (2) S-shaped body, (3) capillary loop development, and (4) maturing glomerulus (Figs. 1-4).

These stages have been chosen because of their close correlation with certain events in glomerular fine structure development. The renal vesicle (Fig. 1) represents the earliest structure identifiable as a developing glomerulus. It will be shown that at the S-shaped stage (Fig. 2), the glomerular epithelium is columnar with junctions along the



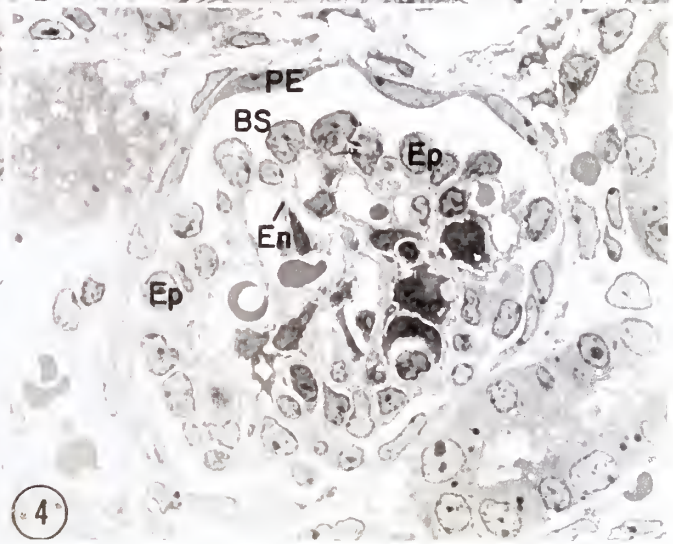
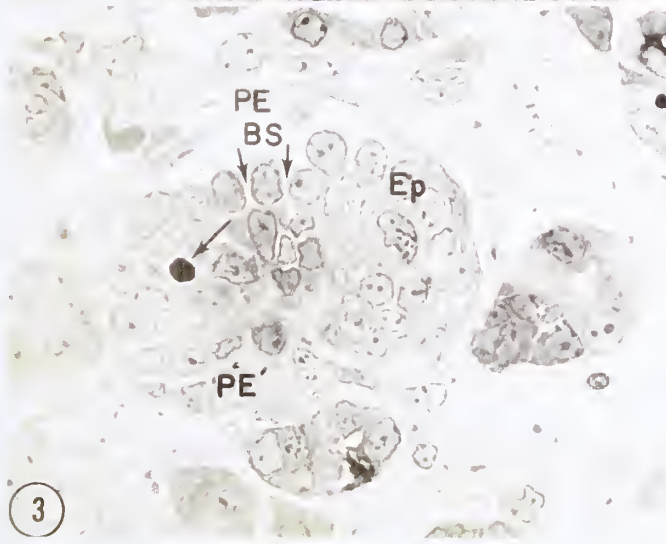
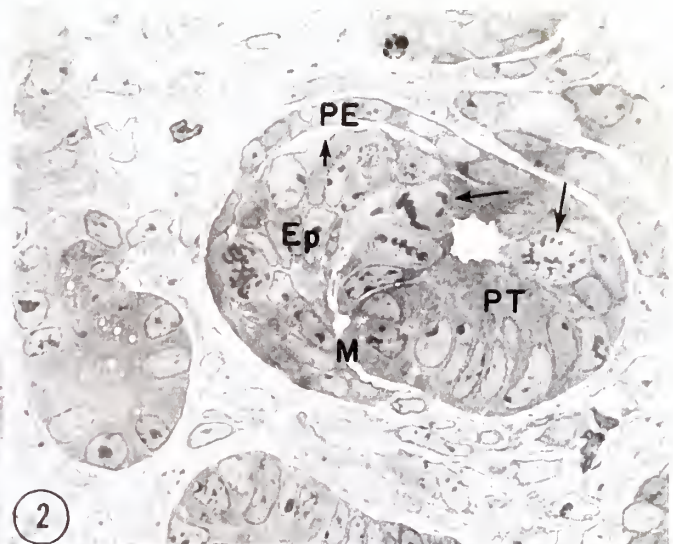
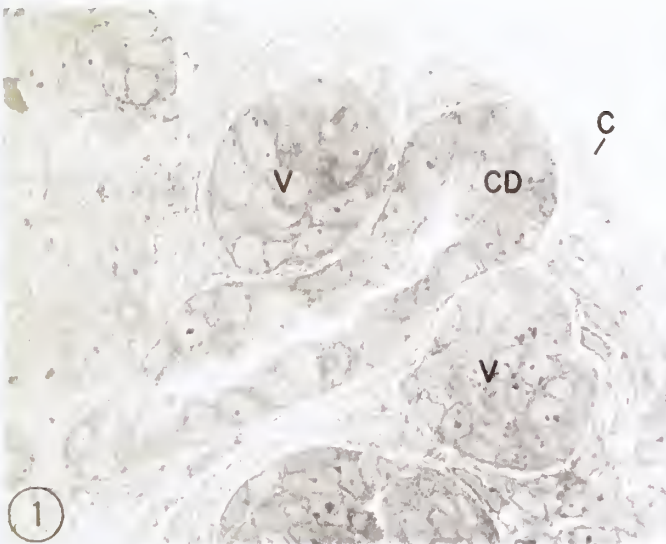
FIGS. 1 to 4. Light micrographs of stages in glomerular development.

FIG. 1. Vesicle (earliest) stage. Vesicles (V) are clusters of cells located near, but apparently not connected to a collecting duct (CD). Note that the vesicles are located just beneath the kidney capsule (C). Fig. 1, X1100.

FIG. 2. S-shaped body stage. The vesicle has begun to differentiate into parietal epithelium (PE), visceral epithelium (Ep) and proximal tubule (PT) and has been invaginated by mesenchymal tissue (M). Bowman's space (short arrow) is recognizable where the parietal epithelium has begun to separate from the visceral epithelium (Ep). The proximal tubule lumen is visible in the plane of section. Note numerous mitotic figures (long arrows), indicating that extensive cell proliferation takes place at this stage. Fig. 2, X1400.

FIG. 3. Developing capillary loop stage. Visceral epithelial cells (Ep) have proliferated and are separated by intercellular spaces (short arrows) which are continuous with Bowman's space (BS). Bowman's space is more prominent and the parietal epithelium (PE) has become flattened at the top of the glomerulus but is still cuboidal below (PE'). Several capillary loops can be recognized (long arrow). Fig. 3, X1400.

FIG. 4. Maturing glomerulus stage. Multiple capillary lumina containing red blood cells are evident. The parietal epithelium (PE), visceral epithelium (Ep) and endothelium (En) have become flattened, but have not yet reached their mature configuration. Fig. 4, X1400.



lateral cell membranes. There are no foot processes at this stage. The capillary loop stage (Fig. 3) will be shown to correlate with the formation of early capillary loops; junctions are located at the bases of epithelial cells at this stage and early foot processes are seen. The maturing glomerulus stage (Fig. 4) will be shown to correlate with the formation of mature slits. These correlations of fine structure development with LM stages have resulted from studies of the process of glomerular development using uranyl acetate and tannic acid en bloc.

DEVELOPMENT OF THE VISCERAL EPITHELIUM, BASEMENT MEMBRANE AND ENDOTHELIUM IN NEWBORN RAT.

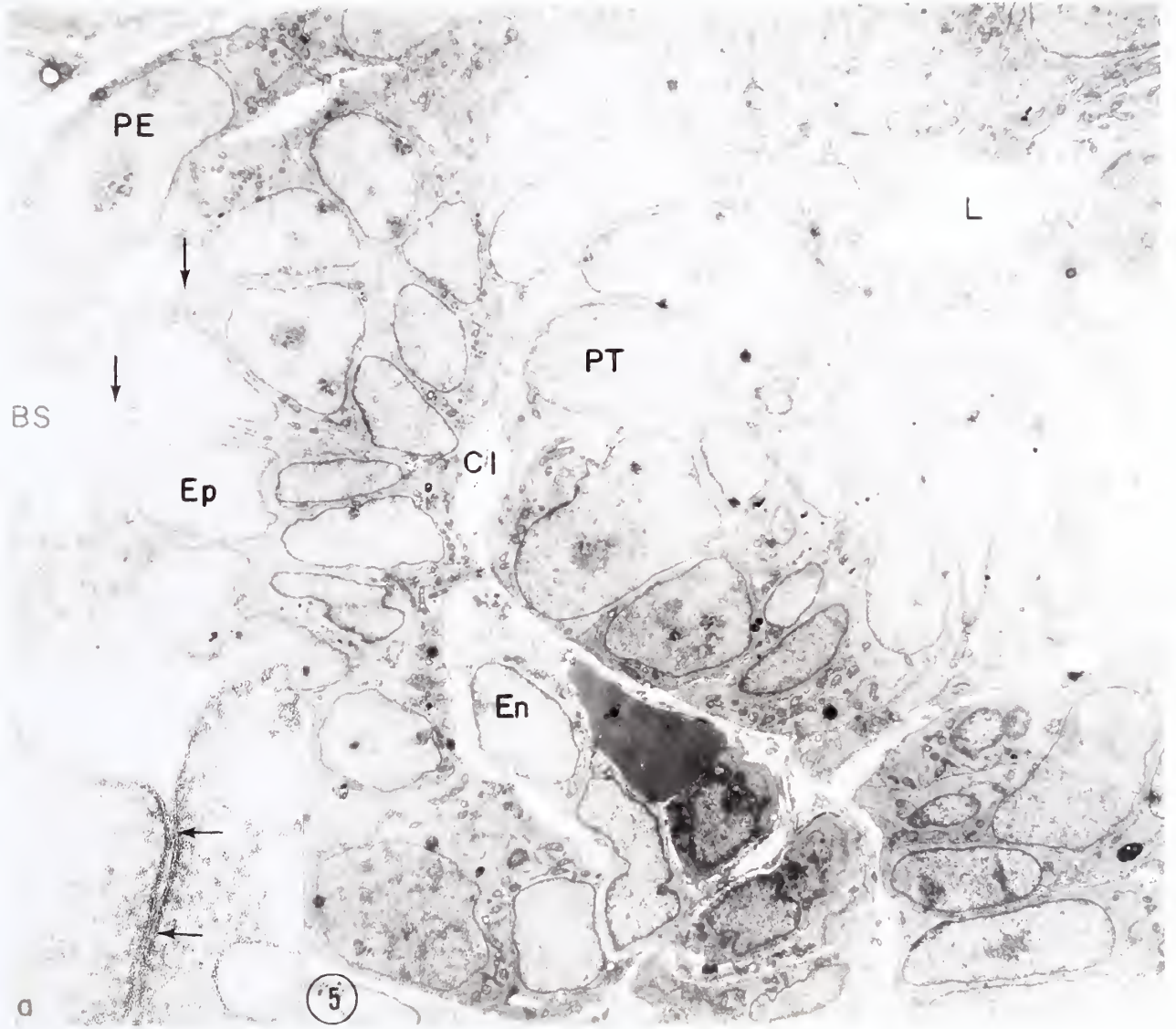
Vesicle Stage. The vesicle consists of a cluster of columnar epithelial cells which form the lining of the vesicle lumen. The cells are sealed at their apices by typical occluding junctions (30, 34, 98). The portion of the vesicle which will form glomerular epithelium cannot be distinguished from the portion that will form tubule epithelium at this stage and for this reason, the vesicle stage was not studied in great detail.

S-Shaped Stage. Early in this stage (Figs. 2 and 5) the visceral epithelium appears to be two or more cells deep (based on numbers of nuclei) (103). Those cells which face the presumptive Bowman's space are joined by junctions at their apices (Fig. 5). When examined at high magnification in appropriately fixed and stained preparations it can be seen (Fig. 5a) that these junctions have the properties of occluding or "tight" junctions, rather than adhering junctions as suggested by Aoki (3). In grazing section, these junctions run for considerable distances between cells, and thus they are presumed to consist of occluding zonulae or fasciae (belts or bands) (30) rather than maculae (focal spots) at this stage. This interpretation is in agreement with the freeze-fracture findings



FIG. 5. Electron micrograph of an S-shaped body (early), comparable to the light micrograph shown in Fig. 2. The parietal epithelium (PE) is thick and Bowman's space (BS) has started to form. The visceral epithelium (Ep) appears to be several cells thick, but many cells extend from Bowman's space to the basement membrane. Mesenchymal tissue with endothelial cells (En) has pushed into the cleft (Cl). The glomerulus forms to one side of this cleft and the proximal tubule (PT) forms to the other. Note the junctions at the apices of the visceral epithelial cells (arrows) and the proximal tubule lumen (L). Fig. 5, X3000.

Inset a. An occluding junction is shown at the apex of the visceral epithelium (Ep) at high magnification. Two areas of fusion of the adjoining cell membranes are present (arrows). Tannic acid staining. Fig. 5a, X115,000.



of Humbert, et. al. (40). Initially, the basement membrane at the base of the epithelial cell layer is minimally developed, and the endothelial cell cytoplasm is continuous -- i.e., it lacks fenestrae.

Late in this stage the visceral epithelium appears as a simple columnar layer with nuclei preferentially located toward Bowman's space (Fig. 7). It appears that as this stage progresses and the capillary loop stage begins, the epithelium undergoes a reorganization from a haphazard, pseudo-stratified arrangement (Figs. 5 and 6) to a simple polarized cell layer (Fig. 7). As the cells become polarized, occluding junctions are seen at different levels partway down the lateral cell membranes between the cells (Fig. 7). This is not a random event; occluding junctions are seen at levels progressively closer to the basement membrane between each succeeding pair of epithelial cells as one moves along the epithelium away from the transition point where parietal epithelium becomes visceral epithelium. Moving from cell to cell in sequence in the direction away from the visceral-parietal cell reflection, the junctions are found progressively near the cell apex, partway down the lateral cell membranes, and near the base of the cells or between early developing foot processes (Fig. 7). This suggests that as the cells differentiate the junctions migrate along the lateral cell surface from apex to base. As the junctions move down, intracellular spaces which are in continuity with Bowman's space become visible between the visceral epithelial cells (Figs. 3 and 7).

By the end of this stage a more distinct basement membrane layer is present between the visceral epithelium and the endothelium. The basement membrane of the S-shaped body is 70-80 nm or less in depth and consists of a loose layer of fibrils embedded in an amorphous matrix, closely applied to the epithelial cell base. Little or no such material is seen adjacent to the mesenchymal/endothelial cells in the cleft. The endothelium contains

FIG. 6. S-shaped body stage. The visceral epithelium (Ep) is not yet polarized uniformly. Some nuclei are located near Bowman's space (BS) and others near the developing basement membrane (B) which is visible between the epithelium and endothelium (En). Occluding junctions are extensive and are seen at the apices between epithelial cells (arrows). PE, Parietal epithelium. Uranyl acetate staining. Fig. 6, X7000.

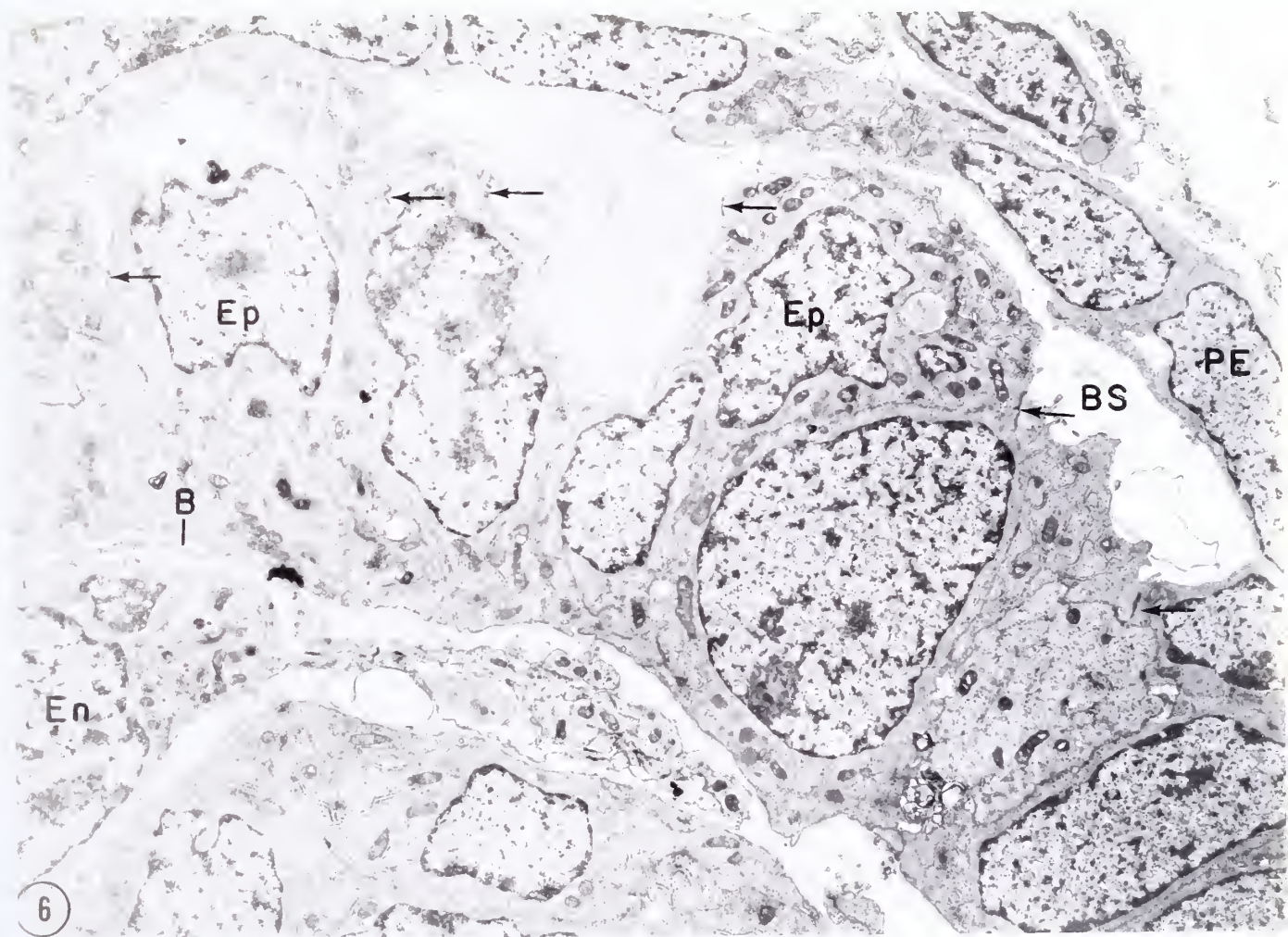
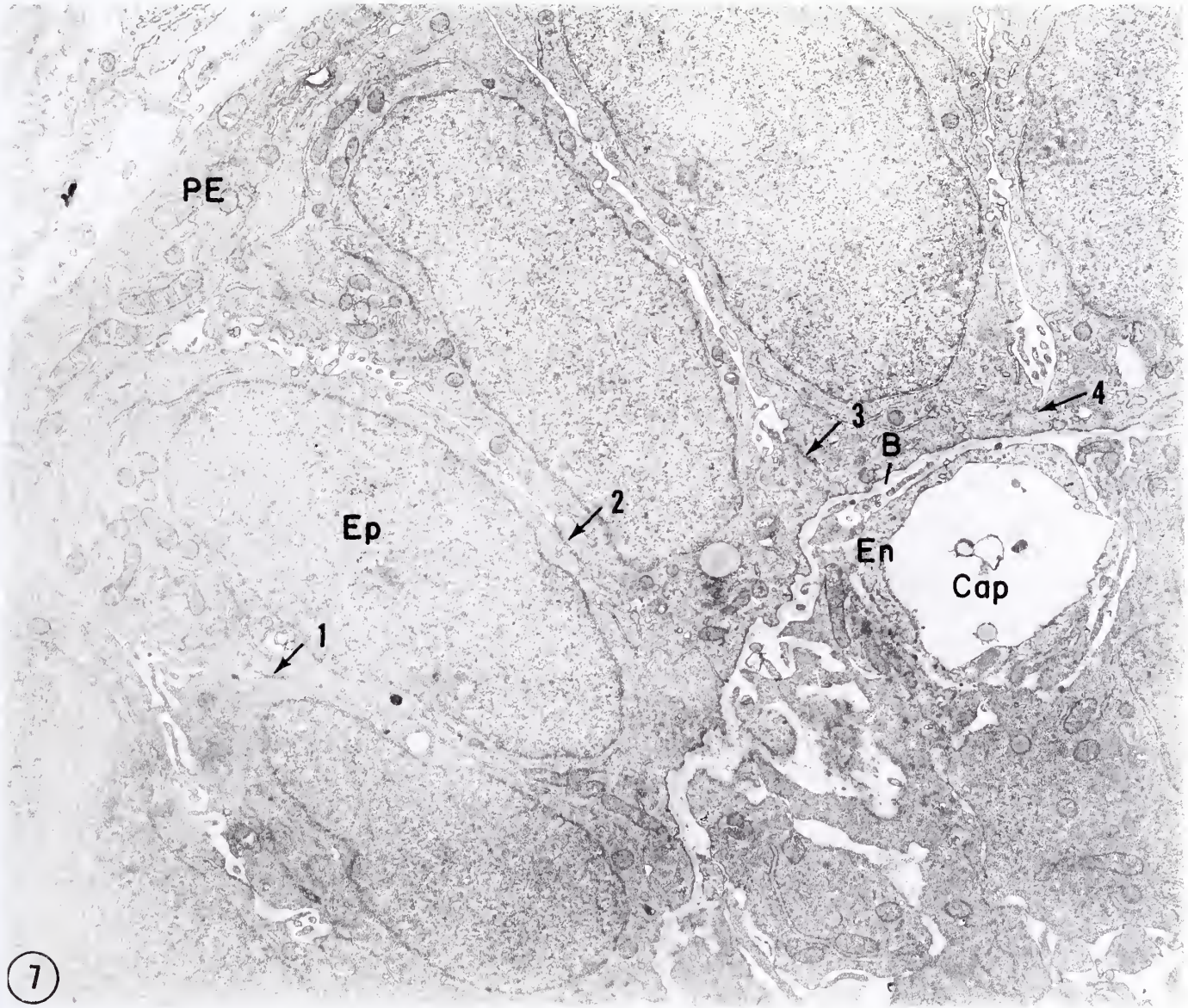


FIG. 7. Late S-shaped body stage. At a stage of development somewhat later than that seen in Fig. 6, the visceral epithelium (Ep) becomes simple columnar. Junctions are seen at progressively lower levels along the lateral cell membrane (arrows 1 to 4), suggesting that migration of the junctions occurs from apex to base. The intercellular spaces above the junctions are open and continuous with Bowman's space. Cap, capillary lumen; PE, parietal epithelium; B, basement membrane; En, endothelium. Tannic acid staining. Fig. 7, X9000.



7

a few fenestrae by the end of this stage, most of which appear to be closed by diaphragms (Fig. 31). These diaphragms are ~ 7 nm wide and contain a central dense particle. Diaphragms of similar appearance are seen closing vesicles which open from the developing endothelium into the GBM (Fig. 31a).

Developing Capillary Loop Stage. This stage is recognized by the presence of several capillary loops at various stages of maturation and the presence of conspicuous intercellular spaces along the lateral margins between the visceral epithelial cells, due to the aforementioned movement of occluding junctions to the cell base (Fig. 8). During this stage, interdigitation of the epithelium begins. Initially, there are only a few interdigitations with broad processes, but gradually the interdigitation progresses so that the epithelial processes become more numerous and less broad. Initially, the cell membranes between adjoining cells are closely apposed along the interdigitations, and occluding junctions are frequently seen between them (Figs. 9 and 12). As the interdigitations become more elaborate a gradually increasing number of the intercellular spaces are open (Figs. 9 to 11) suggesting, in accord with freeze-fracture findings (40), that the occluding junctions are discontinuous -- i.e., they are maculae or fasciae rather than zonulae at this stage. In general, the greater the frequency of interdigitations, the smaller is the percentage of intercellular spaces that are closed by occluding junctions.

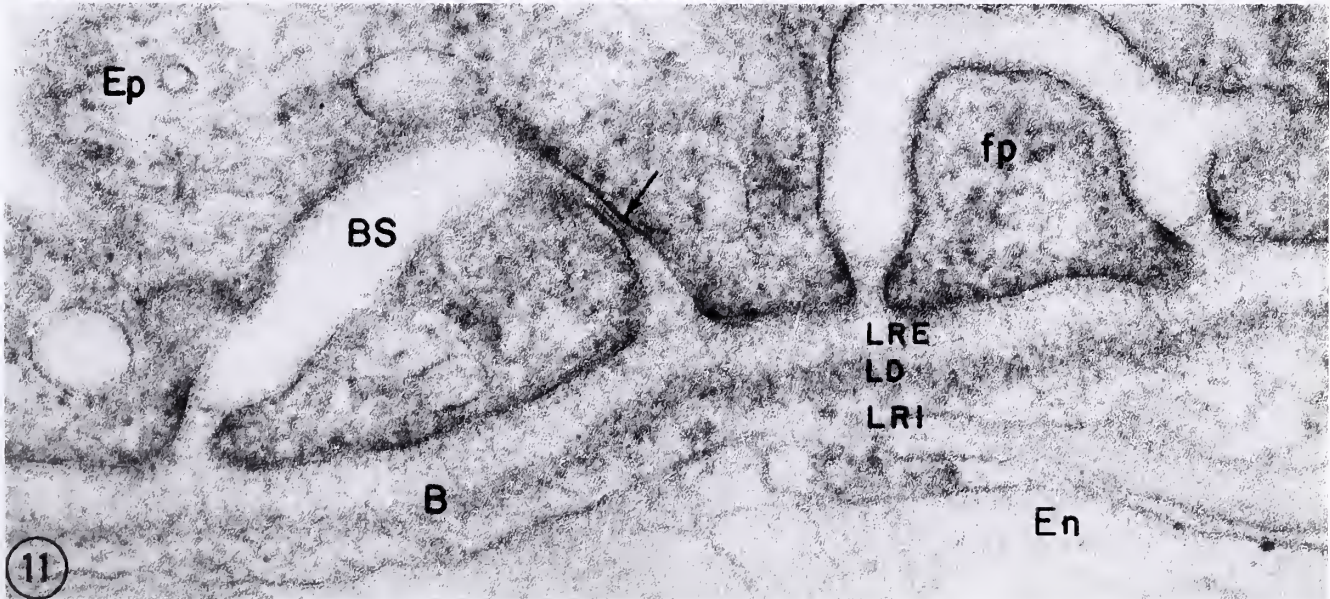
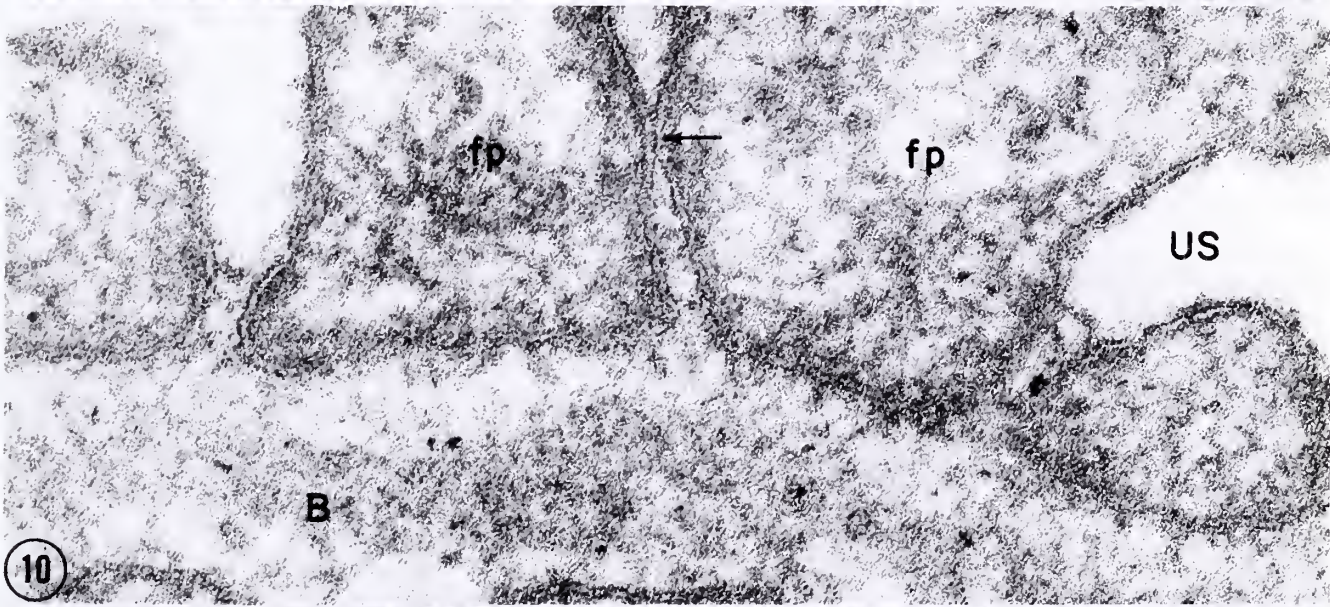
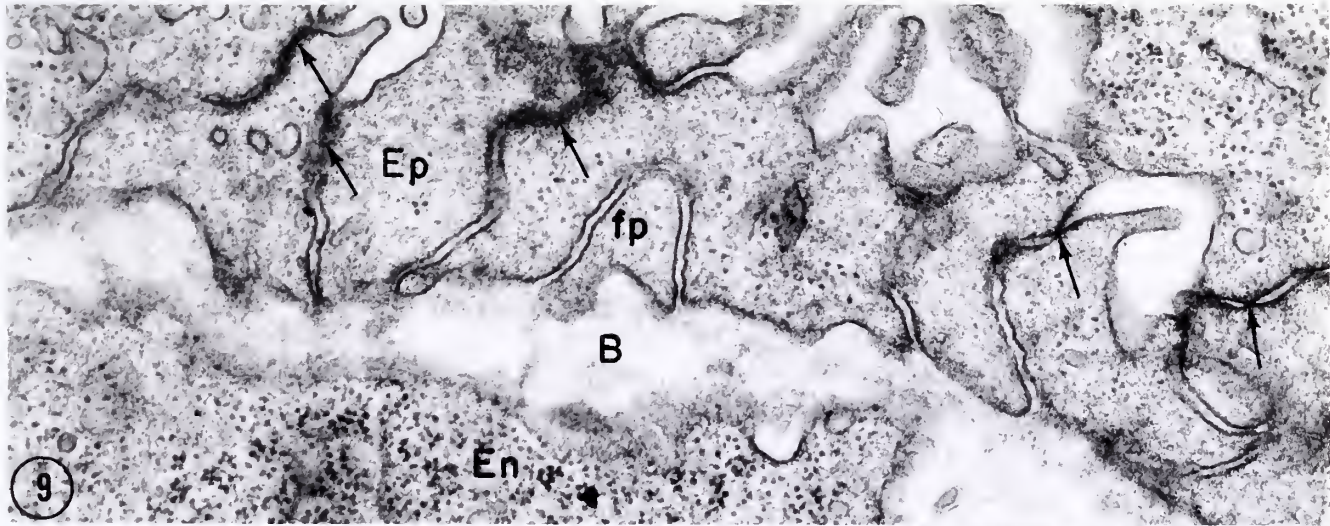
The junctions between the visceral epithelial cells located along the visceral-parietal reflection seem to represent a special case (Fig. 8). These junctions are located much higher on the lateral cell membrane (closer to the cell apex), and they are more extensive (zonulae or fasciae) than the junctions in the main mass of the visceral epithelium.

FIG. 8. Developing capillary loop stage. The parietal epithelium (PE) is flattened and the visceral epithelium (Ep) is cuboidal. Junctions are located between the visceral epithelial cells, primarily at their base (short arrows). The exception is at the reflection of the epithelium where parietal becomes visceral epithelium. The visceral epithelial cells are joined by junctions located partway down the lateral cell membranes (long arrows). The endothelium (En) has begun to flatten and several capillary loops are seen. BS, Bowman's space. Fig. 8, X3200.

Inset a. High magnification of an occluding junction located partway down the lateral margins of the visceral epithelium, showing focal areas of fusion between adjoining cell membranes (arrows). Inset a, X114,000.



FIGS. 9 to 11. Development of foot processes, capillary loop stage. Broad epithelial processes, the early foot processes (fp), are joined by occluding junctions (arrows). As the glomerulus matures, the epithelium (Ep) matures from a configuration in which practically all of the slits are closed by occluding junctions (Fig. 9, arrows) to one in which the slits gradually open (Fig. 10), leaving some slits open and others closed by junctions (Figs. 10 and 11, arrows), and finally, to one in which most of the slits are open and only a few occluding junctions remain between relatively mature-looking foot processes (Fig. 11). As the foot processes develop, the basement membrane also matures into a structure (B) containing lamina rara interna (LRI), lamina densa (LD), and lamina rara externa (LRE). Here, the lamina densa is narrower and the laminae rarae are wider than in the mature glomerulus. The specimen in Fig. 9 was stained en bloc with uranyl acetate, and those in Figs. 10 and 11 were stained en bloc with tannic acid. En, endothelium; US, urinary space; BS, Bowman's space. Fig. 9, X32,000; Fig. 10, X150,000; Fig. 11, X130,000.



In addition to occluding junctions, ladder-like structures comparable to those described in the filtration slits in aminonucleoside-nephrotic animals (19, 85) are commonly found between epithelial cells at this stage (Fig. 13). Their structure is best seen in specimens treated with tannic acid en bloc. Like those in the nephrotic rat, the ladders are typically present in the widened intercellular spaces above the level of the occluding junctions; and they consist of a series of dense ridges (90 nm to 7 nm) spanning the intercellular spaces. As will be discussed later, they also resemble septate junctions closely (see p. 58).

The reduction in the number of foot processes and slits and the presence of occluding junctions as well as ladders are reminiscent of the epithelial changes seen in aminonucleoside nephrosis (19, 29) (Fig. 12).

As this stage progresses, occluding junctions and ladders become increasingly less frequent, slit membranes appear in the slits and increasing numbers of slits take on a mature configuration (Figs. 10 and 11) in which the usual ~ 25 nm intercellular gap is bridged by a typical ~ 7 nm slit diaphragm.

The basement membrane and endothelial fenestrae also differentiate at the same time as the foot processes. Initially (before the slits are open) the basement membrane is a loose layer (~ 100 nm in depth) with indistinct margins (Figs. 9 and 13). However, as foot processes develop, the basement membrane increases in thickness and develops its typical, mature structure with a central dense layer, the lamina densa, and lamina rarae interna and externa, adjoining the endothelium and epithelium, respectively (Fig. 11). The endothelium initially shows few fenestrae and

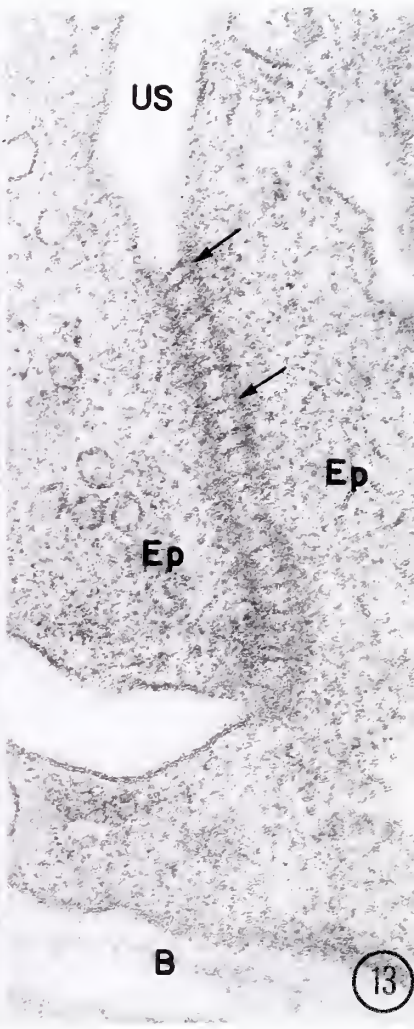
FIGS. 12 and 13. Developing capillary loop stage.

FIG. 12. The appearance of the glomerulus at this stage is reminiscent of its appearance in aminonucleoside nephrosis: broad epithelial processes (Ep) and occluding junctions (arrows) predominate, and few normal slits are present. In addition, the endothelial cytoplasm forms a nearly continuous layer (En) containing few fenestrae. Cap, capillary lumen. Fig. 12, X22,000.

FIG. 13. Ladder-like structure located in the slit between two epithelial cells (Ep) above the basement membrane (B). Such structures are quite common throughout the developing capillary loop stage. Note that the cross-bridges are often paired (arrows) and that the ladders are best visualized in grazing section. The lamina densa of the basement membrane (B) is thin at this stage. US, urinary space. Stained en bloc with tannic acid. Fig. 13, X67,000.



12



13

forms a thick layer nearly covering the luminal aspects of the basement membrane (Fig. 12). As development proceeds, the layer becomes progressively more attenuated and fenestrae are more frequent in number and less frequently closed by diaphragms.

Maturing Glomerulus Stage. This stage merges imperceptibly with the previous stage, the distinction between the two being quite arbitrary. Glomeruli are considered to be "maturing" when they contain multiple patent capillary loops, but the visceral epithelium has not yet achieved its normal, more flattened configuration, and differentiation of the foot processes and slits is largely but not entirely complete. During this stage, occluding junctions and ladder-like structures become less and less frequent and finally disappear altogether, and normal slit architecture prevails. The endothelium and parietal epithelium take on their mature, flattened configuration.

COLLOIDAL IRON STAINING OF DEVELOPING GLOMERULI.

Light Microscopy. Hyaluronidase-resistant staining of developing glomeruli with colloidal iron was minimal or absent at the LM level prior to the capillary loop stage (Fig. 14). The first conspicuous staining was detected in glomeruli early in the capillary loop stage in which a blue staining rim was seen along the apical and lateral cell margins of visceral epithelial cells where they face Bowman's space (Fig. 15). The staining appeared only in glomeruli in which occluding junctions had begun to migrate toward the base of the cells since early staining was detected only in those cells in which Bowman's space was open between the cells. Later in the capillary loop stage, staining was heaviest at the base of the cells (Fig. 16). Thus, the staining for epithelial polyanion is first detectable at the LM level along the apical and

FIGS. 14 to 16. Colloidal iron staining of developing glomeruli, paraffin sections, treated with hyaluronidase before staining for light microscopy.

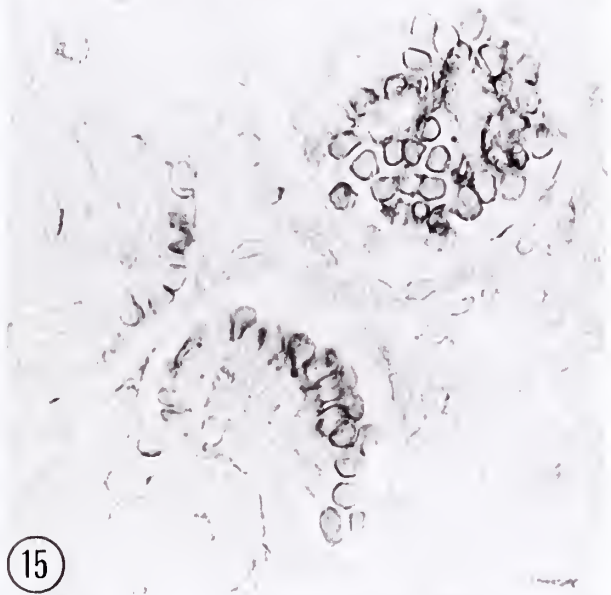
FIG. 14. S-shaped body stage. Note complete lack of colloidal iron staining at this stage. Fig. 14, X1300.

FIG. 15. Cluster of three glomeruli, all in the developing capillary loop stage. In the least mature glomeruli (left and below), colloidal iron stainable material is seen along the apical and lateral surfaces of a row of epithelial cells facing Bowman's space (arrow). In one glomerulus (upper right), the epithelium is cut mostly in grazing section and colloidal iron staining is seen all around the cell periphery. Fig. 15, X1300.

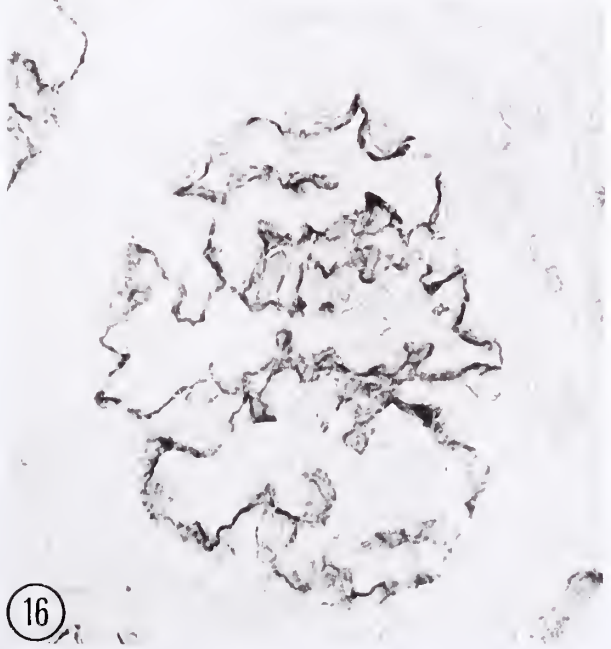
FIG. 16. Maturing glomerulus. Colloidal iron staining is seen mostly at the base of the epithelial cells where they face the basement membrane, and the lateral cell surfaces show relatively less staining. This is most evident on those cells at the periphery of the glomerulus which face Bowman's space (arrows). Fig. 16, X1300.



14



15



16

lateral cell surfaces at a stage prior to the differentiation of the foot processes and slits, and it becomes progressively more concentrated at the cell base at a time when foot processes are differentiating.

Electron Microscopy. To better determine the distribution of colloidal iron staining in developing glomeruli, tissue chopper sections were stained for electron microscopy using colloidal iron. During the S-shaped body stage, only a very small amount of colloidal iron stainable material is present above the apical occluding junctions (Figs. 17 and 17a). Colloidal iron staining is not seen below the level of the occluding zonulae along the lateral cell membranes, nor is it seen on the cell membranes at the base of the cells. In contrast, the basement membrane is quite heavily stained at this stage (Fig. 17b) and the endothelial cell surface (Fig. 17b) is lightly stained as well.

Late in the S-shaped body stage, as the junctions migrate toward the developing basement membrane, large amounts of colloidal iron stainable material are present on the apical and lateral cell surfaces above the level of the occluding junctions (Fig. 18). The lateral cell membranes below the level of these junctions remain unstained as do the basal cell membranes adjoining the basement membrane. The basement membrane does not contain three layers at this point in development, but colloidal iron stainable material is present in the outer face of the developing basement membrane (Fig. 18a) which is destined to become the lamina rara externa. The colloidal iron stainable material on the cell surface has a lumpy or globular distribution with ~20 nm diameter clumps of colloidal iron positive material spaced 50 nm apart (Figs. 18 to 21). This pattern is best seen in grazing sections (Fig. 18 and arrow Fig. 20); it is not known whether this pattern represents a fixation

FIG. 17. Colloidal iron staining of early S-shaped body. Only small amounts of colloidal iron stainable material are seen at the visceral epithelial cell (Ep) apices, and none is seen along the lateral cell membranes below the apical occluding junctions (arrows) at this stage. Note that the parietal epithelium (PE) is closely applied to the visceral epithelium. Fig. 17, X18,000.

Inset a. Higher magnification of an occluding junction (arrow) at the apex of the visceral epithelium (Ep) corresponding to the arrow in Fig. 17. Small amounts of colloidal iron stainable material are seen at the cell apices above the junctions where Bowman's space (BS) has begun to form. Fig. 17a, X48,000.

Inset b. Higher magnification of the very early basement membrane (B) corresponding to arrowhead in Fig. 17, showing colloidal iron staining of the basement membrane and the endothelial cell (En) surface coat. Note absence of colloidal iron staining of the basal epithelial cell membrane. Fig. 17b, X90,000.

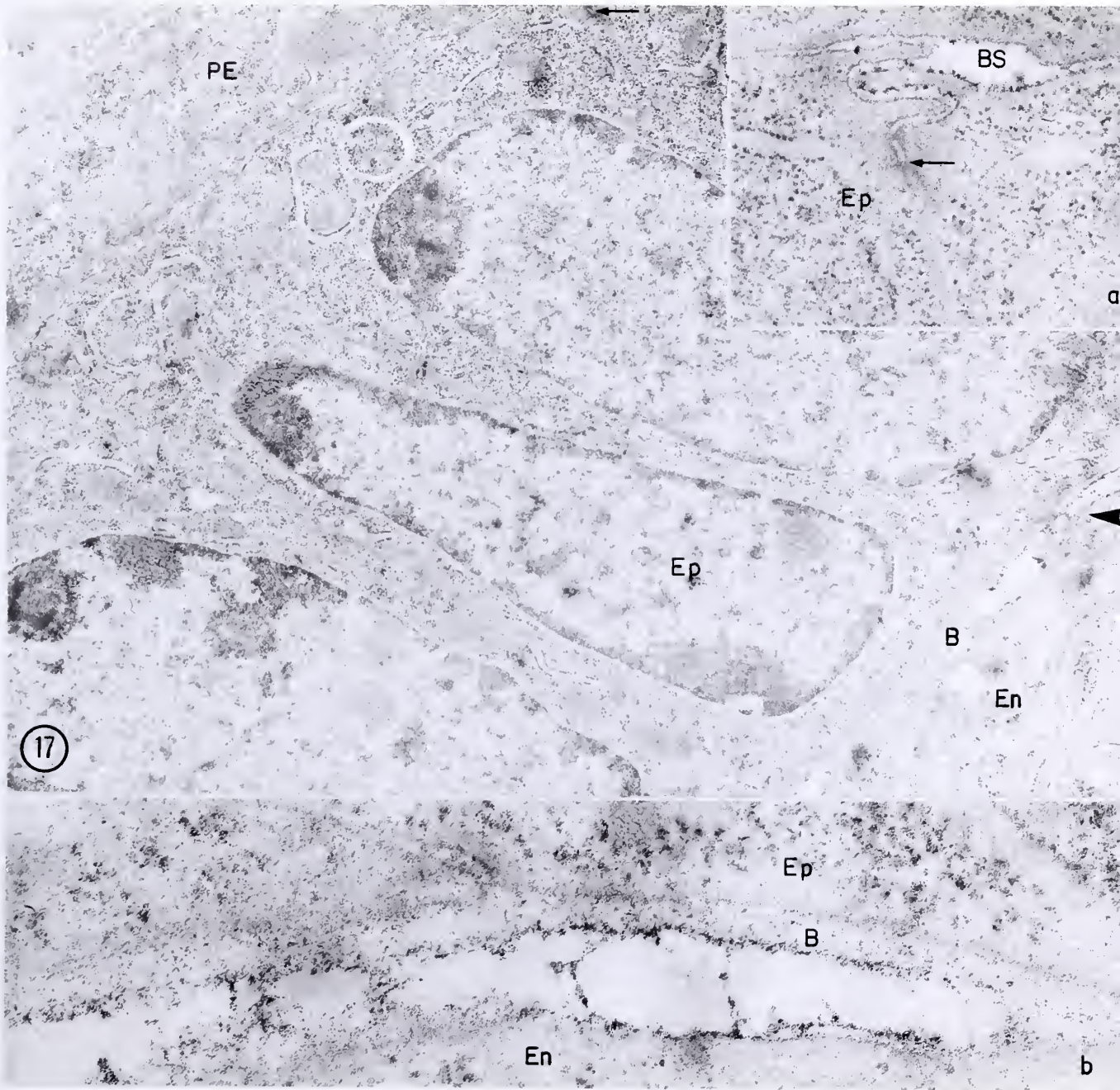
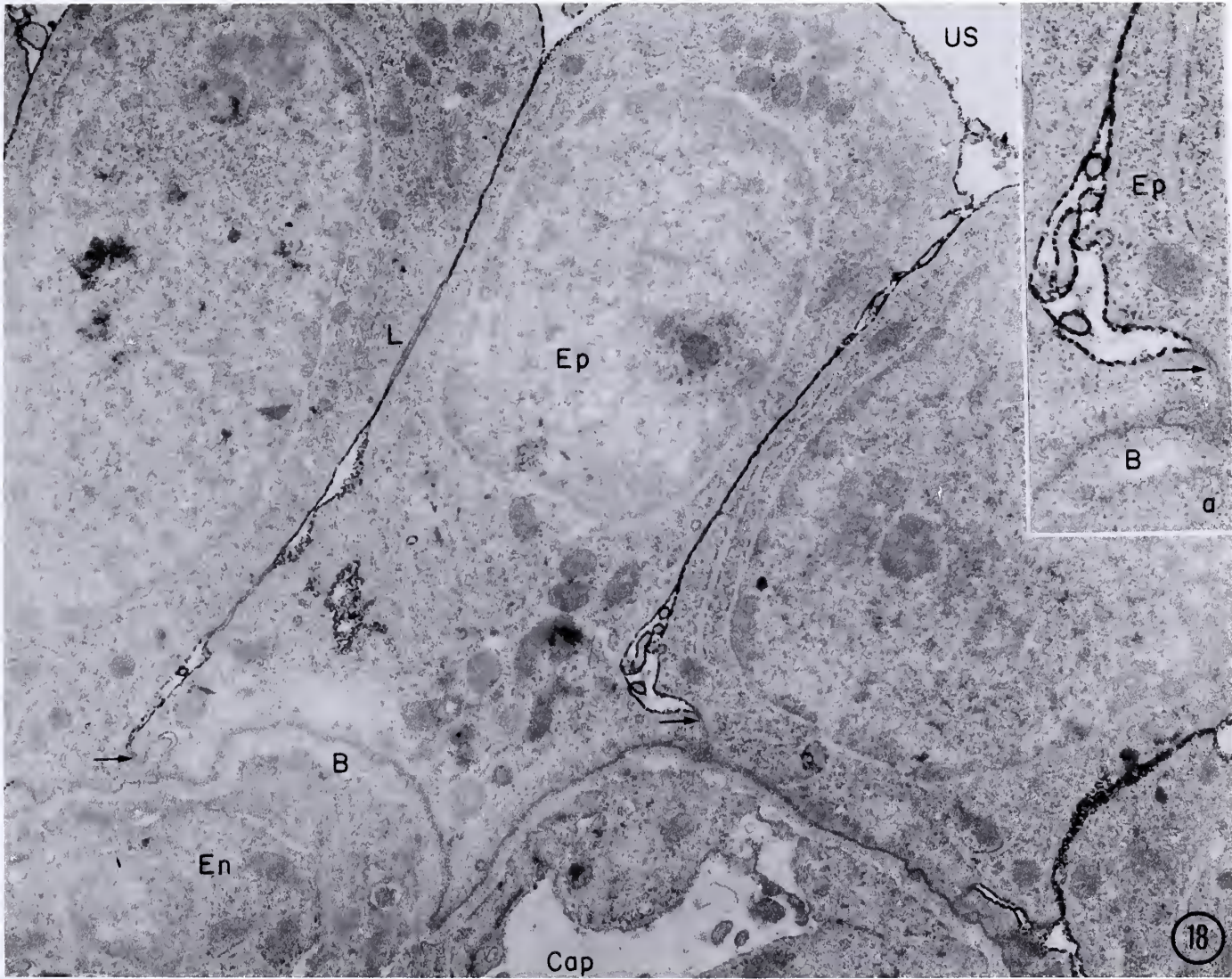


FIG. 18. Colloidal iron staining of late S-shaped body. Occluding junctions (arrows) have nearly reached the epithelial cell (Ep) bases and heavy colloidal iron staining is seen at all levels of the lateral cell membrane above the junctions, but is absent along the lateral cell membranes below the junctions and along the basal cell membrane. A structure (L) that may represent a poorly stained ladder (cf. Fig. 13) is seen in the intercellular space between two epithelial cells. Note the absence of colloidal iron staining inside this structure and the close apposition of the two epithelial cells in the region of this structure, suggesting a possible function in intercellular contact. Fig. 18, X18,000.

Inset a. View of a portion of Fig. 18 showing at higher magnification the wide intercellular space above a junction. Note the lumpy or globular distribution of colloidal iron stainable material on the cell surface and the colloidal iron staining of the basement membrane (B) which is more easily seen at higher magnification (cf. Figs. 19 and 21). En, endothelium; Cap, capillary lumen; US, Bowman's space. Fig. 18a, X36,000.



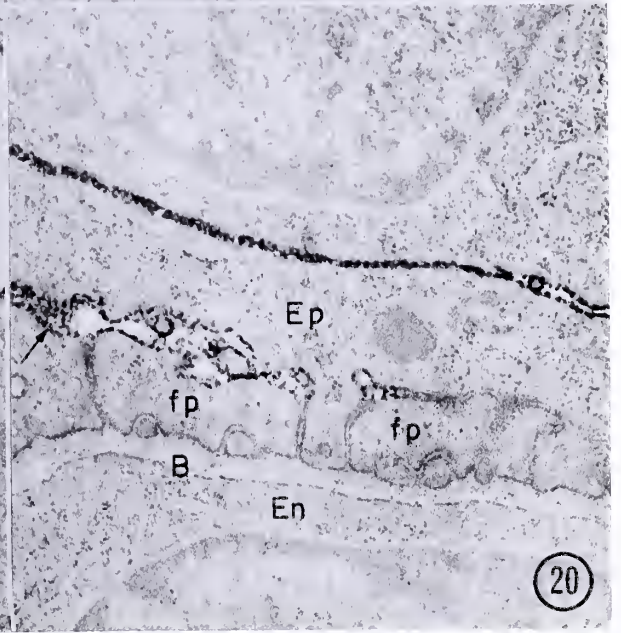
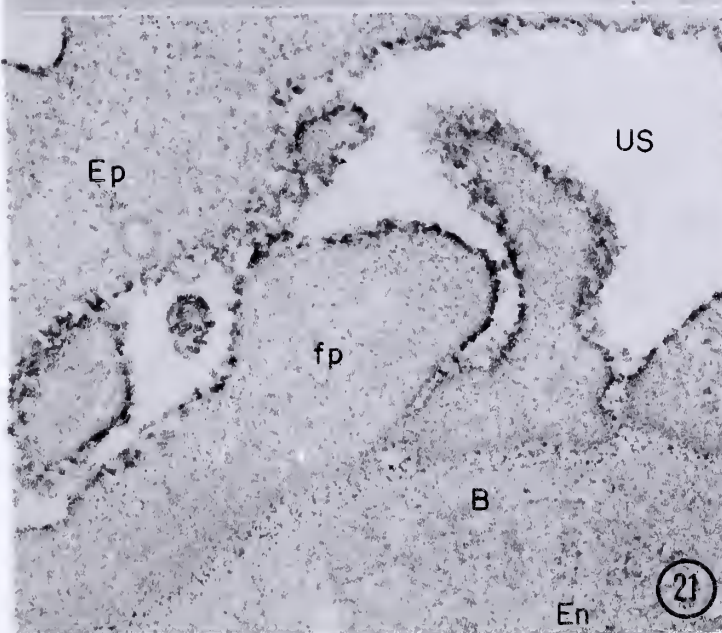
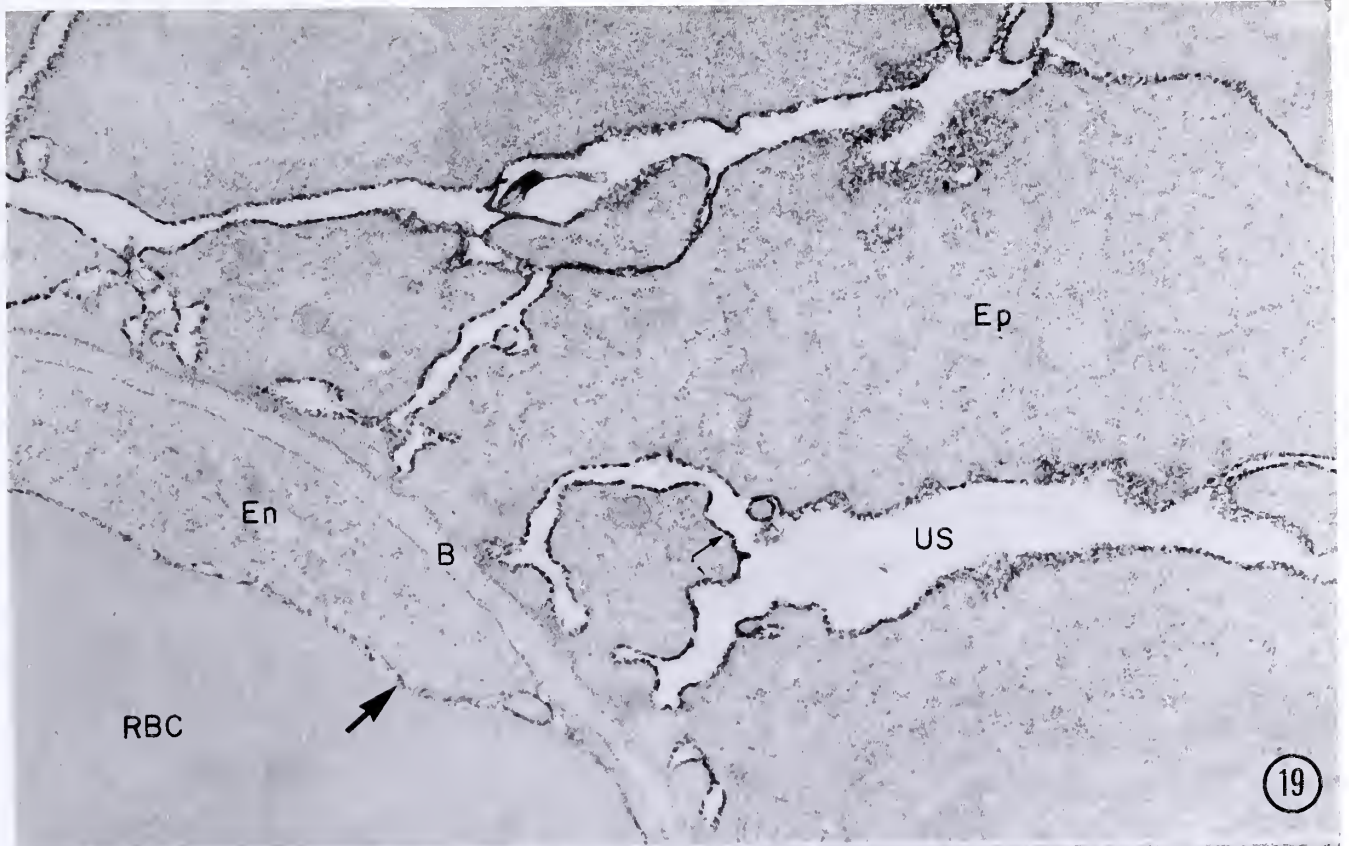
artifact or whether it represents staining of a cell surface component.

As the epithelium matures, colloidal iron stainable material is seen progressively nearer to the basement membrane along the lateral cell membranes (Figs. 18 and 19). The earliest foot processes (Fig. 20) are not stained by colloidal iron, despite the fact that the underlying lamina rara externa is moderately stained. More mature foot processes (Fig. 21) are heavily stained by colloidal iron, but the stain appears to be excluded from the slits, even those which do not have occluding junctions closing them and which have a mature configuration. As in the S-shaped body stage, the basal cell surface does not stain despite adjacent basement membrane staining.

The developing endothelium and parietal epithelium stain much less heavily with colloidal iron than does the visceral epithelium (Fig. 18). Although the basement membrane stains lightly throughout, most staining is concentrated in the region of the developing lamina rara externa. The fact that red blood cells in the capillary lumen stain heavily with colloidal iron (Fig. 19) suggests that this finding is not an artifact of poor penetration of the stain and that the outer (subepithelial) face of the basement membrane may contain more colloidal iron stainable material than the inner (subendothelial) face.

Thus, electron microscopy confirms the LM finding that the epithelial cell surface polyanion is minimal in very early stages of glomerular differentiation and that a rim of colloidal iron stainable material along the apical and lateral cell margins form as the junctions begin to migrate toward the base of the cells. The apparent concentration of colloidal iron stainable material at the cell base (as seen by LM) later in development can be explained by the large surface area of the developing foot processes

FIGS. 19 to 21. Colloidal iron staining of developing foot processes, capillary loop stage. The broad epithelial processes preceding foot process development are stained heavily with colloidal iron in a lumpy pattern (small arrow, Fig. 19) above the level of the occluding junctions. Very early foot processes (fp, Fig. 20) are unstained at this stage. Access of colloidal iron to their membranes should not be restricted at this stage since the junctions consist of incomplete maculae occludentes at this stage rather than zonulae. Both the basement membrane (B) and the red blood cell (RBC) and/or endothelial (En) cell membrane (Fig. 19, large arrow) stain with colloidal iron, showing adequate penetration of the stain. Slits and wide intercellular spaces are seen concomitant with colloidal iron staining of the maturing foot processes (fp, Fig. 21). Note staining of the basement membrane (B) and the absence of staining in the slits (Fig. 21) or on the basal foot process membrane. Also note the granular distribution of colloidal iron stainable material on the epithelial cell surface cut in grazing section (arrow, Fig. 20). Ep, epithelium; En, Endothelium; US, urinary space. Fig. 19, X30,000; Fig. 20, X30,000; Fig. 21, X69,000.



which stain heavily with colloidal iron, rather than by a "ripening" of the basement membrane as suggested by Klinger and Geyer (53). Indeed, basement membrane staining by colloidal iron does not appear to increase significantly between the S-shaped body stage and the maturing glomerulus stage (cf. Figs. 17b and 21).

Enzyme Digestion. Digestion with bovine testicular hyaluronidase for 8 hours at 37° C did not result in any change in distribution or intensity of colloidal iron staining (Figs. 22 and 23). Staining of both basement membrane (Figs. 22 and 23) and epithelial cell surface (Fig. 23) remained virtually unchanged by hyaluronidase treatment. Neuraminidase treatment (8 hours at 37° C), however, removed colloidal iron stainable material from the surface of the epithelial cells in both immature (Fig. 24) and maturing (Fig. 25) glomeruli. Basement membrane staining was not noticeably reduced (Figs. 24a, 25a, and 25b). Thus, as in adult glomeruli (43), colloidal iron staining appears to be due to the presence of sialic acid on the epithelial cell surface, presumably in the form of sialoglycoprotein.

TRACER STUDIES

Native Ferritin. In the early S-shaped body stage, ferritin is not seen in the cleft with the invading mesenchyme, and no conclusions concerning the ability of the basement membrane to exclude it can be made (Fig. 26). Near the end of the S-shaped body stage or at the beginning of the capillary loop stage, when foot processes are first seen (Fig. 27), ferritin is found in the developing capillary lumen and in the basement membrane. At this stage, ferritin is found more or less evenly distributed in the GBM, all the way around the capillary loop (i.e., ferritin is seen in the GBM at all points as one proceeds laterally around the capillary

FIGS. 22 and 23. Colloidal iron staining after hyaluronidase digestion. Digestion with hyaluronidase under the conditions used resulted in no change in the distribution of colloidal iron staining over the epithelial cell body (Ep, Figs. 22a and 23), in the basement membrane (B) or over maturing foot processes (fp). Colloidal iron stains the epithelial cell membrane above the level of the junctions (Fig. 22) but does not stain the surface of the earliest foot processes (fp, Fig. 22). As the foot processes mature, they first stain at the apical portion of their cell membrane (fp, Fig. 22a) above the level of the occluding junctions. As the junctions disappear and slits open, staining is seen over the apical and lateral surfaces of the foot processes (fp, Fig. 23), but not on the portion of the cell membrane nearest to the basement membrane and lying within the slit. This pattern of staining is identical to that seen in undigested specimens. En, endothelium; US, urinary space; Cap, capillary lumen. Fig. 22, X52,000; Fig. 22a, X52,000; Fig. 23, X69,000.

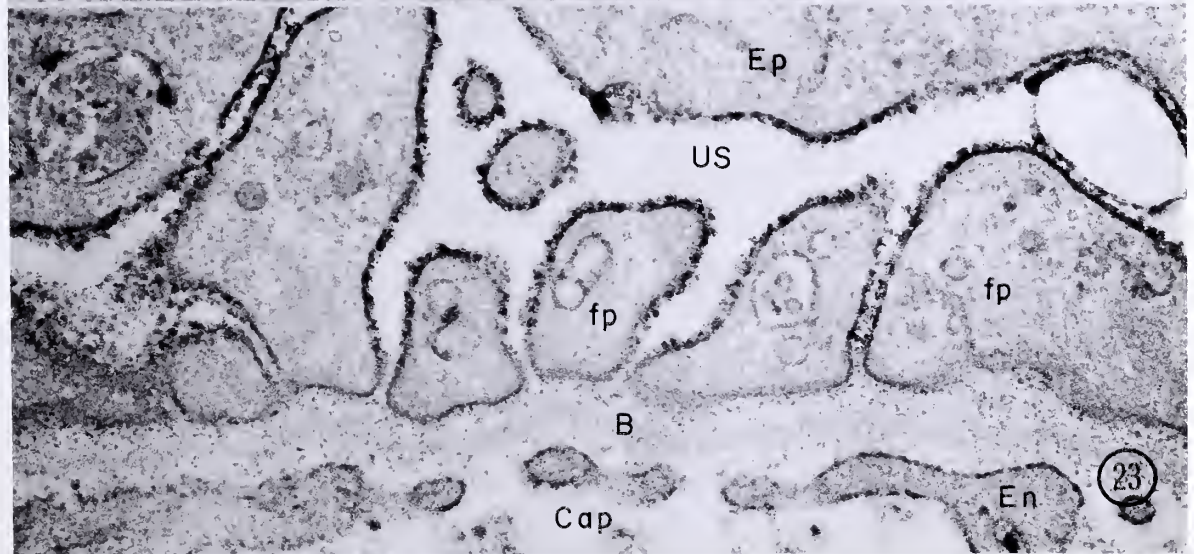
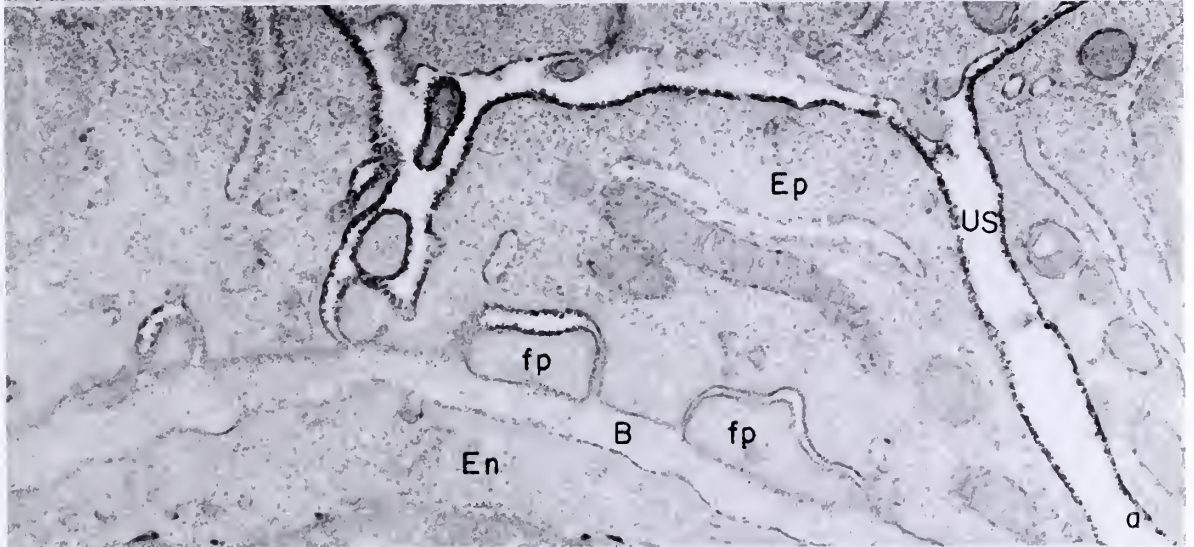
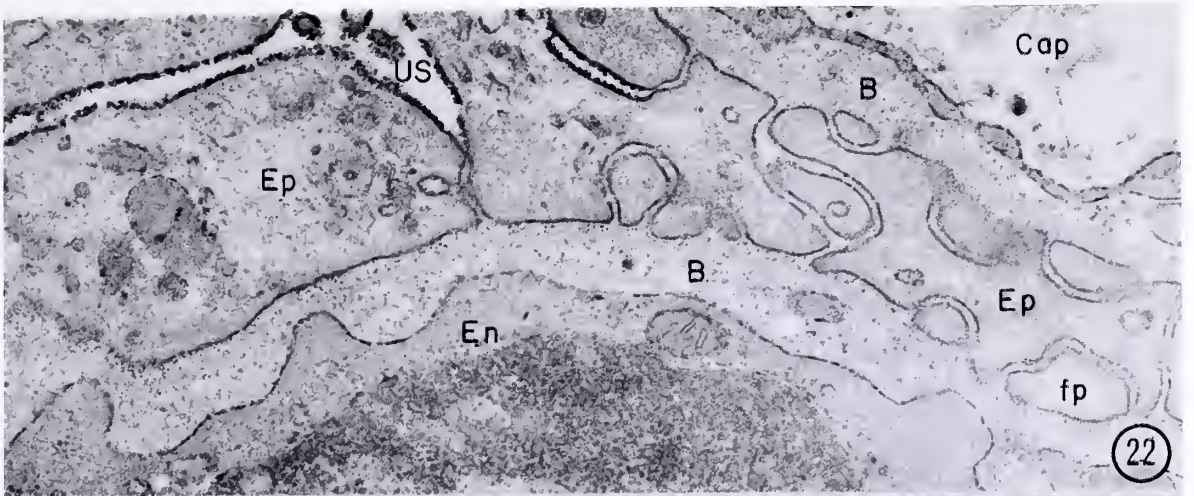


FIG. 24. Colloidal iron staining after neuraminidase digestion. Neuraminidase digestion under the conditions used removed colloidal iron stainable material (presumably sialoglycoprotein) from the epithelial cell surface (Ep) (cf. Fig. 18). Basement membrane (B) staining was unaffected (Fig. 24a) by neuraminidase treatment, indicating that the absence of cell surface staining was not due to poor penetration of the colloidal iron. Early foot processes (Fig. 24a) are also unstained after neuraminidase treatment. BS, Bowman's space; US, urinary space; PE, parietal epithelium; En endothelium; Cap, capillary lumen. Fig. 24, X15,000; Fig. 24a, X69,000.

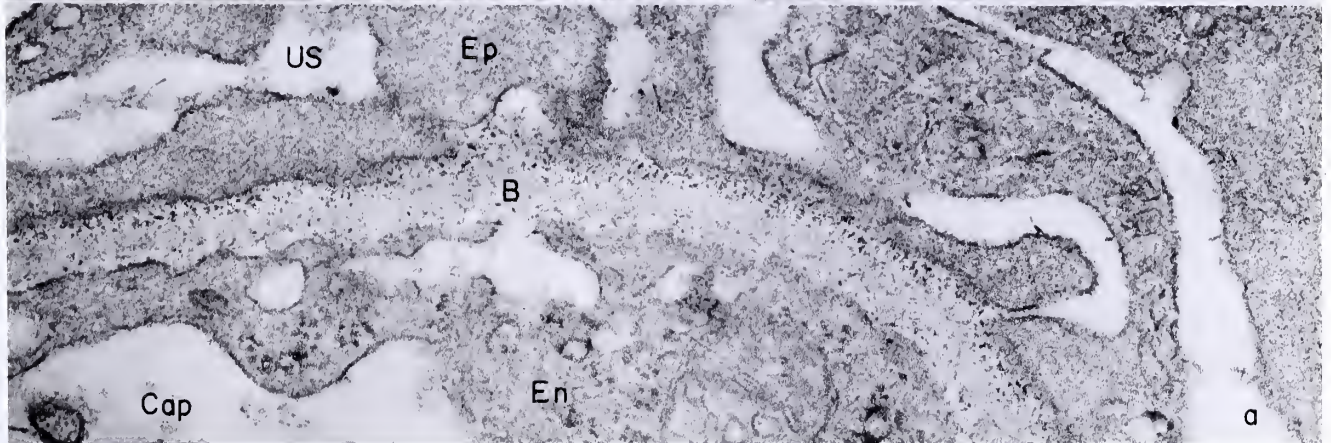
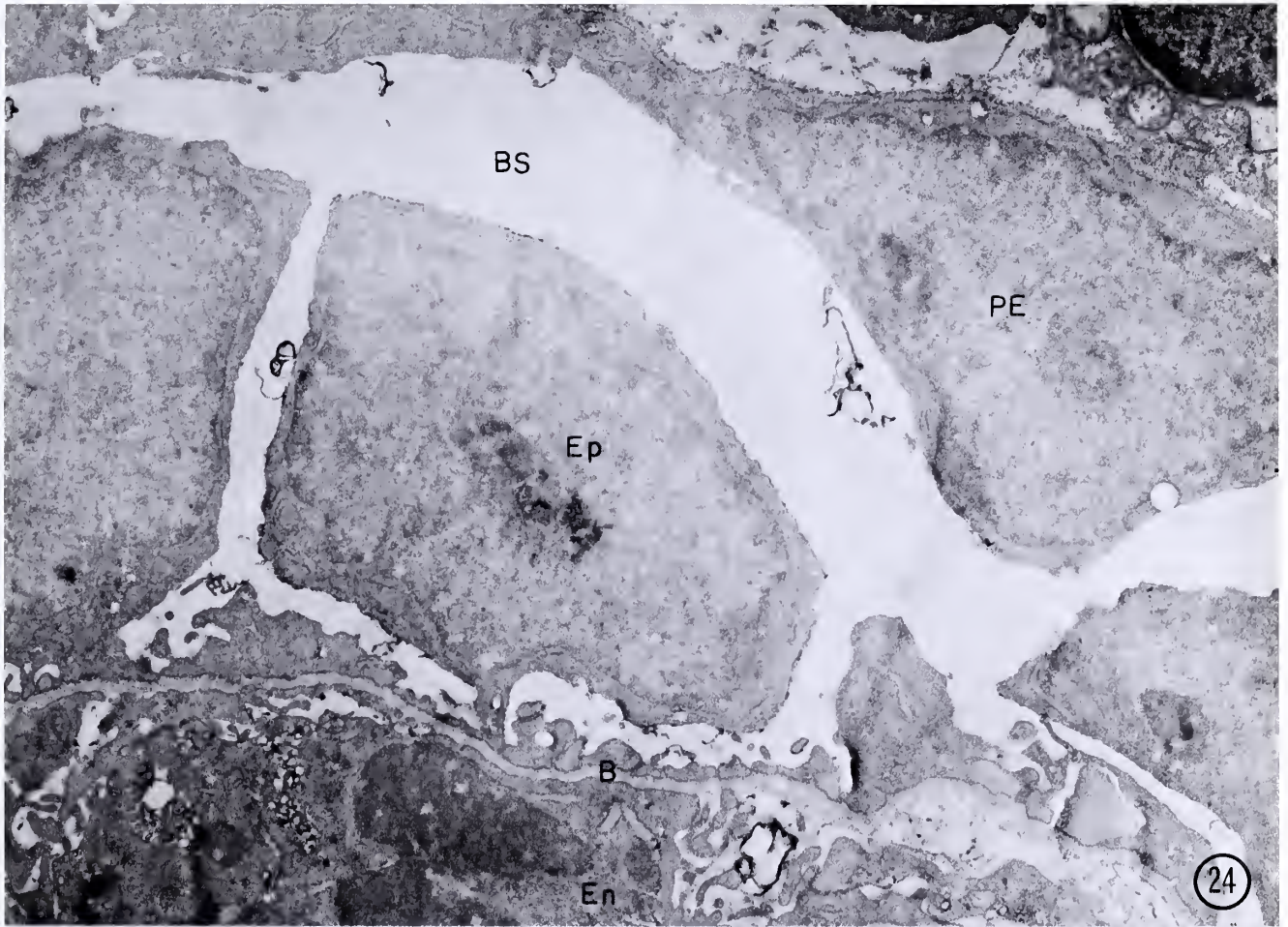
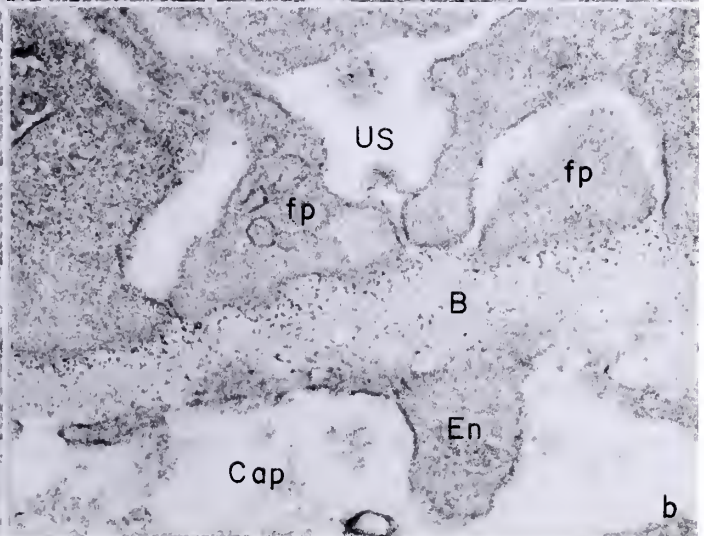
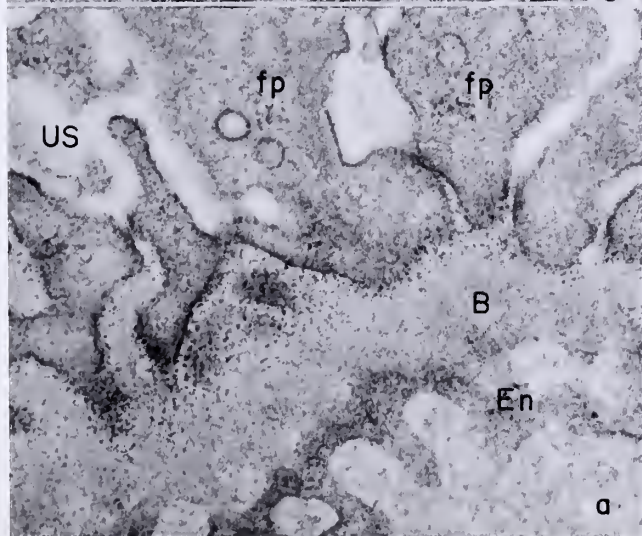
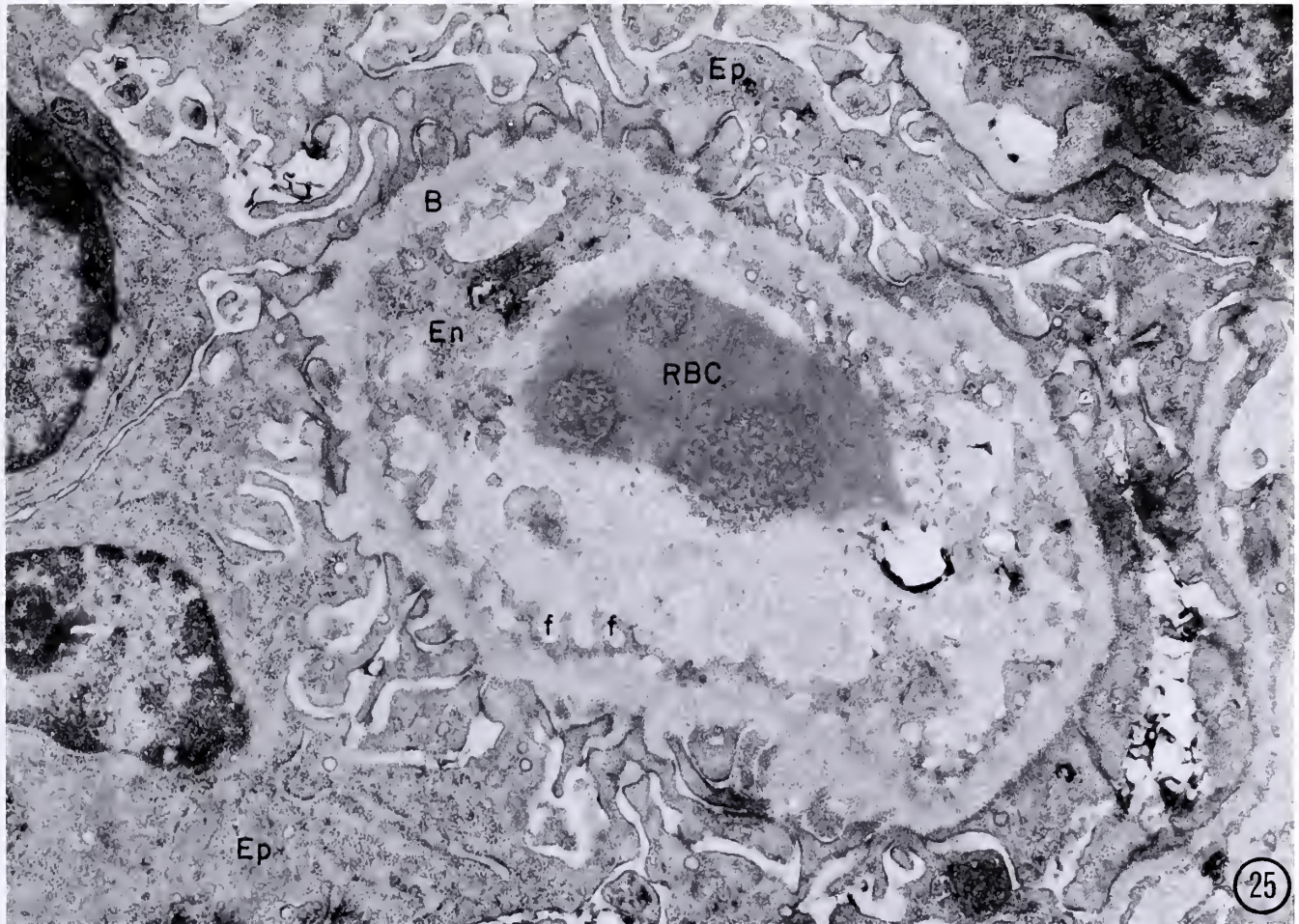


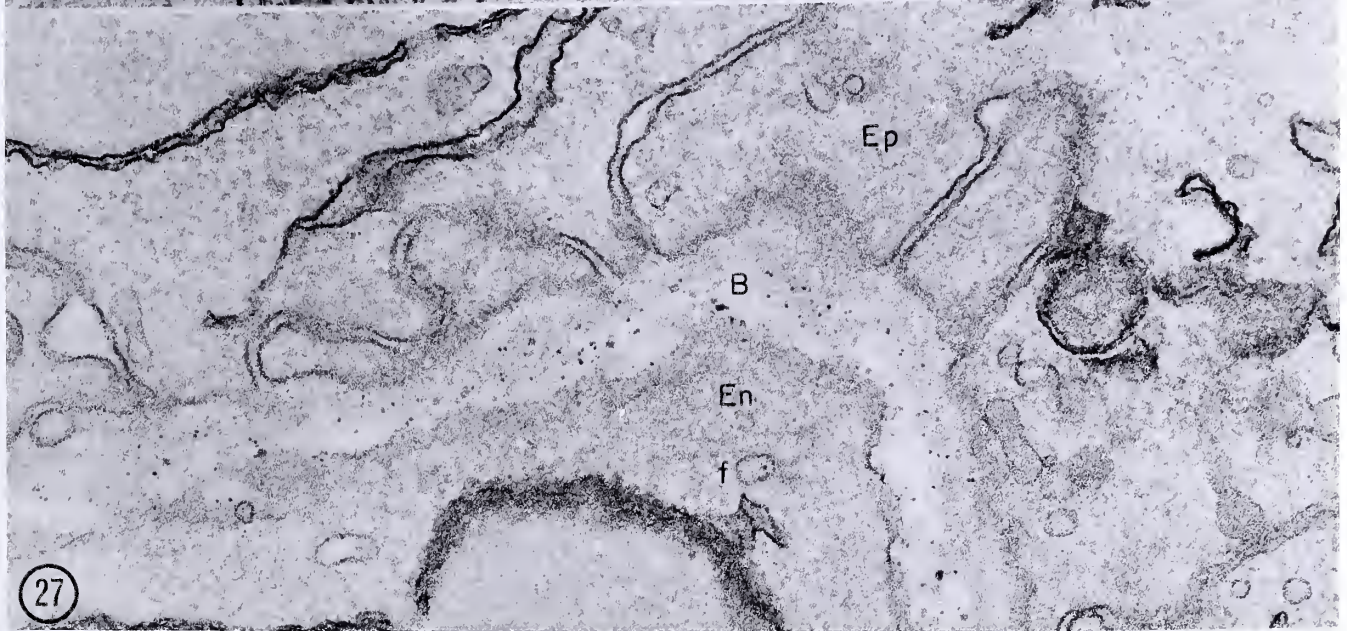
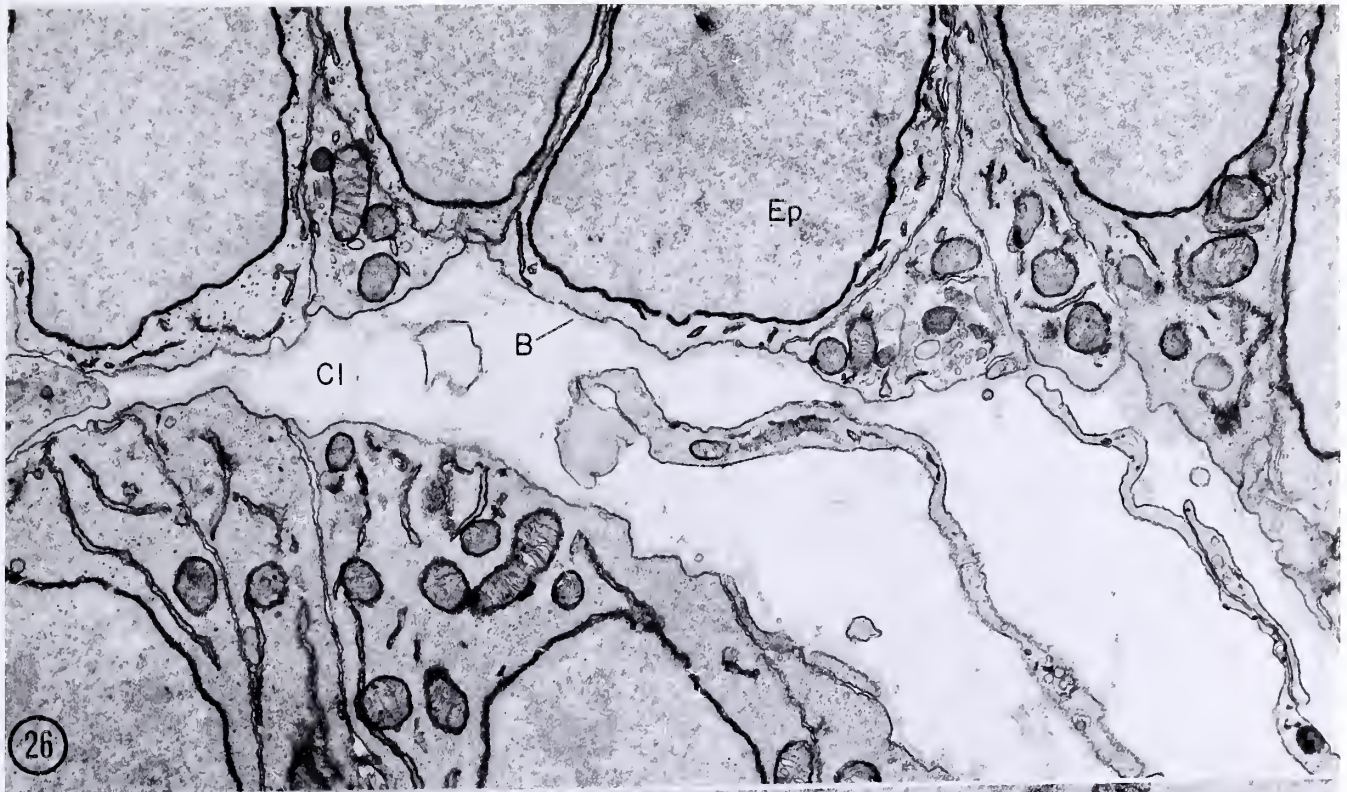
FIG. 25. Colloidal iron staining after neuraminidase digestion. A grazing section through a developing capillary loop (Fig. 25) shows the absence of colloidal iron staining on the red blood cell membrane (RBC), on the endothelial cell membrane (En) or on the maturing epithelial (Ep) foot processes. At high power (Figs. 25 a and b), the absence of staining of the foot processes (fp) can be seen to be almost complete (cf. Figs. 19-21). The basement membrane (B) stains heavily, showing adequate penetration of the colloidal iron. Whether the failure of neuraminidase treatment to prevent basement membrane staining is due to poor penetration of the enzyme or whether the colloidal iron stains a polyanion other than sialic acid in the basement membrane remains to be determined. Note endothelial fenestrae (f); Cap, capillary lumen; US, urinary space. Fig. 25, X24,000; Fig. 25a, X57,000; Fig. 25b, X69,000.



FIGS. 26 and 27. Native ferritin tracer studies.

FIG. 26. Ferritin is absent from the cleft (C1) of the early S-shaped body, indicating that circulation through the cleft has not yet been established. The basement membrane (B) is closely applied to the columnar epithelium (Ep). Note the heavy staining of the nuclear membrane, endoplasmic reticulum and mitochondrial membrane resulting from on grid staining with alkaline bismuth. Fig. 26, X24,000.

FIG. 27. Native ferritin in the basement membrane (B) at the early capillary loop stage. Tracer particles are scattered throughout the basement membrane, but are concentrated in the inner two thirds (ie. the sub-endothelial regions) of the basement membrane. The fact that much larger amounts of the tracer are found in the subendothelial portions of the basement membrane than in the subepithelial portions indicates the function of the basement membrane as a filter at this stage. The thickness of the endothelium and the small numbers of fenestrae seen at this stage may be of importance in regulating access to the incompletely developed basement membrane. Stained with alkaline bismuth on grid. Fig. 27, X75,000.



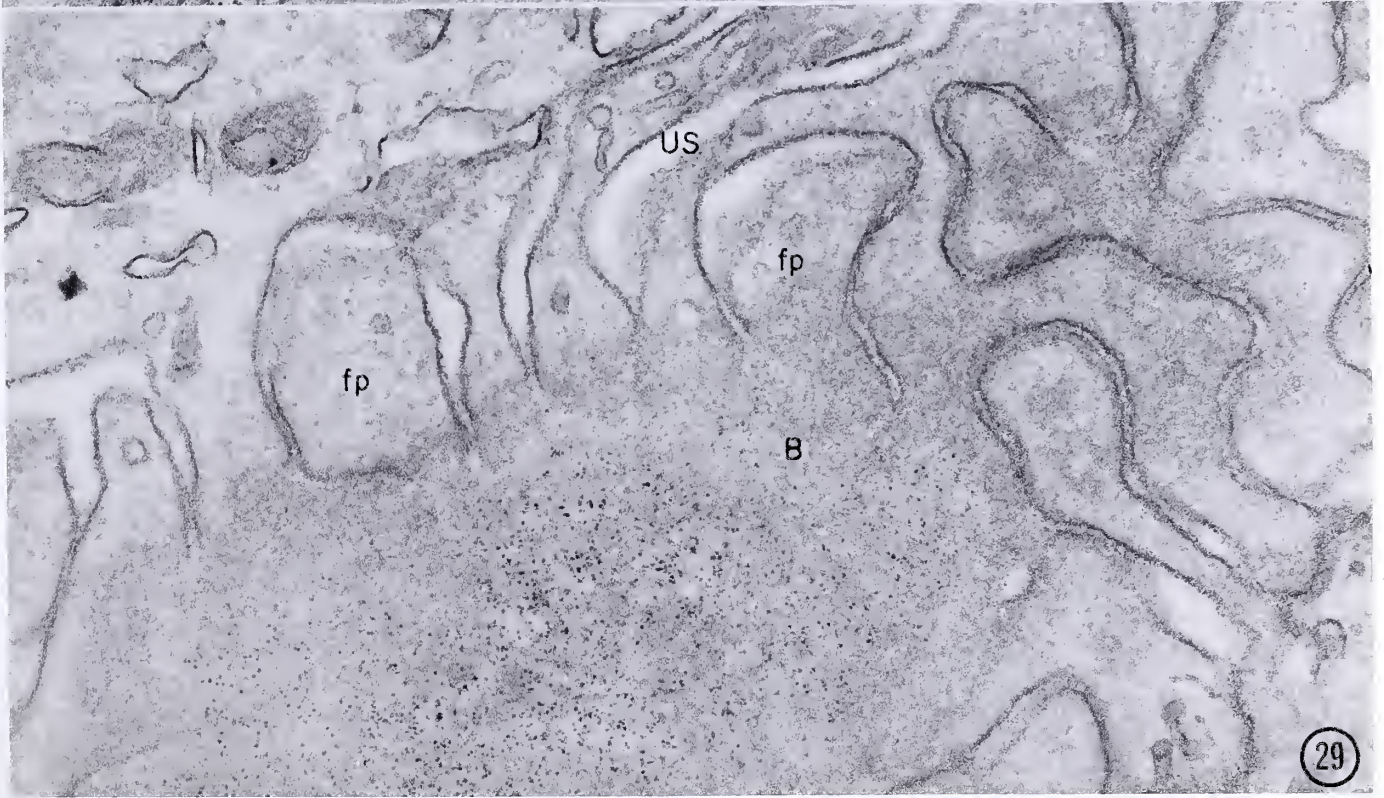
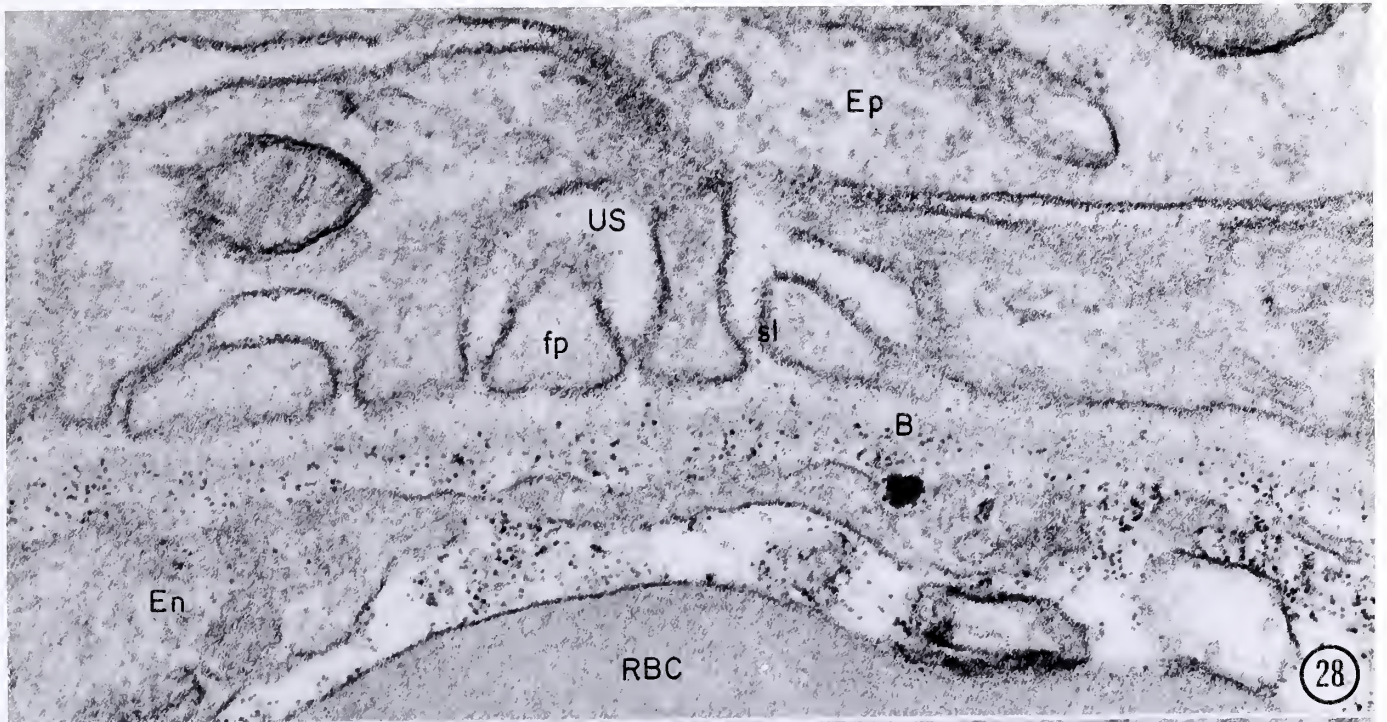
loop). In contrast, ferritin concentration is less in the deeper layers of the GBM (i.e., in subepithelial as opposed to subendothelial regions). This suggests that diffusion of ferritin is relatively unrestricted in the lateral plane of the basement membrane (parallel to the endothelium), since ferritin is seen in all regions of the basement membrane despite the paucity of fenestrae, while movement of ferritin through the basement membrane (from subendothelial to subepithelial regions) is retarded. Ferritin is largely confined to the subendothelial one third of the basement membrane in normal mature rats (i.e., to the lamina rara interna), with only small amounts of the tracer present in deeper layers, while in the fetal (and nephrotic) glomerulus, ferritin molecules are found scattered at various levels throughout the depth of the GBM and an occasional molecule is seen in the slits or in the urinary spaces; there is no detectable accumulation of tracer at the level of the epithelial slits. Tracer molecules are occasionally seen within epithelial membrane invaginations or small epithelial cytoplasmic vesicles as in the nephrotic rat 30 minutes after injection of ferritin. Because of difficulties in keeping the animal alive for more than 5 to 10 minutes following inferior vena caval administration of ferritin (due to blood loss and poor oxygenation), observations extended to later time points in which these invaginations and cytoplasmic vesicles might have been expected to have been more frequent were not possible.

At more mature stages (i.e., capillary loop and maturing glomerulus), the transport of ferritin across the GBM is more restricted than at earlier stages (Figs. 28 and 29). Few tracer molecules are seen in the lamina rara externa (Fig. 28), but ferritin is seen in the lamina densa in moderate amounts, and small amounts are seen in the slits and urinary spaces (Fig. 28).

FIGS. 28 and 29. Native ferritin tracer studies.

FIG. 28. Late capillary loop stage. Native ferritin is seen in all layers of the basement membrane (B) but is present in much smaller amounts in the lamina rara externa than in the lamina rara interna. In contrast to the mature GBM, the lamina densa contains large numbers of tracer molecules. Ferritin is also seen in the slits (Sl) and in the urinary spaces (US) in small amounts. The relatively deep penetration (in comparison to the mature glomerulus) of native ferritin into the GBM and its presence in the urinary spaces in small amounts suggest that the developing GBM is more permeable to large, anionically charged molecules than the mature. Note the presence of endothelial (En) fenestrae. Ep, epithelium; fp, foot process. Stained with alkaline bismuth on grid. Fig. 28, X90,000.

FIG. 29. Maturing glomerulus stage. Grazing section of a capillary loop, showing ferritin in the subendothelial regions of the basement membrane (B), but relatively rarely in the lamina rara externa. The capillary shown here approaches more closely the adult situation (with regards to ferritin permeability) than does that shown in Fig. 28. Foot processes are elaborately interdigitated, few occluding junctions are seen between the cells, and slits of nearly mature appearance are seen. US, urinary space. Stained with alkaline bismuth on grid. Fig. 29, X60,000.



These findings indicate that the immature GBM is more permeable to native ferritin than the mature GBM, but that it is nonetheless a filter for anionic particles the size of ferritin, even at the earliest stages of development in which ferritin gains access to the vascular glomerulus, since a gradient of ferritin concentration is seen as one moves across the GBM from subendothelium to subepithelium. As in the mature glomerulus, the epithelium may serve as a monitor for tracer particles that pass through the filter.

STAINING WITH CATIONIC PROBES

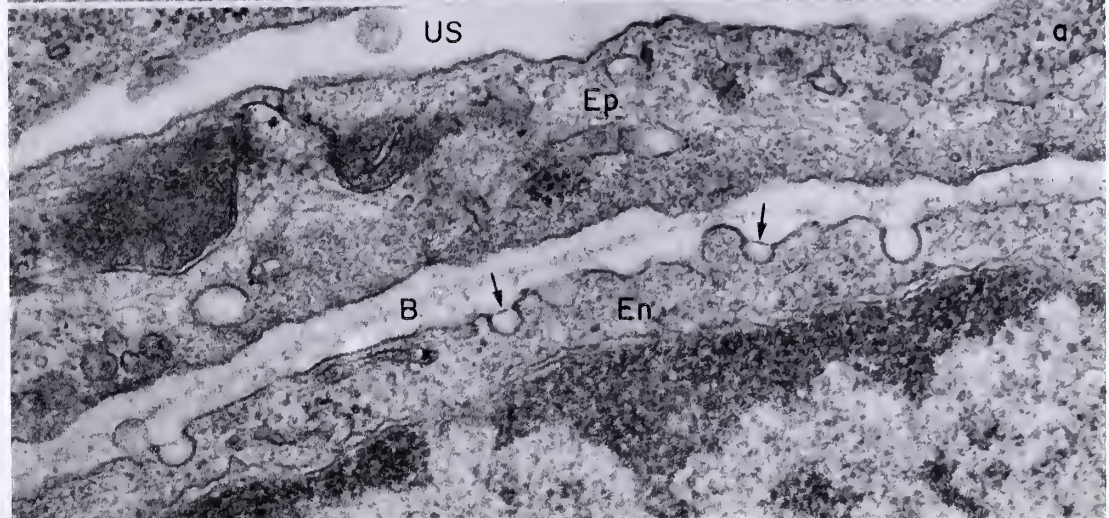
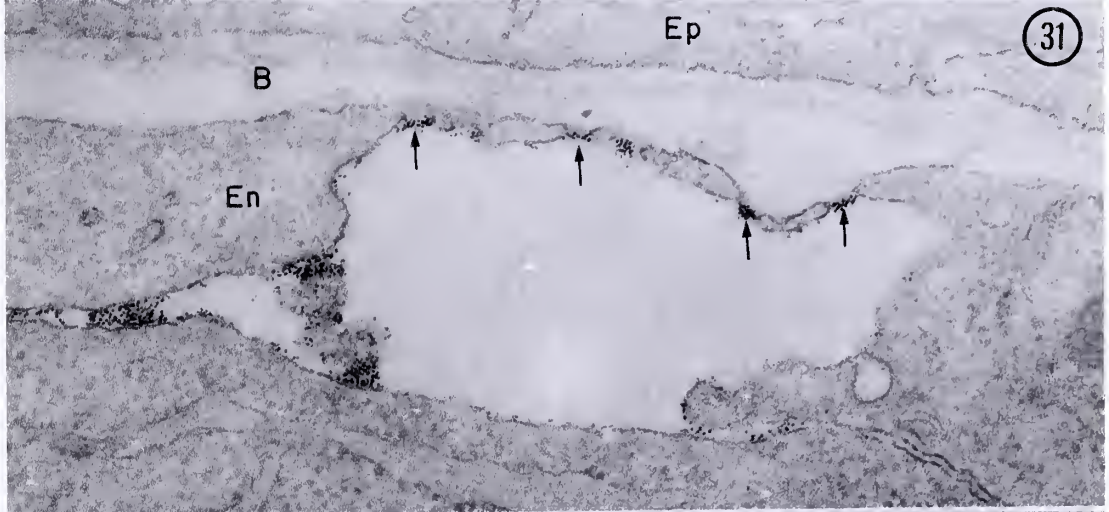
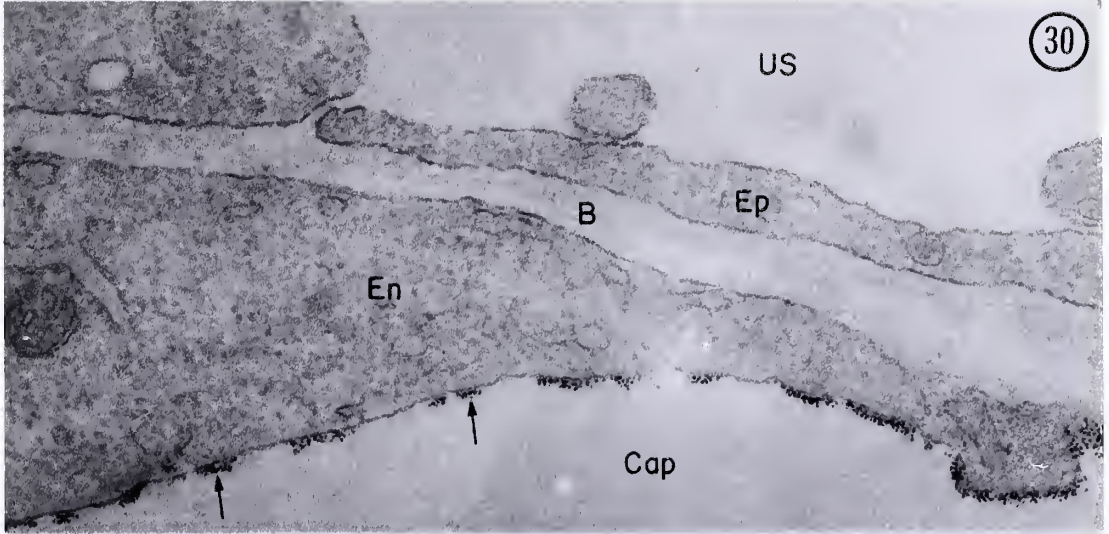
Cationized Ferritin. The distribution of cationized ferritin across the glomerular capillary wall differs in several important respects from that of native ferritin. At the early stages in which fenestrae are infrequent (i.e., the late S-shaped body stage or early capillary loop stage), cationized ferritin (pI 7.3) binds to the endothelial cell surface in a patchy distribution, but is not seen in the basement membrane (Fig. 30). In planes of section which contain fenestrae, cationized ferritin is concentrated on the luminal side of the fenestrae (Fig. 31) and fails to enter the GBM. Most fenestrae at this stage are closed by fenestral diaphragms which bind cationized ferritin and appear to physically prevent the entry of cationized ferritin into the basement membrane, since fenestrae which are not closed by one of these structures appear to allow cationized ferritin ready access to the basement membrane (Fig. 32). Once the cationized ferritin has gained access to the basement membrane through an open fenestrae, it appears to pass readily through the immature GBM, staining discrete sites in the GBM and passing on through to the urinary spaces (Fig. 32). This is unlike the situation in the mature GBM since a) discrete cationized ferritin stainable sites in the GBM appear to be randomly

FIGS. 30 and 31. Cationized ferritin injection.

FIG. 30. Early capillary loop stage showing section of capillary loop containing a thick, unfenestrated endothelium (En). Cationized ferritin binds in patches (arrows) to the endothelial cell surface. Cationized ferritin is not seen in the basement membrane (B) or in the urinary spaces (US), suggesting that the endothelium may play a role in retarding the transit of large molecules across the glomerular capillary wall. Ep, visceral epithelium; Cap, capillary lumen. Fig. 30, X69,000.

FIG. 31. Same stage as Fig. 30, but a portion of the endothelium which contains developing fenestrae. In contrast to the situation in the adult glomerulus, the fenestrae are closed by diaphragms which bind cationized ferritin (arrows) in large amounts, preventing its entry into the basement membrane (B). Note the similarity of the cationized ferritin binding pattern to the endothelial surface in Fig. 30 and to the diaphragms in Fig. 31. Fig. 31, X69,000.

FIG. 31a. Same stage as Figs. 30 and 31, showing the presence of vesicles with diaphragms (arrows) in the developing capillary endothelium (En) of the capillary loop stage. Diaphragms are best stained by alcian blue and uranyl acetate en bloc as in this figure. The relationship of these vesicle diaphragms, if any, to the fenestral diaphragms remains to be determined. Fig. 31a, X69,000.



distributed throughout the structure rather than arranged in two layers located in the lamina rara interna and externa as in the mature GBM (cf. ref. 45); b) cationized ferritin is seen in the urinary spaces (Figs. 32 and 33) in the fetal glomerulus but does not reach the urinary spaces in the mature glomerulus.

Cationized ferritin binds to anionic sites and for this reason appears to be more restricted in its lateral movement in the GBM than is anionic ferritin (Fig. 32). Cationized ferritin is seen in the GBM beneath open fenestrae for a distance of $\sim 0.8-1.0 \mu$, suggesting that it was able to diffuse this distance laterally in the GBM before fixation 5 to 10 minutes later (Fig. 32). This contrasts sharply with the even distribution of anionic ferritin administered under identical conditions.

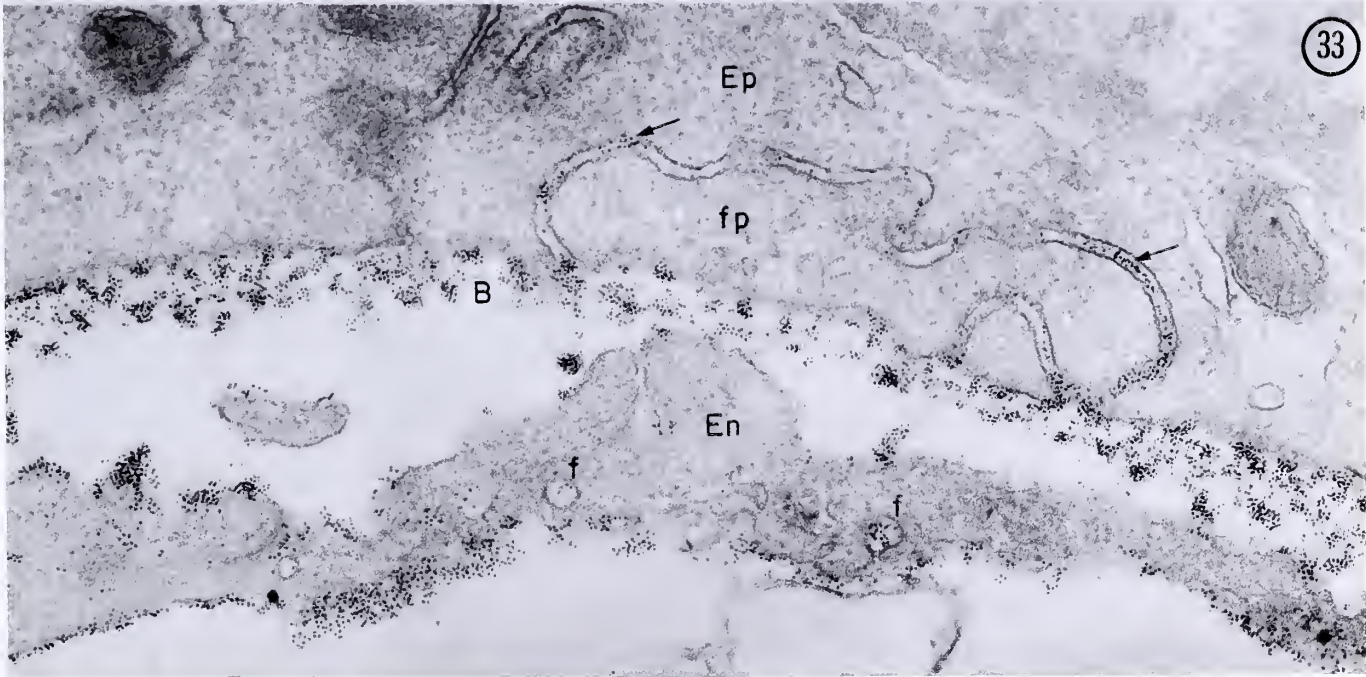
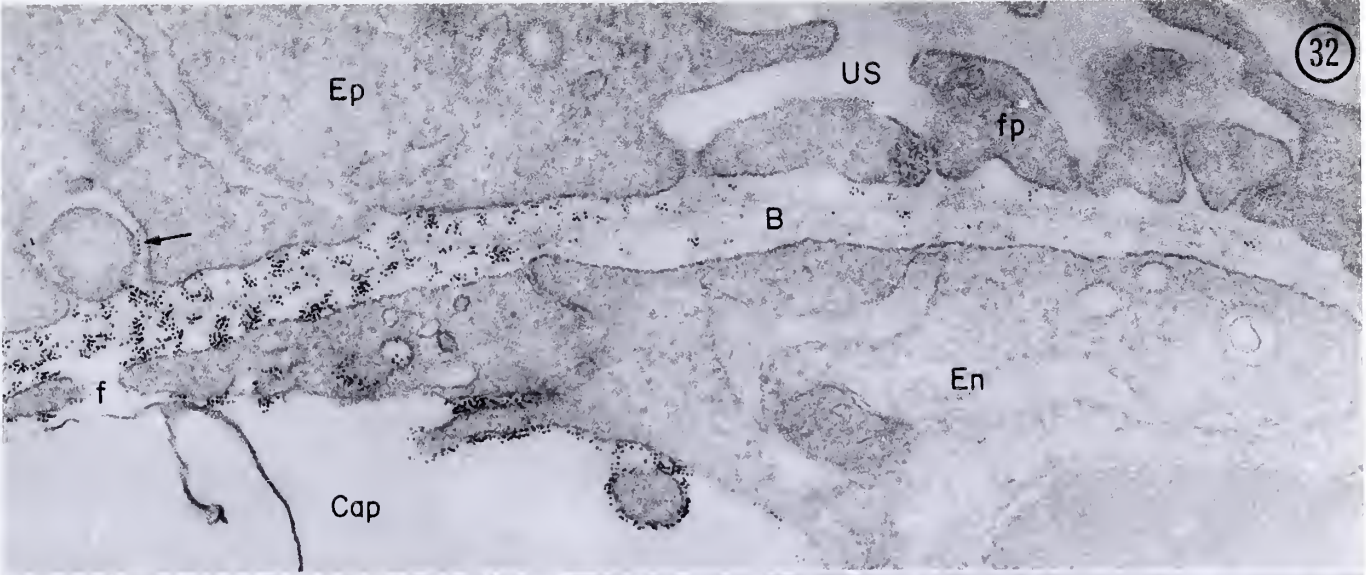
At later stages (Fig. 33) in which a large number of fenestrae are open (i.e., not closed by diaphragms), cationized ferritin is seen staining discrete sites throughout the GBM. As the glomerular capillary wall matures, two layers of cationized ferritin stainable sites (one in the lamina rara interna, the other in the lamina rara externa) are seen and cationized ferritin is prevented from reaching the urinary spaces, as in the adult GBM.

Ruthenium Red. Immature glomeruli (S-shaped body stage) contains ~ 30 nm diameter, randomly arranged ruthenium red stainable granules beneath the epithelial cells, often associated with the thin basement membrane (Fig. 34), inside the cleft. A lightly stained tail (Fig. 34) is associated with some of these large granules. At later stages (i.e., at the early developing capillary loop stage) the large granules are not seen but instead, smaller, $\sim 10-15$ nm diameter ruthenium red positive granules are found randomly distributed within the basement membrane

FIGS. 32 and 33. Cationized ferritin injection.

FIG. 32. Capillary loop stage. Cationized ferritin stains randomly distributed anionic sites in the basement membrane (B) on either side of an open fenestra (f). Note the paucity of tracer molecules at a lateral distance of greater than 1μ from the fenestra and the presence of tracer molecules in the urinary space above a developing foot process (arrow). Ep, epithelium; fp, foot process; US, urinary space; En, endothelium. Fig. 32, X69,000.

FIG. 33. Capillary loop stage. Cationized ferritin has gained access to the basement membrane (B) and stains randomly distributed anionic sites. Note tracer molecules in the urinary spaces (arrows) and in the fenestrae (f). Detachment of the endothelium is artifactual. En, endothelium; fp, foot process; Ep, epithelium. Fig. 33, X69,000.



FIGS. 34 and 35. Ruthenium red perfusion.

FIG. 34. S-shaped body stage. Large (~ 30 nm diameter) ruthenium red stained granules are seen in the cleft (arrows) and associated with the early basement membrane (B). Smaller granules located within the basement membrane near the epithelial cells may represent the precursors of the heparan sulfate rich granules (cf. Figs. 35 and 36) which are seen at later stages. Lightly stained tails are associated with many of the large (~ 30 nm diameter) granules which are seen in the cleft and associated with the portion of the GBM facing the cleft. Ep, epithelium; En, endothelium. Fig. 34, X69,000.

FIG. 35. Early capillary loop stage. Large, 30nm diameter granules such as are seen in Fig. 34 are absent, and instead, smaller, 10-15nm diameter ruthenium red stainable granules (arrows) are found randomly distributed in the basement membrane (B). These granules have a similar distribution to the anionic sites stained by cationized ferritin at this stage (cf. Figs. 32 and 33). En, endothelium; Ep, epithelium; US, urinary space; Cap, capillary lumen. Fig. 35, X75,000.

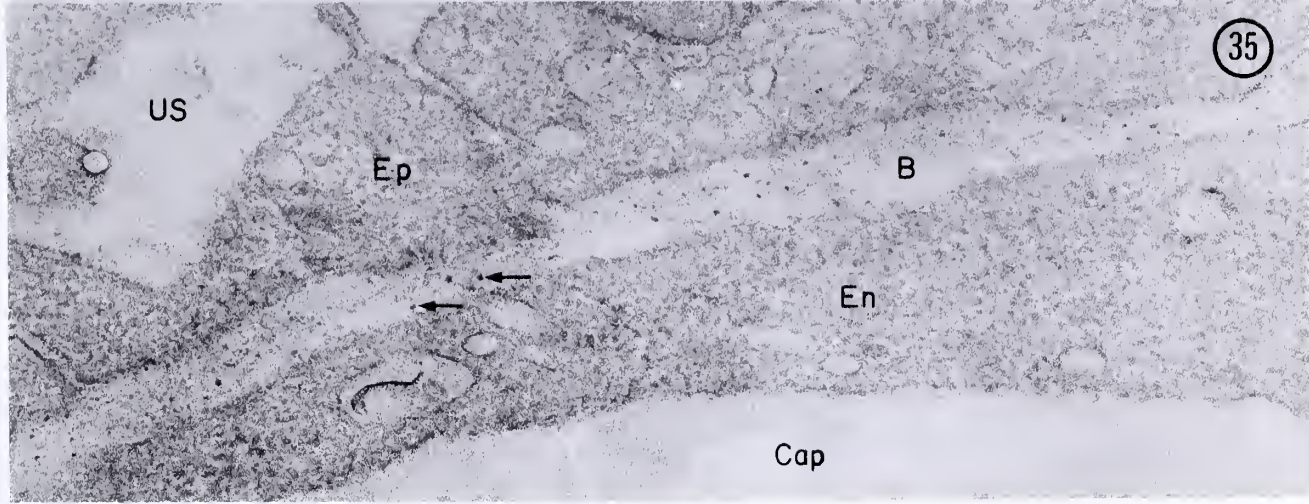
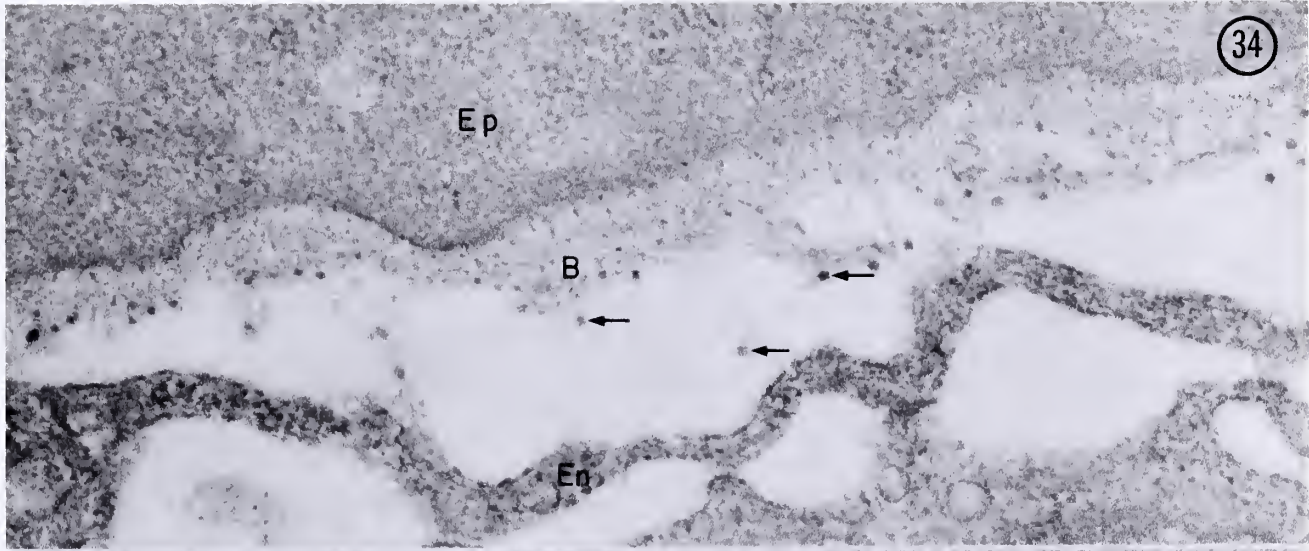


(Fig. 35). Ruthenium red stainable granules are regularly spaced in a lattice-like arrangement in the mature GBM viewed in grazing section (45), but this regularity of spacing is far less evident in grazing sections of the fetal GBM during the capillary loop stage (Figs. 36 and 36a). As the GBM develops its mature three layered structure, the ruthenium red positive granules become concentrated in two layers (Fig. 37), one located in the lamina rara interna and the other located in the lamina rara externa. Each layer consists of $\sim 10-15$ nm diameter ruthenium red positive granules regularly spaced $\sim 40-45$ nm apart in a staggered arrangement. This arrangement closely resembles the arrangement in the mature GBM (44) except that the particles are somewhat smaller in appearance and are located somewhat closer together (mature granules are 20 nm in diameter and spaced 60 nm apart). The reasons for these dimensional differences are unclear, but the spatial arrangement of the granules at this stage is very similar to that of the heparan sulfate containing granules previously identified in the mature GBM (45).

Thus, morphologically, there are two classes of ruthenium red positive granules in developing glomeruli -- one consisting of large (~ 30 nm diameter) particles which are seen in the clefts of S-shaped bodies, the other consisting of smaller ($\sim 10-15$ nm diameter) particles, at early stages randomly arranged, at later stages arranged in two layers in the lamina rara interna and externa, which probably represent the precursors of the proteoglycan granules recently found in the mature GBM.

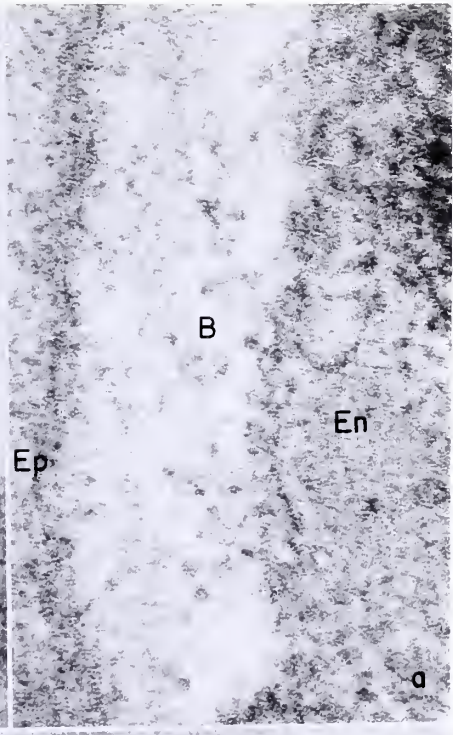
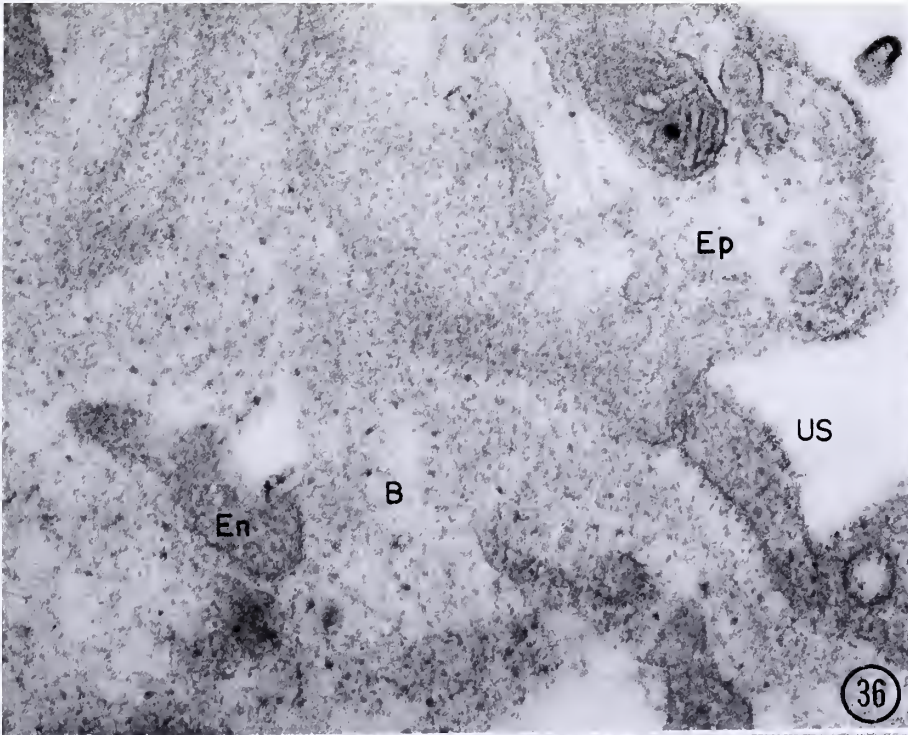
Alcian Blue. At pH 6.5 (Fig. 38), the epithelial cell surface stains non-specifically and in normal section, densely staining fibrils are seen in the GBM, some more or less perpendicular and others parallel to the plane of the GBM. This pattern is similar to that seen in the mature GBM (14). Grazing sections (Fig. 38a) show a reticular pattern as seen in

FIGS. 36 and 37. Ruthenium red perfusion.

FIG. 36. Early capillary loop stage. Grazing section of the basement membrane (B) showing irregular arrangement of ruthenium red positive granules. En, endothelium; Ep, epithelium; US, urinary space. Fig. 36, X90,000.

FIG. 36a. High magnification of a normal section through the GBM showing ruthenium red positive granules, early capillary loop stage. Fig. 36a, X150,000.

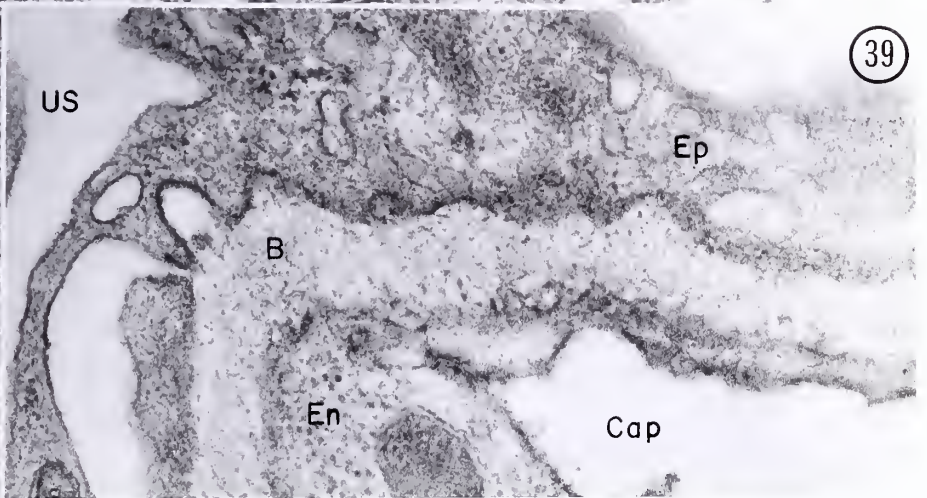
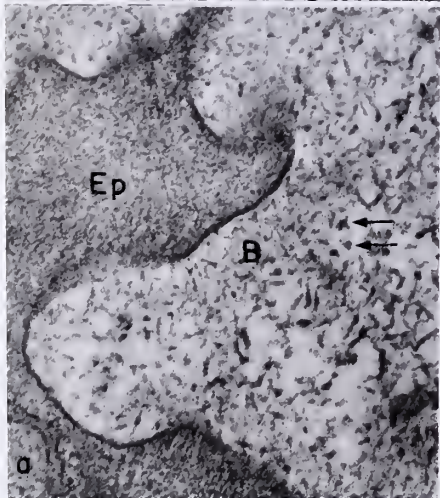
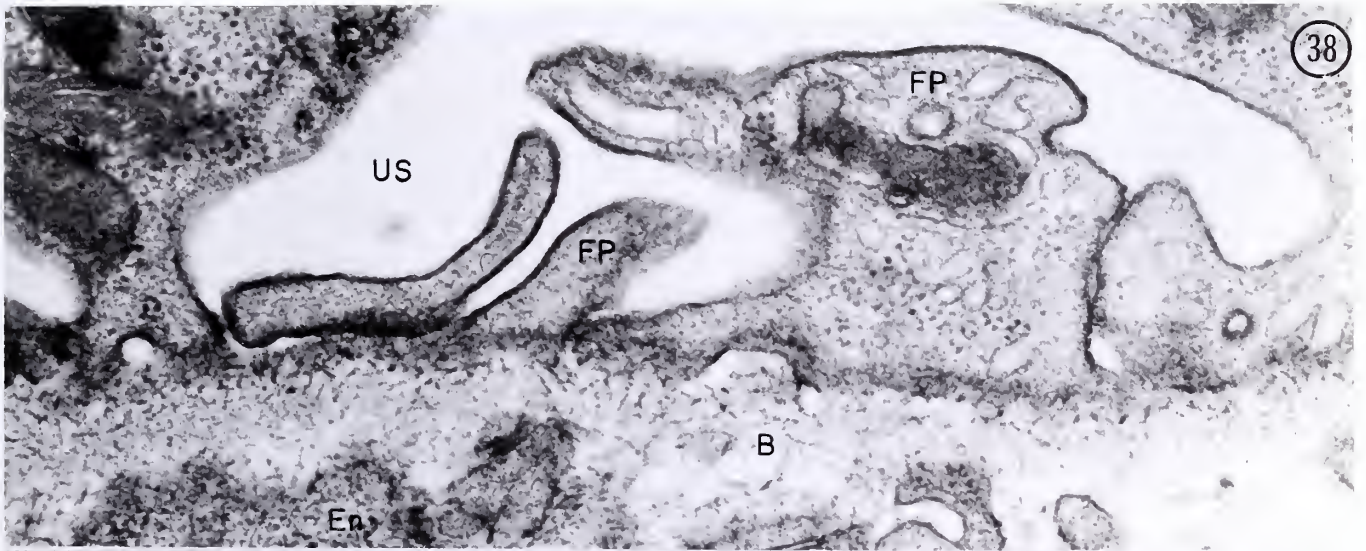
FIG. 37. Late capillary loop stage. The lamina densa (ld) is present at this stage, and ruthenium red positive granules occupy two layers in the lamina rara interna and lamina rara externa. The granules are 10-15 nm in diameter and closely resemble the randomly distributed granules seen at earlier stages (cf. Fig. 35) as well as the heparan sulfate rich granules seen in the mature GBM. Note the slit diaphragms between several of the foot processes (fp), some of which are still displaced above the basement membrane at this stage. Cap, capillary lumen; En, endothelium; B, basement membrane; US, urinary space; Ep, epithelium. Fig. 37, X75,000.



FIGS. 38 and 39. Alcian blue perfusion.

FIG. 38. Alcian blue perfused at pH 6.5, developing capillary loop stage. Alcian blue stains the cell coat of the foot processes as well as the basement membrane (B). Fibrils in the basement membrane run in two directions- either approximately parallel to or perpendicular to the plane of the GBM. In grazing sections (inset a), these fibrils form a reticular pattern and on occasion (arrows, inset a), appear to have a somewhat granular appearance. These granules may represent cross sections of the fibrils or else points where two fibrils cross one another. En, endothelium; Ep, epithelium; FP, foot process. Fig. 38, X69,000; Inset a, X69,000.

FIG. 39. Alcian blue perfused at pH 5.7, developing capillary loop stage. The basement membrane stains in a distribution similar to that seen in Fig. 38, but the epithelial cell (Ep) membrane staining is absent, indicating that alcian blue is more specific for sites in the GBM at this pH than at pH 6.5. En, endothelium; Cap, capillary lumen; US, urinary space. Fig. 39, X69,000.



the adult (14).

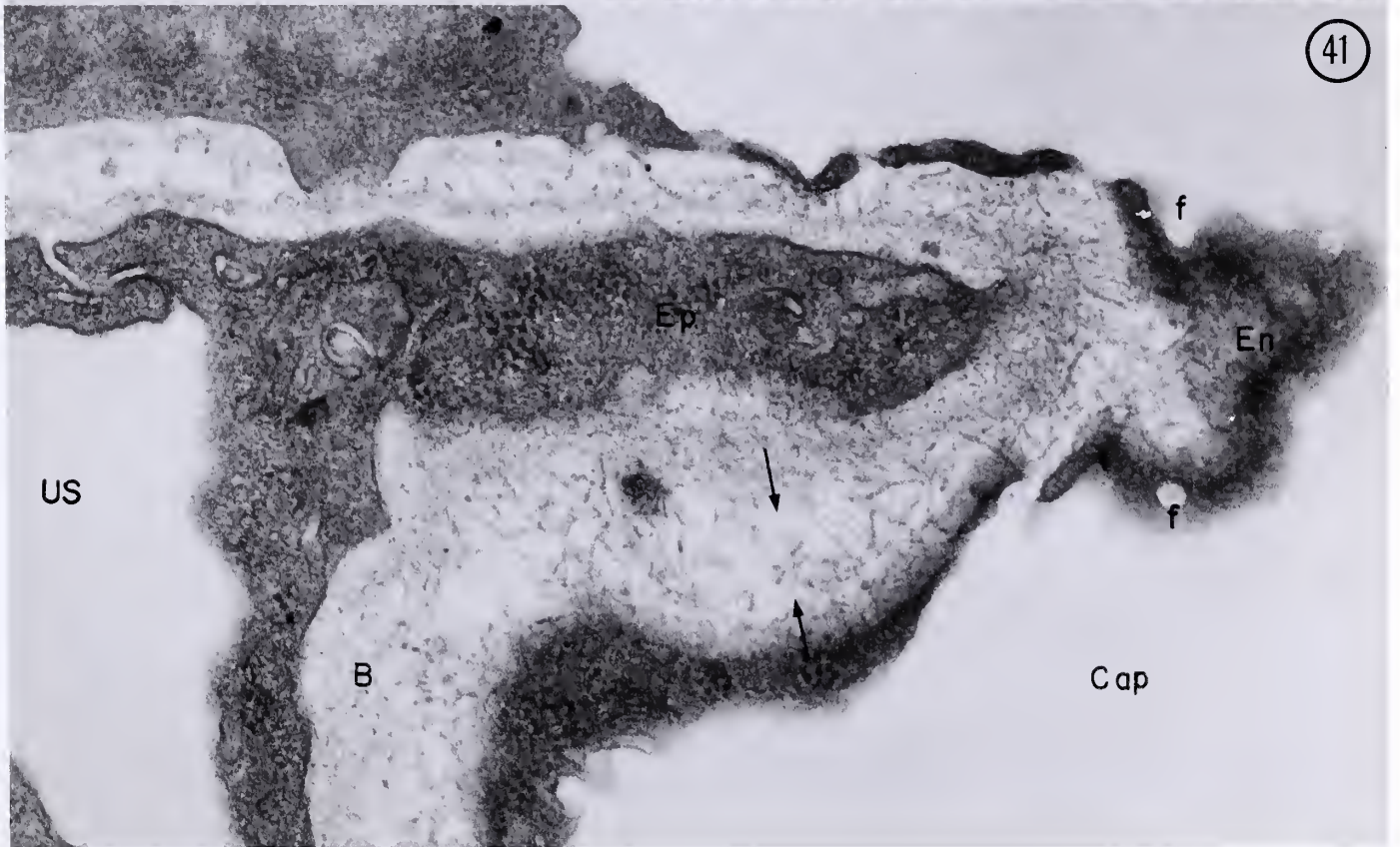
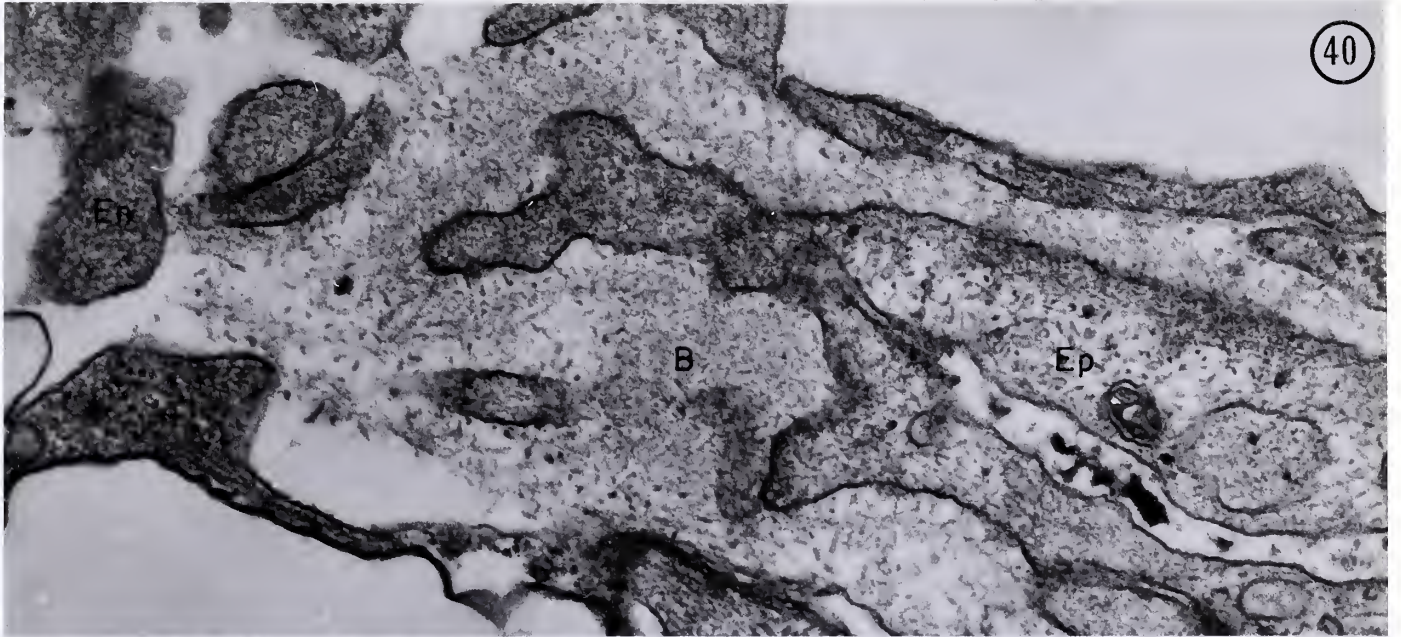
At pH 5.7, alcian blue is more specific and the epithelial cell surface is minimally stained while the staining pattern of the GBM remains virtually unchanged (Figs. 39 and 40). To make alcian blue specific for mucopolysaccharides would require staining at pH 1, but at that pH, a larger number of tissue polycations are ionized and interact with the tissue polyanions, preventing their complete binding with the dye (75).

For this reason, the critical electrolyte concentration method outlined above (see methods) was used instead of varying the pH of the staining mixture, in an attempt to increase the specificity of alcian blue for sulfated mucopolysaccharides. At low $MgCl_2$ concentrations (0.4 and 0.8 M) (Fig. 41) large, subendothelial fibers seem to be preferentially stained (cf. Figs. 40 and 41). At 1.2 M $MgCl_2$ concentration, these large, densely staining fibrils are poorly visualized and instead, a feltwork of fine alcianophilic fibrils is seen throughout the developing GBM (Fig. 42). The large subendothelial fibrils seen at low $MgCl_2$ concentrations are 10 nm in diameter while the fine fibrils seen throughout the basement membrane at high $MgCl_2$ concentration are roughly 3 nm in diameter. The two patterns of alcian blue staining described above are seen during the capillary loop stage and maturing stage of glomerular development, but another pattern of alcian blue staining is evident in early (S-shaped body stage) glomeruli. At this stage, very large, densely staining fibers are found in the cleft between the early mesenchymal/endothelial cells and the columnar epithelial cells or associated with (but not inside) the early GBM (Fig. 43). They are approximately 20 nm in diameter and are not seen at later developmental stages.

FIGS. 40 and 41. Alcian blue perfusion.

FIG. 40. Alcian blue perfused at pH 5.8, no $MgCl_2$, capillary loop stage. The section contains both grazing and normal sections of the basement membrane (B), showing the reticular pattern of the alcianophilic fibrils. En, endothelium; Ep, epithelium. Fig. 40, X69,000.

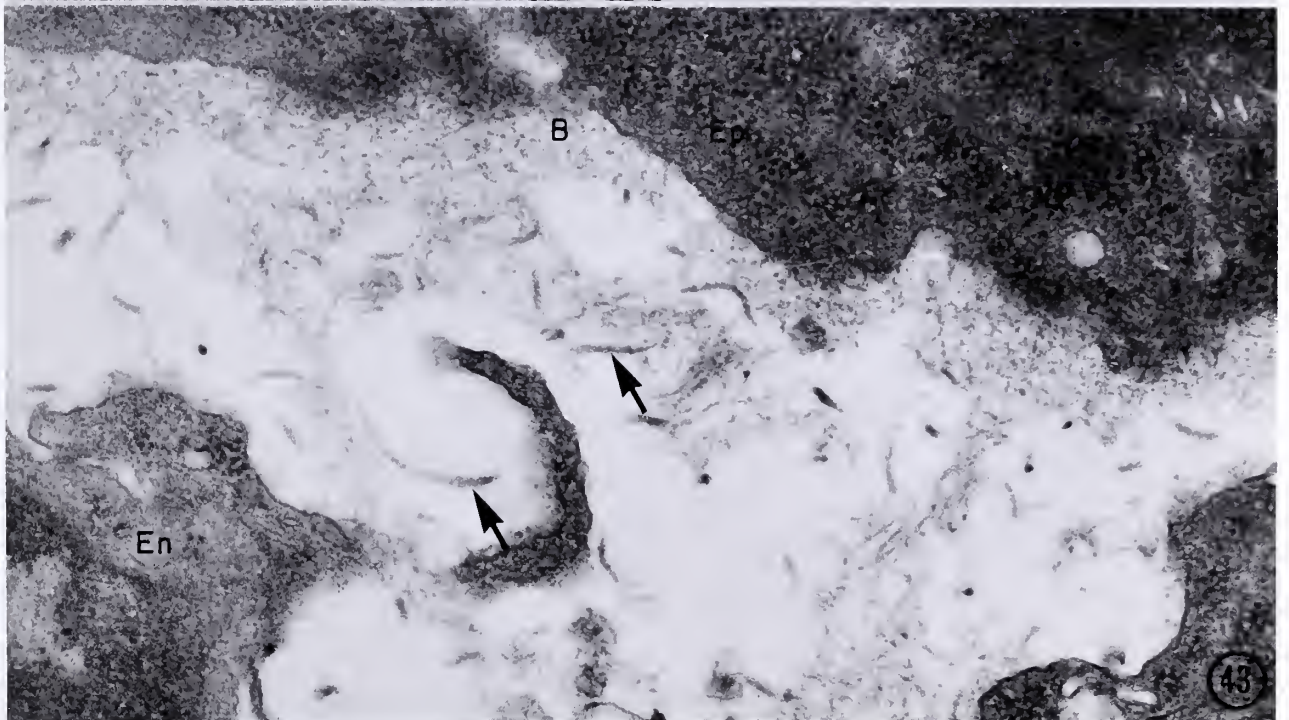
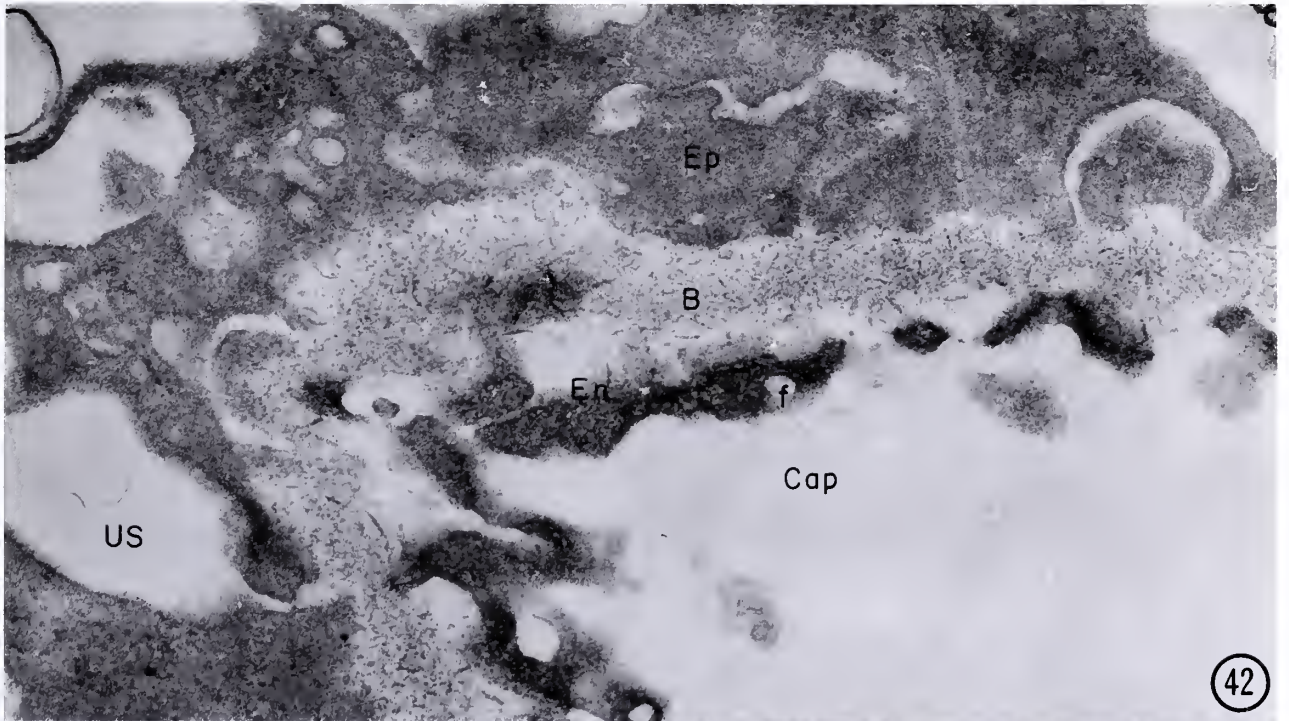
FIG. 41. Alcian blue + 0.4M $MgCl_2$ perfused at pH 5.8, capillary loop stage. In the presence of 0.4 (or 0.8)M $MgCl_2$, alcian blue stains 10nm wide subendothelial fibrils preferentially (region between arrows). These fibrils are seen in both normal and grazing section. Little structural detail can be seen in the subendothelial amorphous material which makes up the early lamina rara externa and lamina densa. Cap, capillary lumen; En, endothelium; f, fenestra; Ep, epithelium; US, urinary space. Fig. 41, X69,000.



FIGS. 42 and 43. Alcian blue perfusion.

FIG. 42. Alcian blue + 1.2M MgCl₂, perfused at pH 5.8, capillary loop stage. In the presence of 1.2M MgCl₂, the large fibrils stained at 0.4 and 0.8M MgCl₂ are poorly visualized, and instead, a fine felt-work of ~3 nm wide fibrils is seen throughout the basement membrane (B), both in grazing and in normal section. Cap, capillary lumen; En, endothelium; f, fenestra; Ep, epithelium; US, urinary space. Fig. 42, X69,000.

FIG. 43. Alcian blue + 0.4M MgCl₂, perfused at pH 5.8, S-shaped body stage. Coarse alcianophilic fibrils measuring ~20nm in width are seen in the cleft (arrows) beneath and adjacent to the epithelial portion of the early basement membrane (B). Note the deeper staining of one end of these fibrils and the long tails. This increase in staining density at one end of the fibrils might represent bent fibrils or possibly staining of the same early proteoglycan granules as are stained by ruthenium red at this stage (cf. Fig. 34). On close inspection of Fig. 34, many of the deeply staining granules appear to have lightly staining tails. It is possible that alcian blue stains the tails preferentially while ruthenium red stains one end of the fibrils specifically. Also, note the presence of banded collagen fibers at the lower right in this micrograph. En, endothelium. Fig. 43, X69,000.



DISCUSSION

Based on the observations made in this thesis and taking into account what is already known about glomerular development, one can reconstruct the differentiation of glomerular fine structure. This process will be considered in sections, following the path of an albumin molecule from the capillary lumen through the glomerular capillary wall to the urinary space. The following sections will deal sequentially with endothelial development, basement membrane formation and epithelial differentiation, after which the similarities between epithelial differentiation and glomerular diseases and the function of the developing glomerular capillaries will be considered.

DEVELOPMENT OF THE GLOMERULAR ENDOTHELIUM

The mature glomerular endothelium is a very thin layer (down to ~ 20 nm) which extends around the capillary lumen (31). Fenestrae, 50 nm-100 nm in diameter occupy about 30% of the total surface area of the endothelium. These fenestrae are freely permeable to native ferritin and are not closed by diaphragms such as those in other capillaries with a fenestrated endothelium (64, 93), e.g., peritubular capillaries of the kidney, those of intestinal mucosa, endocrine glands, etc. Rhodin (81) describes fenestral diaphragms in the adult murine glomerular capillary endothelium, but no other investigator has ever confirmed this finding and the fact that cationized ferritin readily reaches the GBM in adult animals without binding to the diaphragm is evidence against their existence, at least in the adult rat.

From the results of these studies, the sequence of endothelial differentiation can be reconstructed. The developing endothelium is derived from mesenchymal cells (23, 42) occupying the cleft of the S-

shaped body. During the S-shaped body stage, these cells are broad and undifferentiated, containing few, if any fenestrae. During the capillary loop stage, the endothelium begins to attenuate and increasing numbers of fenestrae are seen. Unlike the fenestrae in the mature glomerular endothelium, these early fenestrae are closed by diaphragms such as those seen in fenestrated capillaries in other tissues. As the glomerulus approaches the end of the capillary loop stage, these fenestral diaphragms are lost and open fenestrae appear. Like the fenestral diaphragms in mouse capillary endothelium (94), the transient glomerular fenestral diaphragms exhibit a high density of anionic charges as demonstrated by large amounts of cationized ferritin binding to them. When such diaphragms are present, cationized ferritin is not seen in the underlying basement membrane, but later in endothelial development when the diaphragms are absent, cationized ferritin readily enters the basement membrane as in the adult (44).

Since due to its net positive charge, the cationized ferritin binds to these diaphragms, one cannot say whether or not the diaphragms are open, i.e., permeable to ferritin. Evidence from other endothelia (64, 93) using native ferritin indicates that most fenestral diaphragms are not permeable to molecules of this size. Studies are now in progress using anionic ferritin as a tracer which does not bind to the diaphragms in order to directly determine their permeability. So far, only longer time points (10 minutes) after injection of the tracer have been examined and because of the rapid diffusion of native ferritin in the subendothelial plane of the basement membrane, it was not possible to test the permeability of the fenestrae. In the future, earlier timepoints (30 sec. to 5 min.) after injection of the tracer will be examined in hopes

of determining whether or not the tracer enters the GBM only through fenestrae that are not closed by diaphragms.

The presence of a complete layer of endothelium prior to differentiation of the GBM and slits serves the function of preventing leakage of protein when these layers are still incomplete. The loss of fenestral diaphragms during the course of development might be viewed as resulting from a differentiation of the glomerular endothelium to perform a more specialized function -- that of allowing access to the glomerular filter.

FORMATION OF THE BASEMENT MEMBRANE

The mature basement membrane measures 120 nm-150 nm (from endothelial cell membrane to foot process membrane) and consists of two relatively electron lucent layers (the lamina rara interna and externa) separated by the electron dense lamina densa (31). Poorly outlined 3 nm-4 nm fibrils are seen throughout the basement membrane, and 20 nm proteoglycan granules containing heparan sulfate are found in the lamina rara interna and externa, spaced \sim 60 nm apart in an amorphous matrix (44).

It is usually assumed that the GBM results from fusion of the endothelial and epithelial basement membrane (99). There is direct evidence for the epithelial origin of the GBM, but although an endothelial contribution to the basement membrane seems likely, this has not yet been proved, although it has been demonstrated that the endothelium makes basement membrane in other tissues (41).

The earliest GBM (S-shaped body stage) consists of a 70-80 nm colloidal iron stainable layer closely applied to the epithelial cell base, consisting of fine fibrils in an amorphous matrix. The electron density and width of this layer gradually increases until the GBM assumes a mature appearance.

Development of Anionic Sites in the Laminae Rarae. The development of charged sites in the GBM appears to involve several steps. Very early in the S-shaped body stage, large, negatively charged granules, stainable with ruthenium red, are seen inside the cleft. These deeply staining particles bear a close resemblance to the ruthenium red positive proteoglycan granules secreted by embryonic cornea (101) and other embryonic tissues (37). The granules in embryonic cornea are known to be rich in GAG's most notably hyaluronate, since staining of the granules is markedly reduced by hyaluronidase treatment (37, 101). Hyaluronic acid is thought to be of great importance in association with mesenchymal cell migrations (100) because of the striking increase in its synthesis at these times. This matrix is thought to serve as a scaffolding for mesenchymal invasion in the embryonic cornea, and by analogy, the ruthenium red positive granules seen in the cleft of the S-shaped body might serve as a scaffolding for the invasion of mesenchyme into the cleft.

There is indirect evidence to support this interpretation: 1) in cultured fragments of renal cortex, S-shaped bodies form with clefts devoid of cells (23), suggesting that cleft formation precedes (and is not dependent upon) mesenchymal invasion, indeed, the cleft might induce mesenchymal invasion; 2) the large ruthenium red positive granules are not seen once the developing capillary loop stage is reached, in keeping with the known increase in hyaluronidase activity and increases in sulfated GAG synthesis in other embryonic tissues which are known to occur during periods of cell differentiation (see above and refs. 8, 9, 100).

Hyaluronidase digestion prior to ruthenium red staining is needed in order to state with more certainty that these large ruthenium red

stainable granules are similar in composition to the proteoglycan granules in other developing systems, but it seems reasonable to assume that they are.

During the developing capillary loop stage, smaller ruthenium red positive granules become visible at the interface between endothelium and epithelium. Before the presence of the lamina densa, these granules are randomly distributed in the developing GBM, but as the lamina densa forms (during the capillary loop stage), they become localized in the lamina rara interna and lamina rara externa, in a pattern very similar to that seen in the mature GBM. Although these granules are smaller and more closely spaced than the ruthenium red positive granules in the mature GBM, it seems likely on the basis of morphology after ruthenium red staining that they are the precursors of the proteoglycan granules rich in heparan sulfate which have recently been identified in the mature GBM (45). Removal by digestion with heparitinase will be necessary to prove this interpretation. These granules appear to stain with cationized ferritin as well, since randomly distributed clumps of this cationic probe are seen in the developing capillary loop stage while at later stages, the cationized ferritin stains sites in the laminae rarae interna and externa only. Simultaneous use of ruthenium red and cationized ferritin (technically difficult in the newborn rat) could be used to confirm that the anionic sites stained by the two probes are the same. This has been shown in the adult rat, in which cationized ferritin and ruthenium red were found to stain identical sites in the GBM (45).

Thus, it appears from these studies that two types of proteoglycan granules are formed during development: one type is secreted into the cleft of the S-shaped body during or before the period of mesenchymal

invasion; a second type of proteoglycan granule is secreted into the GBM during the early developing capillary loop stage. The latter granules polarize during the course of development of the lamina densa to occupy their adult position in the laminae rarae interna and externa by the time the maturing glomerulus stage is reached. The distribution of proteoglycans has not previously been studied in developing glomeruli.

Colloidal Iron and Alcian Blue Staining. Previous studies of colloidal iron staining in mature glomeruli have been contradictory (43, 65). In some studies (43) colloidal iron staining in the GBM was removed and cell surface staining was reduced by hyaluronidase treatment, while in others (65) no change in the staining pattern was seen after hyaluronidase treatment; it has been concluded by both groups that neuraminidase has no effect on basement membrane staining by colloidal iron. The reason for this discrepancy in the results of hyaluronidase treatment is not clear¹, but the results reported in this thesis support the latter finding that colloidal iron staining of the GBM is unaltered by hyaluronidase treatment. The negative results of these enzyme digestions in the fetal GBM are difficult to interpret, however, since cross-linking within the GBM may protect sialic acid or hyaluronic acid which might be present from enzyme digestion by sterically hindering access of the enzyme to its substrate.

Alcian blue stains fibrils in the GBM and discrete anionic sites (such as those stained by ruthenium red and cationized ferritin) concentrated in the laminae rarae are poorly visualized. Early in development,

¹These differences may have been due to technical factors such as relative purity of the enzyme, method of fixation, incubation conditions, penetration of the colloidal iron, etc.

fibrils measuring ~ 20 nm in diameter are stained by alcian blue in the clefts of the S-shaped bodies. One end of these fibrils stains heavily and might either correspond to bending of the fibrils or else to the ruthenium red positive granules seen at that stage, which, upon close inspection (Fig. 34) appear to have poorly stained tails. Thus, ruthenium red might specifically stain only one end of a thick fiber while alcian blue stains the entire fiber non-specifically. The smaller, presumptive heparan sulfate rich granules, seen at later stages in development are not distinctly recognizable with alcian blue. The changes in staining pattern between 0.4 M $MgCl_2$ and 1.2 M $MgCl_2$ might be attributable to loss of carboxyl group staining at high $MgCl_2$ concentration, but little else can be said regarding the nature of the alcianophilic fibers.

Thus, although colloidal iron and alcian blue also stain anionic groups in the GBM, the relationship between these stained groups and the ruthenium red stainable proteoglycan granules is uncertain. The presence of colloidal iron staining in the GBM well before the development of the proteoglycan granules suggests that colloidal iron must stain some other type of polyanion in the GBM beside heparan sulfate. The nature of the anionic groups stained by both colloidal iron and alcian blue remains to be determined.

EPITHELIAL DIFFERENTIATION.

The mature glomerular epithelium consists of a single layer of cells remarkable for their elaborate branching and foot processes that interdigitate with the foot processes of adjacent epithelial cells. The foot processes are club-shaped in normal section with relatively more cytoplasm located toward the GBM than toward the urinary space. The foot processes

are separated near the basement membrane by 25-30 nm slits and slit diaphragms are frequently seen bridging the slits.

The development of the early columnar epithelium to its highly differentiated mature form has been reconstructed on the basis of the studies reported in this thesis, taking into account previous knowledge concerning this process.

The visceral as well as the parietal and proximal tubule epithelium differentiate from a common precursor cell layer known as the renal vesicle epithelium. The latter forms the lining of the renal vesicle and its cells are joined along their apical or luminal surfaces by occluding junctions. From this layer, some cells differentiate into visceral and some into parietal epithelium, and the vesicle lumen at this level represents the precursor of Bowman's space. The visceral epithelium starts out as a pseudostratified layer with a haphazard arrangement of nuclei -- some at the cell apex, some at the base -- but gradually becomes uniformly polarized to form a simple columnar cell layer with the nuclei located next to Bowman's space. Initially, cells of both the visceral and parietal epithelium maintain occluding zonulae between adjoining cells at their apices where they border on Bowman's space. As development continues, the junctions between cells of the parietal epithelium maintain this position, whereas those between the cells of the visceral epithelium migrate along the lateral cell margin from their apex (near Bowman's space) to their base where they rest on the basement membrane. In the process of migrating, the junctions become discontinuous or interrupted so that they represent fasciae (or bands) rather than zonulae (or belts) completely encircling each cell. At this time, epithelial cell cytoplasm appears as a continuous,

uninterrupted layer -- without foot processes or slits -- applied to the outer aspect of the developing basement membrane, with occluding junctions located between adjoining cells. Shortly after migration of the junctions, rearrangement of the basal pole of the epithelium begins with the cytoplasm of adjoining cells sliding over one another in such a way that interdigitation between the cells occurs. At this time, the occluding junctions become progressively more fragmented into maculae, and ladder-like structures appear in the intercellular spaces. Finally, normal slit membranes appear, the interdigitating processes become separated by the usual 25 nm gap, foot processes take on their usual club-shaped configuration and the occluding junctions and ladders disappear.

Junctions in Developing Glomeruli. Several interesting aspects of the junctional arrangements found in developing glomeruli are worthy of mention. One is the relocation of occluding junctions from apex to base that occurs along the lateral intercellular spaces. Such occluding junctions are known to be composed of intramembranous particles in ridge-like or linear arrays (14, 40, 98). The relocation of the junctions could be accomplished by removal of particles at the top followed by addition of particles to the bottom of the junctions. Alternatively, the junctions could partially fragment and the fragments could migrate more or less intact by a kind of membrane flow phenomenon involving directed movement of the ridges and particles. In order to maintain cell contact, the specializations on one cell would have to move in phase with those on the adjoining cells. Fragmentation of junctions has been seen following dissociation of pancreatic exocrine cells of the guinea pig (2) and in regenerating rat liver after partial hepatectomy (98, 108) in which it was suggested that fasciae occludentes arise by fragmentation of zonulae occludentes as a

result of cell movements which occurred during reorganization of these tissues.

Another interesting problem is the fate of the occluding junctions and the relationship between occluding junctions, ladders, and normal slit membranes, since the former two elements disappear and are replaced by normal slits. At the moment, there is no information as to the fate of these two types of structures. The present study finds no evidence that they are incorporated intact into lysosomes as described in dissociated cells (2). Moreover, there is no information concerning the source of the slit diaphragms. Finally, the absence of regular junctional complexes (i.e., zonula occludens, zonula adherens and macula adherens) in the glomerular epithelium is of interest. Such tripartite junctional complexes, with minor variations in the precise arrangement, are found in most other epithelia -- e.g., GI tract, uterus, glandular epithelia of the liver, pancreas, parotid, thyroid and stomach, as well as in the proximal tubule, distal tubule and collecting duct of the nephron (30). Thus, the junctional arrangement encountered in developing glomeruli represents an exception to the junctional pattern seen in most other epithelia. The reason for these differences is not presently known.

Epithelial Cell Surface Sialoprotein. A thick layer of negatively charged, colloidal iron stainable material has been found to coat the cell bodies and foot processes of the mature glomerular epithelium down to the level of the slits (43, 65). Because this epithelial polyanion is removed by treatment with neuraminidase or proteases, it has been assumed to consist of sialoglycoprotein. This assumption is supported by the fact that sialoglycoproteins have recently been isolated biochemically from the glomerulus (69).

In this thesis, the development of epithelial sialoglycoprotein has been studied. The colloidal iron stainable material present on the surfaces of developing visceral epithelial cells, like that on the mature cells, is digested by neuraminidase and thus is likely to consist of sialoglycoprotein. During the early S-shaped body stage, occluding junctions are located at the apices of epithelial cells and minimal staining of the apical cell surface is detected either at the LM or at the EM level. Shortly after the junctions begin to migrate, epithelial polyanion becomes detectable (both by LM and EM) along the apical and lateral aspects of the epithelial cell surfaces. By EM, this staining has not been shown to extend below the level of the junctions. This is not due to poor penetration of the colloidal iron, since the adjacent basement membrane stains with colloidal iron, and individual particles can be seen in the intercellular spaces between two epithelial cells. Thus, the differentiating columnar epithelial cell becomes polarized with a thick coat of sialoprotein above the level of the migrating junctions and with no staining below this level. As the junctions migrate toward the cell bases, epithelial polyanion continues to be seen adjacent to the junctions in amounts that are not decreased from that seen on the more apical portions of the cell membrane, suggesting that sialoglycoprotein may migrate toward the bases of the cells by a membrane flow process at the same time as the junctions migrate. An alternative explanation would be the random insertion of new molecules. This would explain the fact that dilution of colloidal iron stainable material is not seen as the plasmalemma expands to cover the interdigitating foot processes. A combination of these two processes might also occur.

The polarity of the epithelial cell surface could be explained by differentiated plasmalemma domains (with and without sialoglycoproteins). Separation of the domains by occluding zonules could be rationalized, but separation after the disappearance of the occluding zonules poses some questions. Differentiated plasmalemmal domains could conceivably be maintained in a fluid membrane by structures beneath the plasmalemma -- e.g., spectrin.

As epithelial cell polyanion appears at progressively lower levels along the lateral cell membranes, widened intercellular spaces appear which may be opened by the mutual repulsion of the anionic groups located on the surfaces of two adjacent cells, or by migration of the junctions or by a combination of these two processes. It can be seen, however, (Fig. 18) that often the adjacent cells are closely apposed, with epithelial polyanion completely filling the narrow intercellular space. In some planes of section, cell surface specializations are seen in these areas of close apposition which resemble poorly stained ladders in having electron dense material on either side of the intercellular space and poorly stained filaments inside this space. There is no colloidal iron staining between the cells in these areas, either because of the absence of epithelial polyanion or because of poor penetration of the stain. Further studies using uranyl acetate en bloc along with colloidal iron are needed to further define the morphology of these areas; if these specializations prove to be ladders, as their appearance suggests, it might be that the ladders are important in maintaining contact between the cells above the level of the occluding junctions.

There is no direct evidence from these studies concerning the origin of the surface sialoglycoprotein, but if the steps in its synthesis are

like that of other glycoproteins, it can be assumed that the protein is synthesized and partially glycosylated in the rough endoplasmic reticulum, and the terminal hexoses and sialic acid are added in the Golgi complex before the sialoglycoprotein is transported to and inserted into the cell membrane (72).

The only reservation about the interpretation of the results of these studies of epithelial cell surface polyanion is that the neuraminidase used in this study (and all previous enzyme digestion studies in adult glomeruli -- e.g., refs. 38, 65) contained trace amounts of protease activity (by the Azocoll assay). Recently, a protease-free preparation of the enzyme has become available, and experiments are now in progress in which an attempt has been made to digest the epithelial polyanion with the purified enzyme. The results should remove any doubt as to the validity of the enzyme results and aid in determining the nature of the surface polyanion.

Function of Sialoprotein. Evidence is now accumulating which suggests that the presence of colloidal iron stainable sialoprotein on the epithelial cell surface may be required for the maintenance of normal foot process and slit organization. This association between epithelial polyanion and normal slit and foot process architecture was first suggested by Michael, Blau and Vernier (65) and was clearly indicated by the experiments of Seiler, et. al. (90, 91) who showed that neutralization of the cell surface polyanion by perfusion with polycations (e.g., protamine sulfate and poly-L-lysine) causes a reduction in the number of foot processes and a narrowing and reduction in the number of slits. These findings were reversible by reperfusion with heparin, a polyanion which neutralizes the perfused polycation. The demonstration in the

present study that epithelial polyanion (detected by colloidal iron staining) appears on the surface of the differentiating epithelial cell at a stage before foot processes and slits differentiate is in keeping with this assumption.

ANALOGY WITH AMINONUCLEOSIDE NEPHROSIS.

Epithelium. The development of the visceral glomerular epithelium may be divided into two broad periods: the first is the period of commitment and proliferation of the visceral epithelial cells which encompasses the vesicle and S-shaped body stages. The second is the period of foot process differentiation which occurs after vascularization and migration of the junctions to the base of the epithelium. This period correlates roughly with the latter part of the capillary loop stage of development. There is little similarity between glomerular organization in the first period and that in aminonucleoside nephrosis; however, the similarities between findings during the second period and those in aminonucleoside nephrosis are striking (Fig. 12): 1) Foot processes are reduced in number and broad epithelial processes replace the usual foot processes, with the filtration slits in both the nephrotic and the immature glomerulus. 2) Focal occluding junctions which appear similar in thin section (19, 85) as well as in freeze fracture preparations (19, 40, 74, 84) are present between foot processes in both cases. 3) Slit diaphragms are often displaced to a position above occluding junctions in nephrotic (19) as well as in immature glomeruli. 4) Ladder-like structures are seen in both the nephrotic (19, 85) and the developing glomerulus. In the nephrotic glomerulus, such ladders have been suggested (85) to represent redundant slit diaphragm, but there is little evidence one way or another to indicate whether or not this is the case, and it is not known why the slit diaphragm should be formed in a redundant configuration during fetal

development. An alternative explanation is that these ladders represent septate-like junctions, previously reported in invertebrates (98), and in Sertoli cells in mammals, which they resemble closely. 5) Presence of foot processes is correlated with the presence of colloidal iron stainable epithelial polyanion, and diminished numbers of foot processes is correlated with a decrease or absence of such material in both the developing and the nephrotic (11, 65) glomerulus. In the developing glomerulus, foot processes are seen to form only after the appearance of epithelial sialoprotein near the base of the cells.

Thus, it can be concluded that the changes undergone by the glomerular epithelium in aminonucleoside nephrosis represent a dedifferentiation -- or rerun in reverse -- of events that take place during normal glomerular differentiation. Studies of the epithelial changes associated with other experimental models of the nephrotic syndrome are less complete. However, both occluding junctions and ladder-like structures have also been described (51, 87) in immune complex nephritis, indicating that these alterations are not limited to the aminonucleoside model.

Basement Membrane and Endothelium. The similarity between the fetal basement membrane and endothelium and the changes seen in aminonucleoside nephrosis is more tenuous. The endothelium of the S-shaped body bears no resemblance to the endothelium of nephrotic animals, however, the endothelium late in the capillary loop stage bears some resemblance to the endothelium of the 10 day nephrotic animal (16) in that the number of fenestrae is reduced in comparison to the normal mature endothelium. There is no report of the presence of fenestral diaphragms in any glomerular disease, and until evidence is found to the contrary, this structure must be considered unique to the fetal

glomerular endothelium.

The basement membrane is more permeable to native ferritin and contains reduced anionic charge in both the nephrotic (18, 29) and in the developing glomerulus, but it is not known whether or not the same factors account for these alterations in glomerular disease and for the findings in the developing basement membrane. There is no reason, a priori to suspect that this is the case and the resemblance between these two situations may be merely a superficial one.

TRACER STUDIES.

Native Ferritin. In the mature glomerulus, ferritin concentration drops sharply along the subendothelial surface of the lamina densa. Little native ferritin reaches the deeper layers of the GBM.

In this thesis, the development of the glomerular size barrier was studied with the general conclusion that while the permeability of the developing GBM is greater than that of the mature, the developing GBM still serves as a barrier to the movement of tracer molecules across the glomerular capillary wall, even at very early stages of development.

The very interesting case of the basement membrane at the earliest stages of development (i.e., early S-shaped body) could not be studied since ferritin did not reach the cleft of the glomerulus at this stage. This may be of functional significance in preventing access of protein to the GBM at a stage when the filter is too immature to be an efficient barrier to protein transport.

At the earliest stages in which ferritin reaches the vascular glomerulus (i.e., late in the S-shaped body stage or early in the capillary loop stage), native ferritin is seen throughout the inner two thirds of the basement membrane. The concentration of tracer is less on the sub-epithelial side of the GBM (i.e., a gradient exists), indicating the

role of the GBM as a filter. The absence of large numbers of fenestrae may be expected to reduce access to the developing glomerular filter, but the tracer is apparently not significantly retarded at the level of the endothelial fenestrae (or for that matter, at the level of the slits). As in the adult, the epithelium may serve as a monitor for tracer molecules that leak through the filter. Quantitation of the amount of ferritin leaking through the filter is difficult (compared with cationized ferritin) since native ferritin does not bind to the epithelial cell surface and could be washed away during fixation.

Cationized Ferritin as a Tracer. In addition to serving as a cationic probe, cationized ferritin can also be regarded as a tracer by virtue of its large size. The results obtained with any cationic particle as a tracer must be interpreted with caution, however, since such molecules will bind to fixed polyanion on the endothelial cell (13, 79), the basement membrane (44) and the epithelial cell (43, 59, 66). Karnovsky and associates, for example, overlooked this problem in interpreting their studies using peroxidatic tracers, and as a result, concluded that the slits represent the primary glomerular filter (see above and ref. 27). Keeping this limitation in mind, it seems likely that at early stages of development, the primary glomerular mechanism responsible for retaining cationized ferritin is the fenestral diaphragms covering the small numbers of fenestrae which are present. Cationized ferritin appears to enter the GBM only through fenestrae that are patent (i.e., not closed by diaphragms), and once into the GBM, to stain anionic sites and pass readily through the GBM (Figs. 30 to 33) to the urinary spaces where it binds to the epithelial cell surface.

No conclusions can be made as to whether or not cationized ferritin passes more readily through the developing GBM than does anionic ferritin (as might be suggested by the physiologic studies of the mature glomerulus, cf. ref. 13), since cationized ferritin is more likely to remain in the urinary spaces (bound to epithelial cell surface polyanion) than is anionic ferritin.

The fact that cationized ferritin penetrates the GBM more readily than native (anionic) ferritin (despite their similar size) reinforces the concept that both size and charge barriers exist in the GBM, and that any particle travelling across the basement membrane is affected to a greater or lesser degree by both of these barriers. Thus, while useful conceptually, a distinction between these barriers may be artificial.

It can be concluded that both the endothelium (as suggested by Weber and Blackburn, ref. 106) and the basement membrane (as suggested by Vernier and Birch-Anderson, ref. 103) appear to play a role in regulation of the transport of particles through the early developing glomerular capillary wall and that the functions of the three layers of the glomerular capillary wall postulated by Farquhar and associates (25, 26, 27, 31) in filtration seem particularly applicable in the case of the fetal glomerulus. The endothelium probably regulates access to the basement membrane by virtue of its relatively small numbers of fenestrae which are closed (and impermeable to cationized ferritin and probably to native ferritin as well) by diaphragms at early stages of development. That the basement membrane serves as a filter, even at early stages of development has been shown above, as has the fact that the epithelium may serve as a monitor of protein leaking through the filter. The reduced filtration surface resulting from fewer slits and the presence of occluding junctions

closing the few slits that are present early in epithelial development might serve to limit protein leakage as well. The large amount of cationized ferritin seen in the urinary spaces, however, shows that the immature glomerular capillary wall is less efficient in retaining positively charged particles than is the mature.

CONCLUSIONS

A number of new findings and concepts have resulted from this study of the developing glomerulus.

1. Four stages of glomerular development have been identified at the LM level which correlate with specific events in the differentiation of glomerular fine structure.

2. Fenestral diaphragms have been identified for the first time in the early glomerular endothelium of the rat (cf. p.93). These diaphragms are anionically charged and appear to retard the movement of cationized ferritin (and probably anionic ferritin as well) into the GBM. Such fenestral diaphragms are not seen in the mature glomerular endothelium, and appear to largely disappear by the end of the capillary loop stage.

3. The process of development of anionic sites in the basement membrane of the developing glomerulus has been delineated. These sites are stainable by ruthenium red and cationized ferritin, appear early in the capillary loop stage of development, and later become organized into two layers located in the laminae rarae interna and externa as the lamina densa forms.

4. Large, presumably proteoglycan, granules have been seen for the first time in developing glomeruli, in the clefts of S-shaped bodies.

As in other developing systems, these granules may play an important role in mesenchymal cell migration into the cleft. These granules disappear by the beginning of the capillary loop stage.

5. The sequence of events in the process of epithelial development from an undifferentiated simple columnar epithelium to the flattened, mature epithelium containing interdigitating foot processes and slits has been determined. Occluding junctions have been identified between developing epithelial cells which are seen at progressively lower levels of the epithelium during development, a finding which has led to the conclusion that zonulae occludentes migrate from epithelial cell apex to base, where the junctions apparently fragment into fasciae and maculae occludentes which appear between the developing foot processes. As foot process interdigitation increases in complexity and increased numbers of mature slits are formed, these focal junctions are eventually lost entirely.

6. Ladder-like structures, previously seen only in glomerular disease, have been identified in the intercellular spaces between developing glomerular epithelial cells. This had led to the realization that these structures represent a recapitulation of events in normal fetal development rather than a pathologic alteration of the glomerular epithelium as was previously thought. A possible function for these structures in maintaining intercellular contact has been proposed.

7. It has been shown that the changes in aminonucleoside nephrosis (i.e., ladders, occluding junctions, wide foot processes, narrow slits and decreased epithelial polyanion) bear a striking resemblance to the epithelium of the normal differentiating glomerulus during the late

capillary loop stage, which has led to the conclusion that the epithelial changes in aminonucleoside nephrosis (an experimental model of minimal change disease in children) may represent a dedifferentiation to a more primitive organization and that the events that occur early in this disease process represent a rerun in reverse of events that occur during normal glomerular development.

8. The differentiation of glomerular epithelial sialoprotein has been studied. The time of its appearance, its increase during early epithelial development and the fact that it is seen at progressively lower levels of the epithelial cell surface as the junctions migrate toward the base of the cells has been shown. These studies support the interpretation that epithelial cell surface sialoprotein is of importance for differentiation and maintenance of foot process and slit architecture, since the appearance of cell surface sialoprotein at the base of the columnar epithelium precedes the formation of foot processes and open slits.

9. The path taken by tracer molecules (i.e., ferritins) through the developing capillary wall has been studied. It has been shown that both the endothelial fenestrae and the basement membrane probably play major roles in regulating movement of ferritin across the developing capillary wall and that the early GBM is less dense and more permeable to ferritin than the mature GBM.

A number of these novel findings have been recently reported in the literature (Reeves, Caulfield and Farquhar, ref. 76), and the other new findings will be reported in a forthcoming paper.

BIBLIOGRAPHY

1. Ainsworth SK, Karnovsky MJ. An ultrastructural method for enhancing the size and electron opacity of ferritin in thin sections. *J Histochem and Cytochem* 20:225 (1972).
2. Amsterdam A, Jamieson JD. Structural and functional characterization of isolated pancreatic exocrine cells. *Proc Natl Acad Sci USA* 69:3028 (1972).
3. Aoki A. Temporary cell junctions in the developing human renal glomerulus. *Devel Biol* 15:156 (1967).
4. Aoki A. Development of the human renal glomerulus. I. differentiation of the filtering membrane. *Anat Rec* 155:339 (1966).
5. Arakawa M. A scanning electron microscopy study of the glomerulus of normal and nephrotic rats. *Lab Invest* 23:489 (1970).
6. Arataki M. On the postnatal growth of the kidney with special reference to the number and size of glomeruli (albino rat). *Am J Anat* 36:399 (1926).
7. Baylis C, Bohrer MP, Troy JL, Robertson CR, Brenner BM. Mechanisms of puromycin-induced defects in transglomerular passage of water and macromolecules (abstr.). *Kidney Intnl* 10:554 (1976).
8. Bernfield MR, Banerjee SD. Acid mucopolysaccharides (glycosaminoglycan) at the epithelial-mesenchymal interface of mouse embryo salivary glands. *J Cell Biol* 52:664 (1972).
9. Bernfield MR, Banerjee SD, Cohn RH. Dependence of salivary epithelial morphology and branching morphogenesis upon acid mucopolysaccharide protein (proteoglycan) at the epithelial surface. *J Cell Biol* 52:674 (1972).
10. Blau EB, Haas JE. Glomerular sialic acid and proteinuria in human renal disease. *Lab Invest* 28:227 (1973).
11. Blau EB, Michael AF. Rat glomerular glycoprotein composition and metabolism in aminonucleoside nephrosis. *Proc Soc Exp Biol Med* 141:164 (1972).

12. Brenner BM, Baylis C, Deen WM. Transport of molecules across renal glomerular capillaries. *Physiol Revs* 56:502 (1976).
13. Brenner BM, Hostetter TH, Humes HD. Molecular basis of proteinuria of glomerular origin. *New Eng J Med* 298:826 (1978).
14. Caulfield JP. Alterations in the distribution of fibrillar anionic sites in the glomerular basement membrane in aminonucleoside nephrosis. *Lab Invest* 1979 (in press).
15. Caulfield JP, Farquhar MG. The permeability of glomerular capillaries to graded dextrans. *J Cell Biol* 63:883 (1974).
16. Caulfield JP, Farquhar MG. The permeability of glomerular capillaries of aminonucleoside nephrotic rats to graded dextrans. *J Exp Med* 142:61 (1975).
17. Caulfield JP, Farquhar MG. Distribution of anionic sites in glomerular basement membranes: Their possible role in filtration and attachment. *Proc Natl Acad Sci USA* 73:1646 (1976).
18. Caulfield JP, Farquhar MG. Loss of anionic sites from the glomerular basement membrane in aminonucleoside nephrosis. *Lab Invest* 39:505 (1978).
19. Caulfield JP, Reid JJ, Farquhar MG. Alterations of the glomerular epithelium in acute aminonucleoside nephrosis: evidence for formation of occluding junctions and epithelial cell detachment. *Lab Invest* 34:43 (1976).
20. Chang RLS, Deen WM, Robertson CR, et. al. Permsselectivity of the glomerular capillary wall. III. Restricted transport of polyanions. *Kidney Intl* 8:212 (1975).
21. Comper WD, Laurent TC. Physiological function of connective tissue polysaccharides. *Physiol Revs* 58:255 (1978).
22. Couser WG, Hoyer JR, Stilmant MM, et. al. Effects of aminonucleoside nephrosis on immune complex localization in autologous immune complex nephritis in the rat. *J Clin Invest* 61:561 (1978).
23. DuBois AM. The embryonic kidney. In *The Kidney: Morphology, Biochemistry, Physiology*, Vol. I, edited by Rouiller C, Muller AF; p.6; New York, Academic Press, 1969.
24. Farquhar MG. In *Small Blood Vessel Involvement in Diabetes Mellitus*, edited by Siperstein MD, Colwell AR, Meyer K; Washington DC, American Institute of Biological Sciences, p.34, 1964.
25. Farquhar MG. The primary glomerular filtration barrier-basement membrane or epithelial slits. *Kidney Intl* 8:197 (1975).

26. Farquhar MG. Structure and function in glomerular capillaries. Role of the basement membrane in glomerular filtration. In Biology and Chemistry of Basement Membranes. Edited by N.A. Kefalides. p.43, New York, Academic Press, 1978.
27. Farquhar MG. Role of the basement membrane in glomerular filtration: Results obtained with electron dense tracers. In Functional Ultrastructure of the Kidney. Edited by A.B. Maunsbach, et. al., Academic Press, 1979, "In Press."
28. Farquhar MG, Palade GE. Cell junctions in amphibian skin. J Cell Biol 26:263 (1965).
29. Farquhar MG, Palade GE. Glomerular permeability. II. Ferritin transfer across the glomerular capillary wall in nephrotic rats. J Exp Med 114:699 (1961).
30. Farquhar MG, Palade GE. Junctional complexes in various epithelia. J Cell Biol 17:375 (1963).
31. Farquhar MG, Wissig SL, Palade GE. Glomerular permeability. I. Ferritin transfer across the normal glomerular capillary wall. J Exp Med 113:47 (1961).
32. Feldman JD, Fisher ER. Renal lesions in aminonucleoside nephrosis as revealed by electron microscopy. Lab Invest 8:371 (1959).
33. Gasic GL, Berwick L, Sorrentino M. Positive and negative colloidal iron as cell surface electron stains. Lab Invest 18:63 (1968).
34. Gilula NB. Junctions between cells. In Cell Communication, edited by Cox RP, p.1, New York, John Wiley and Sons, Inc., 1974.
35. Graham RC, Karnovsky MJ. Glomerular permeability: ultrastructural and cytochemical studies using peroxidases as protein tracers. J Exp Med 124:1123 (1966).
36. Hay ED, Dodson JM. Secretion of collagen by corneal epithelium. I. Morphology of the collagenous products produced by isolated epithelia grown on frozen-killed lens. J Cell Biol 57:190 (1973).
37. Hay ED, Hasty DL, Kiehnau KL. Morphological investigation of fibers derived from various types: Fine structure of collagens and their relation to glucosaminoglycans (GAG). In Collagen-Platelet Interaction, edited by Gastpar H, Kuhn K, Marx R. Stuttgart-New York, F.K. Schattauer Verlag, 1978.
38. Hay ED, Meier S. Glycosaminoglycan synthesis by embryonic inductors: neural tube, notochord and lens. J Cell Biol 62:889 (1974).

39. Hughes RC. Membrane Glycoproteins: A Review of Structure and Function. London, Butterworths, 1977.
40. Humbert F, Montesano R, Perrelet A, Orci L. Junctions in developing human and rat kidney: A freeze fracture study. J Ultrastruc Res 56:202 (1976).
41. Jaffe EA, Minick CR, Adelman B, Becker CG, Nachman R. Synthesis of basement membrane collagen by cultured human endothelial cells. J Exp Med 144:209 (1976).
42. Jokelainen P. An electron microscope study of the early development of the rat metanephric nephron. Acta Anat 52, Suppl. 47:1 (1963).
43. Jones JB. Mucosubstances of the glomerulus. Lab Invest 21:119 (1969).
44. Kanwar YS, Farquhar MG. Anionic sites in the glomerular basement membrane. In vivo and in vitro localization to the lamina rarae by cationic probes. J Cell Biol(1979)(in press).
45. Kanwar YS, Farquhar MG. Presence of heparan sulfate in the glomerular basement membrane. Proc Natl Acad Sci USA, (1979) (in press).
46. Karnovsky MJ. A formaldehyde-glutaraldehyde fixative of high osmolality for use in electron microscopy (abstr). J Cell Biol 27:137a (1965).
47. Karnovsky MJ. Use of ferrocyanide reduced osmium tetroxide in electron microscopy. Abstr. No. 284, Eleventh Annual Meeting of the American Society for Cell Biology, New Orleans, LA (1971).
48. Kefalides NA. Structure and biosynthesis of basement membranes. In International Review of Connective Tissue Research, Vol 6, edited by Hall DA, Jackson DS, p.63, New York, Academic Press, 1973.
49. Kefalides NA. Basement membranes: Current concepts of structure and synthesis. Dermatologica 150:4 (1975).
50. Kefalides NA. Basement membranes: Structural and biosynthetic considerations. J Invest Derm 65:85 (1975).
51. Kelley VE, Cavallo T. An ultrastructural study of the glomerular slit diaphragm in New Zealand Black/White mice. Lab Invest 35:213 (1976).
52. Kelley VE, Cavallo T. Glomerular permeability: Ultrastructural studies in New Zealand Black/White mice using polyanionic ferritin as a molecular probe. Lab Invest 37:265 (1977).

53. Klinger G, Geyer G. Histochemical studies on renal basal membranes during their development. *Acta Histochem* 21:261 (1965).
54. Kreibich G, Debey P, Sabatini DD. Selective release of content from microsomal vesicles without membrane disassembly. I. Permeability changes induced by low detergent concentration. *J Cell Biol* 58:436 (1973).
55. Kreibich G, Sabatini DD. Selective release of content from microsomal vesicles without membrane disassembly. II. Electrophoretic and immunological characterization of microsomal subfractions. *J Cell Biol* 61:789 (1974).
56. Kurtz SM, Feldman JD. Experimental studies on the formation of the glomerular basement membrane. *J Ultrastruc Res* 6:19 (1962).
57. Kurtz SM, McManus JFA. A reconsideration of the development, structure and disease of the human renal glomerulus. *Am Heart J* 58:357 (1959).
58. Latta H, Johnston WH. The glycoprotein inner layer of glomerular capillary basement membrane as a filtration barrier. *J Ultrastruc Res* 57:65 (1976).
59. Latta H, Johnston WH, Stanley TM. Sialoglycoproteins and filtration barriers in the glomerular capillary wall. *J Ultrastruc Res* 51:354 (1975).
60. Lindahl U, Hook Magnus. Glycosaminoglycans and their binding to biological macromolecules. *Ann Rev Biochem* 47:385 (1978).
61. Luft JH. Improvements in epoxy resin embedding methods. *J Biophys Biochem Cytol* 9:409 (1961).
62. Luft JH. Ruthenium red and violet. I. Chemistry, purification, methods of use for electron microscopy and mechanism of action. *Anat Rec* 171:347 (1971).
63. Luft JH. Ruthenium red and violet. II. Fine structural localization in animal tissues. *Anat Rec* 171:369 (1971).
64. Majno G. Ultrastructure of the vascular membrane. In *Handbook of Physiology-Circulation*, Vol III, Chap 64, edited by Hamilton WH, Dow P, p.2293, Washington DC, American Physiological Society, 1963.
65. Michael AF, Blau E, Vernier RL. Glomerular polyanion: alterations in aminonucleoside nephrosis. *Lab Invest* 23:649 (1970).

66. Mohos SC, Skoza L. Glomerular sialoprotein. *Science* 164:1519 (1969).
67. Mohos SC, Skoza L. Histochemical demonstration and localization of sialoproteins in the glomerulus. *Exp Mol Pathol* 12:316 (1970).
68. Mohos SC, Skoza L. Variations in the sialic acid concentration of glomerular basement membrane preparations obtained by ultrasonic treatment. *J Cell Biol* 45:450 (1970).
69. Nevins TE, Michael AF. Isolation of glomerular polyanion. Abstr. American Society of Nephrology, 11th Annual Meeting, New Orleans, LA, 1978.
70. Osathanondh V, Potter EL. Development of the human kidney as shown by microdissection. Development of vascular pattern of the glomerulus. *Arch Pathol* 82:403 (1966).
71. Palade GE. A study of fixation for electron microscopy. *J Exp Med* 95:285 (1952).
72. Palade GE. Intracellular aspects of the process of protein secretion. *Science* 189:347 (1975).
73. Potter EL. Development of the human glomerulus. *Arch Pathol* 80:241 (1965).
74. Pricam C, Humbert F, Perrelet A, Amherdt M, Orci L. Intercellular junctions in podocytes of the nephrotic glomerulus as seen with freeze-fracture. *Lab Invest* 33:209 (1975).
75. Quintarelli G, Dellovo MC. The chemical and histochemical properties of alcian blue. IV. Further studies on the methods for the identification of acid glycosaminoglycans. *Histochemie* 5:196 (1965).
76. Reeves W, Caulfield JP, Farquhar MG. Differentiation of epithelial foot processes and filtration slits: Sequential appearance of occluding junctions, epithelial polyanion and slit membranes in developing glomeruli. *Lab Invest* 39:90 (1978).
77. Renkin EM, Gilmore JP. Glomerular filtration. In *Handbook of Physiology. Section 8. Renal Physiology.* Edited by Orloff J, Berliner RW, p. 185, Washington DC, American Physiological Society, 1973.
78. Renke HG, Cotran RS, Venkatachalam MA. Role of molecular charge in glomerular permeability. Tracer studies with cationized ferritin. *J Cell Biol* 67:638 (1975).
79. Renke HG, Venkatachalam MA. Glomerular permeability: In vivo tracer studies with polyanionic and polycationic ferritins. *Kidney Intl* 11:44 (1977).

80. Reynolds ES. The use of lead citrate at high pH as an electron opaque stain in electron microscopy. *J Cell Biol* 17:208 (1963).
81. Rhodin JAG. The diaphragms of capillary endothelial fenestrations. *J Ultrastruc Res* 6:171 (1962).
82. Rinehart JF, Abul-Haj SK. An improved method for the demonstration of acid mucopolysaccharides in tissues. *AMA Arch Pathol* 52:189 (1951).
83. Ruggeri A, Dell'Orbo C, Quacci D. Electron microscopic visualization of proteoglycans with alcian blue. *Histochem J* 7:187 (1975).
84. Ryan GB, Leventhal M, Karnovsky MJ. A freeze-fracture study of the junctions between glomerular epithelial cells in aminonucleoside nephrosis. *Lab Invest* 32:397 (1975).
85. Ryan GB, Rodewald R, Karnovsky MJ. An ultrastructural study of the glomerular slit diaphragm in aminonucleoside nephrosis. *Lab Invest* 33:461 (1975).
86. Sato T, Spiro RG. Studies on the subunit composition of the renal glomerular basement membrane. *J Biol Chem* 271:4062 (1976).
87. Schneeberger EE, Grupe WE. The ultrastructure of the glomerular slit diaphragm in autologous immune complex nephritis. *Lab Invest* 34:298 (1976).
88. Schneeberger EE, Leber PD, Karnovsky MJ, McCluskey RT. Altered functional properties of the renal glomerulus in autologous immune complex nephritis. *J Exp Med* 139:1283 (1974).
89. Scott JE, Dorling J. Differential staining of acid glycosaminoglycans (mucopolysaccharides) by alcian blue in salt solutions. *Histochemie* 5:221 (1965).
90. Seiler MW, Rennke HG, Venkatachalam MA, Cotran RS. Pathogenesis of polycation-induced alterations ("fusion") of glomerular epithelium. *Lab Invest* 36:48 (1977).
91. Seiler MW, Venkatachalam MA, Cotran RS. Glomerular epithelium: Structural alterations induced by polycations. *Science* 189:390 (1975).
92. Simionescu N, Simionescu M. Galloylglucoses of low molecular weight as mordant in electron microscopy. I. Procedure and evidence for mordanting effect. *J Cell Biol* 70:608 (1976).

93. Simionescu N, Simionescu M. The blood circulatory system. In *Histology*, edited by Weiss L, Greep RO, p.373, New York, McGraw-Hill Book Company, 1977.
94. Simionescu N, Simionescu M. Differential distribution of anionic sites on the capillary endothelium. *J Cell Biol* 79:59a (abstr.) (1978).
95. Spicer SS. A correlative study of the histochemical properties of rodent acid polysaccharides. *J Histochem Cytochem* 8:18 (1960).
96. Spinelli F. Structure and development of the renal glomerulus as revealed by scanning electron microscopy. *Intl Rev Cytol* 39:345 (1974).
97. Spiro RG. Basement membranes and collagens. In *Glycoproteins: Their Composition, Structure, and Function*, edited by Gottschalk A, p.964, Elsevier Publishing Company, America, London, NY, 1972.
98. Staehelin LA. Structure and function of intercellular junctions. *Intl Rev Cytol* 39:191 (1974).
99. Thorning D, Vracko R. Renal glomerular basal lamina scaffold: Embryologic development, anatomy and role in cellular reconstruction of rat glomeruli injured by freezing and thawing. *Lab Invest* 37:105 (1977),
100. Toole BP. Morphogenetic role of glycosaminoglycans (acid mucopolysaccharides) in brain and other tissues. In *Neuronal Recognition*, edited by Barondes SH, p.275, New York, Plenum Publishing Corporation, 1976.
101. Trelstad RL, Hayashi K, Toole BP. Epithelial collagens and glycosaminoglycans in the embryonic cornea. Macromolecular order and morphogenesis in the basement membrane. *J Cell Biol* 62:815 (1974).
102. Velosa JA, Glaser RJ, Nevins TE, et. al. Experimental model of focal sclerosis. II. Correlation with immunopathological changes, macromolecular kinetics and polyanion loss. *Lab Invest* 36:527 (1977).
103. Vernier RL, Birch-Anderson A. Studies of the human fetal kidney. *J Pediatrics* 60:754 (1962).
104. Vernier RL, Birch-Anderson A. Studies of the human fetal kidney. II. Permeability characteristics of the developing glomerulus. *J Ultrastruc Res* 8:66 (1963).

105. Vernier RL, Papermaster BW, Good RA. Aminonucleoside nephrosis. I. Electron microscopic study of the renal lesion in rats. *J Exp Med* 109:115 (1959).
106. Weber WA, Blackbourn J. The permeability of the immature glomerulus to large molecules. *Lab Invest* 23:1 (1970).
107. Wight TN, Ross R. Proteoglycans in primate arteries. I. Ultrastructural localization and distribution in the intima. *J Cell Biol* 67:660 (1975).
108. Yee AG. Gap junctions between hepatocytes in regenerating rat liver (abstr). *J Cell Biol* 55:294a (1972).



YALE MEDICAL LIBRARY

Manuscript Theses

Unpublished theses submitted for the Master's and Doctor's degrees and deposited in the Yale Medical Library are to be used only with due regard to the rights of the authors. Bibliographical references may be noted, but passages must not be copied without permission of the authors, and without proper credit being given in subsequent written or published work.

This thesis by _____ has been used by the following persons, whose signatures attest their acceptance of the above restrictions.

NAME AND ADDRESS	DATE
<i>Isidore Plimley 511 George St New Haven Ct.</i>	<i>10/17/79</i>
<i>R. K. Jackson M.D. 310 Cedar St New Haven Ct. (Pathology)</i>	<i>11/19/80</i>

